A STATE CONTROLLER FOR CLOSED-LOOP FUNCTIONAL ELECTRICAL STIMULATION REGULATED BY NATURAL SENSORY FEEDBACK

by

Kevin D. Strange
B.A.Sc., Simon Fraser University, 1992

THESIS SUBMITTED IN PARTIAL FULFILLMENT OF
THE REQUIREMENTS FOR THE DEGREE OF
MASTER OF APPLIED SCIENCE
in the School
of
ENGINEERING SCIENCE

SIMON FRASER UNIVERSITY
April, 1996

Approval

NAME:	Kevin Daryl Strange
DEGREE:	Master of Applied Science (Engineering Science)
TITLE OF THESIS:	A State Controller for Closed-Loop Functional Electrical Stimulation Regulated By Natural Sensory Feedback

EXAMINING COMMITTEE:

Chair:	Dr. Jim Cavers Professor of School of Engineering Science
Senior Supervisor	Dr. J. Andy Hoffer Professor and Director of School of Kinesiology
Supervisor	Dr. Dejan Popovic Professor of Biomedical Engineering University of Belgrade
Supervisor	Dr. Tom Calvert Professor of School of Engineering Science Director of Centre for Systems Science
Examiner	Dr. M. Ash Parameswaran Assistant Professor of School of Engineering Science
DATE APPROVED:	10 April 1996

PARTIAL COPYRIGHT LICENSE

I hereby grant to Simon Fraser University the right to lend my thesis, project or extended essay (the title of which is shown below) to users of the Simon Fraser University Library, and to make partial or single copies only for such users or in response to a request from the library of any other university, or other educational institution, on its own behalf or for one of its usrs. I further agree that permission for multiple copying of this work for scholarly purposes may be granted by me or the Dean of Graduate Studies. It is understood that copying or publication of this work for financial gain shall not be allowed without my written permission.

Title of Thesis/Project/Extended Essay

"A State Controller For Closed-Loop Functional Electrical Stimulation Regulated By Natural Sensory Feedback"

Author:

_____
(signature)

K. Strange
(name)

April 17th, 96
(date)

Abstract

Functional electrical stimulation (FES) is used in clinical systems to return function to patients with extremities paralyzed by spinal cord injury or stroke. Stimulation pulses are applied through surface or implantable electrodes to nerve or muscle tissue below the level of the lesion, resulting in muscle twitch or sustained contraction in paralyzed muscles. Coordinated stimulation of multiple muscles may be required to return useful function to an entire extremity, and FES is currently being implemented to produce standing and walking in paraplegic patients and pinch grip in quadriplegic patients. Closed-loop FES systems may improve the efficacy of clinical systems by including feedback from artificial sensors external to the body or, in a new approach, from natural physiological sensors that remain viable in affected extremities.

In this thesis, a state controller for FES was developed to demonstrate the viability of implementing natural sensory signals from nerve cuffs in the periphery as feedback for closed-loop FES systems.

In a first study, recording nerve cuff electrodes were implanted on two of the Median, Ulnar, and/or Radial nerves in the forelimb of fourteen cats. The functional condition of the nerves and recording devices was periodically evaluated by monitoring evoked compound action potentials (CAPs) and device impedances under anesthesia. The study demonstrated that implanted nerve cuffs are safe and that stable neural recordings are possible for extended periods of at least six months in freely moving animals.

In a second study, natural sensory signals were recorded from cutaneous nerves in the forelimb of six cats during walking on a motorized treadmill, using chronically implanted tripolar nerve cuffs

on the Median, Ulnar, and/or Radial nerves. Features in the electroneurograms (ENGs) related to foot contact and lift-off were reliably detected and were used by a state controller model to predict the timing of activity of Palmaris Longus, a wrist flexor, for a variety of walking conditions. The cutaneous ENG signals recorded during walking suggested that natural sensory signals may be more generally implemented as a source of feedback for closed-loop control of FES.

In a third study, a real-time state controller for FES was developed which implemented cutaneous neural signals from the cat forelimb as feedback to predict the timing of the stance phase and associated Palmaris Longus (PalL) muscle activity during walking on the treadmill. The state controller was tested in three sets of experiments: 1) to predict the timing of muscle activity in an open-loop configuration with no stimulation, 2) to predict the timing of muscle activity in a closed-loop configuration and stimulate the PalL over a background of natural muscle activity, and 3) to predict the timing of muscle activity in a closed-loop configuration and stimulate the PalL to return function to the wrist during temporary paralysis of the PalL and other wrist planter flexors. The FES state controller was tested in a variety of walking conditions, including treadmill velocities of up to 1.0 m/s and slopes of $\pm 10\%$.

The stability of nerve cuff signals over time and the accuracy of state controller results in a range of walking conditions lend support to the long-term use of nerve cuff recording electrodes for the control of functional electrical stimulation systems and neural prostheses in human applications.

Dedication

My thesis is dedicated to my parents, Phil and Quilla Strange, for their loving support through the last eight years of my life at Simon Fraser University, and to my brother Mike and my fiancee Karen. Thanks for everything.

Acknowledgements

I gratefully acknowledge the guidance and support of my supervisor Dr. Andy Hoffer, and the assistance and friendship of all of the past and present members of the Neurokinesiology Lab: Yunquan Chen, Paul Christensen, David Crouch, Janice Eng, Morten Hansen, Klaus Kallesøe, Catharine Kendall, Josh Lawson, Myriam El Mouldi, Jeff Pugh, Haiming Qi, Sheila Schindler-Ivens, Ignacio Valenzuela, and David Viberg.

I also gratefully acknowledge the helpful discussions I had with Drs. Dejan Popovic, Morten Haugland, and Aleksandar Kostov during my MASc thesis work.

Funding for this research was provided by the National Institutes of Health (contract number NIH-NINDS-NO1-NS-3-2380, J.A. Hoffer, P.I.) and by the Canadian NeuroScience Network of Centres of Excellence (Theme 6, Project A3).

Table of Contents

List of Tables

List of Figures

Chapter 1: General Introduction

The underlying objective of this MASc thesis project is to demonstrate the feasibility of utilizing sensory nerve signals recorded from chronically implanted transducers as a source of feedback for functional electrical stimulation (FES) systems.

The overall goal of FES is to improve the quality of life for patients affected by paralysis and related disabilities resulting from spinal cord injuries or other central nervous system injuries such as stroke. The means of FES are the application of stimulation technology in an intelligent, efficient manner to return function to paralyzed muscle tissue in the extremities or in internal organs.

Voluntary control of muscles in the extremities is removed by a break or lesion of the neural pathways from the higher control centres to the extremities, even though the peripheral nerves and muscles below the level of the lesion or injury remain largely healthy and viable so long as blood supply has not been interrupted and muscle atrophy is minimized through physiotherapy. Nerves and muscles in the extremities can be stimulated with trains of current pulses to evoke muscle contraction, and functionality can be returned to the extremity if the appropriate muscles are stimulated in coordinated patterns. Stimulation patterns are modulated by stimulation rate with a combination of stimulus current amplitude or pulse duration to produce the desired muscle output (Mortimer, 1981, 1990).

Clinical FES systems have been implemented in humans in either open-loop and closed-loop configurations for a range of functional tasks from standing up from a wheelchair (Marsolais et al., 1994), to walking (Popovic, 1992; Stein et al., 1993; Kralj et al., 1994; Haugland and

Sinkjær, 1995), to controlling the grasp of objects in the paralyzed hand (Crago et al., 1991; Peckham and Keith, 1992; Nathan, 1993; Haugland et al., 1995), and controlling internal organ function such as the bladder (Creasey, 1993). Open-loop FES systems, such as those used to control standing and stepping in paraplegics, generally require a user-controlled trigger to initiate a preset program of muscle stimulation which produces a stereotyped muscle output. With this approach, the initial conditions and environment that the system is used in must be rigidly controlled, and the system may not compensate for changes in system variables such as muscle fatigue and changes in the slope, direction or rate of walking.

Closed-loop FES systems may be able to provide the flexibility and adaptability necessary to respond to changing environmental conditions. FES systems for walking that include feedback for foot contact, position, muscle force, joint torque, and/or rate of walking can lead to adjustment in stimulation patterns and accommodate changes in the gait pattern and other variables such as muscle fatigue (Stein, 1992; Chizeck, 1992). Similarly, upper limb FES systems for grasping that include grasp force feedback should allow for changes in object load or slippage of the object without dropping or crushing the object (Crago, 1991; Peckham and Keith, 1992; Nathan, 1993). The musculo-skeletal system naturally uses many forms of sensory feedback to allow for a wide range of operating conditions, and it seems appropriate that FES systems should emulate the natural system to improve accuracy and efficiency (Hoffer, 1988; Stein, 1992).

A current challenge in implementing closed-loop FES systems is to determine and obtain the type of feedback signals that are necessary to improve a desired task, taking into consideration the technical difficulty of instrumenting the body with transducers to provide feedback. Artificial transducers such as force sensitive resistors have been implemented in the soles of shoes to provide contact and force feedback during walking (Stein et al., 1992; Kostov et al., 1995a), and goniometers have been attached to lower limb orthoses to provide joint angle feedback (Andrews et al., 1989; Kostov et al., 1995a), but both of these approaches utilize sensors that may be unreliable over wide ranges of operating conditions and require frequent calibration. In addition,

external sensors normally require some form of orthoses or external framework to attach the transducer to, which may not be cosmetically acceptable to patients unwilling to wear an instrumented orthosis or external brace. In some hybrid systems which utilize bracing technology with FES to stiffen joints and reduce degrees of freedom, external sensors are easily implemented and may be appropriate for obtaining feedback.

Implanted sensors may also be used to provide useful feedback signals, and will be necessary for closed-loop FES systems once the stimulation systems become fully implantable. Implantable sensors may transduce either artificial sensor signals such as contact force or joint angle, or natural physiological signals such as electromyographic (EMG) or electroneurographic (ENG) activity. An attractive approach in closed-loop FES systems is to instrument sensory nerves below the level of the lesion and record sensory activity in the paralyzed extremity. Instrumenting cutaneous sensory nerves could provide feedback regarding contact and force during walking and during grasping, while instrumenting muscle nerves could lead to harnessing feedback signals regarding muscle length and force and joint position.

Instrumenting the peripheral nervous system is proving to be a very promising option for attaining useful physiological feedback signals (Hoffer, 1990; Popovic et al., 1993; Yoshida and Horch, 1994; Haugland et al., 1994; Haugland and Hoffer, 1994a,b; Haugland and Sinkjaer, 1995, Haugland et al., 1995). Fine wire and intrafascicular microelectrodes inserted into peripheral nerves have been used to record single and multi-unit activity in a number of research applications (Hoffer, 1990; Kallesøe et al., 1994; Yoshida and Horch, 1994), but normally the recording environment is very harsh for the fragile electrodes and device breakage, encapsulation, and migration are common. It is proving to be extremely challenging to successfully record in the periphery for longer that one or two days in awake, freely moving animals with silicon-based microelectrodes (Kallesøe and Hoffer, 1994; and personal communications).

Nerve cuff electrodes implanted in the periphery offer a number of distinct advantages to microelectrodes in that nerve cuffs encircle and record from the entire nerve and offer superior device longevity and signal stability. To date, several experimental closed-loop FES systems utilizing nerve cuff feedback from the extremity have been implemented in both animals and humans with promising results. Haugland and Hoffer (1994b) demonstrated that a closed-loop steady state FES controller could control the combined force output from four ankle extensor muscles based on footpad slip signals from a nerve cuff implanted on the Tibial nerve in the cat hindlimb. Further work with the cat hindlimb led to a demonstration of closed-loop stimulation over natural EMG during walking utilizing nerve cuff signals from the Tibial nerve (Kallesøe et al., 1992). Popovic et al. (1993) showed that nerve cuff signals recorded from the Tibial and Superficial Peroneal nerves in the cat hindlimb could be used to accurately detect foot contact during walking and control stimulation. In the first human application where FES was controlled using nerve cuff feedback from the extremity, Haugland and Sinkjær (1995) demonstrated a system to correct for drop-foot that utilized a nerve cuff signal from the Sural nerve as a switch to detect foot contact.

In this thesis, three basic questions are addressed regarding the use of neural signals as a source of feedback for FES: 1) Are nerve signals, recorded from nerve cuffs chronically implanted in the forelimbs of cats stable over long term implant periods? 2) Do sensory nerve recordings provide useful, reliable information regarding foot contact and other gait events? and 3) Can sensory nerve signals be implemented as feedback in a FES system to restore the use of paralyzed wrist plantar flexor muscles during walking?

Chapters 2 to 4 address these three questions. Each chapter represents a full manuscript prepared for submission to IEEE Transactions in Biomedical Engineering.

Chapter 2 addresses the issue of long-term stability of signals recorded from nerve cuffs chronically implanted in the cat forelimb. Fourteen cats were implanted on two of the Median,

Ulnar, and/or Radial nerves in the left forelimb, and the functional condition of the nerves and recording devices was periodically evaluated by monitoring evoked compound action potentials (CAPs) and device impedances under anesthesia. The amplitudes and conduction latencies of the CAPs were used to monitor the condition of the nerves and implanted devices, and to calibrate and verify sensory nerve recordings in the awake cat during walking on a motorized treadmill.

Chapter 3 discusses the development and evaluation of a model FES state controller in which sensory nerve recordings are used as inputs to predict the timing of phases of the step cycle and related muscle activity. In this study, electroneurograms (ENGs) from the implanted nerve cuffs from six cats walking on the treadmill were examined for similarities from cat to cat over the implant periods and for reliable features related to foot contact and lift-off. The model state controller was evaluated for accuracy and reliability with data obtained from different cats in a range of walking conditions (treadmill speeds and slopes).

Chapter 4 discusses the development and evaluation of a real-time state controller (finite state machine) for FES which implemented sensory neural signals from the cat forelimb as feedback to predict the timing of the stance phase and the timing of activation of the Palmaris Longus muscle during walking on the treadmill. The challenge was to record neural signals in the presence of stimulation artifacts and, in real-time, accurately distinguish neural activity related to paw contact and lift-off for a wide variety of walking conditions. The real-time state controller was tested in three sets of experiments: 1) to predict the timing of muscle activity in an open-loop configuration with no stimulation, 2) to predict the timing of muscle activity in a closed-loop configuration and stimulate the muscle over a background of natural muscle activity, and 3) to predict the timing of muscle activity in a closed-loop configuration and stimulate the PalL to return function to the wrist during temporary paralysis of the PalL and other wrist planter flexors. The results of testing the real-time state controller in a range of walking conditions are discussed in terms of transferability of nerve cuff feedback to human applications of FES and neural prostheses.

Chapter 5 presents a general discussion of the results from all three studies, and examines the feasibility and reliability of recording neural signals with implanted nerve cuffs for clinical applications. The advantages and limitations of the FES state controller and the use of sensory nerve feedback are also analyzed, as well as limitations of developing FES technology for human walking in a quadruped model. Chapter 5 also assesses the likelihood of implementing neural feedback in clinical applications of FES.

Appendix A presents a copy of NIH Progress Report #11, submitted to NIH on Sept. 30, 1995, which discusses preliminary nerve cuff recordings from muscle nerves in the cat forelimb during walking.

Chapter 2:

Long-term stability of signals recorded from cat forelimb nerves with cuff electrodes.

Summary

Nerve cuff electrodes were implanted on two of the Median, Ulnar, and/or Radial nerves in cat forelimbs. Conventional cuff recording electrodes utilizing closing sutures were used in a first series of eight cats. Nerve cuffs of a novel design were implanted in a second series of six implants. The cats were group-housed and could jump and move about freely in a holding room equipped with shelves up to 1.5 m high. The viability and stability of the nerves and recording devices were periodically evaluated by monitoring evoked compound action potentials (CAPs) and device impedances for at least six months. The nerve cuff design used in the second series had more stable CAPs and impedances than the nerve cuff design used in the first series. This study demonstrates that stable neural recordings are possible for extended periods in freely moving animals. Our results lend support to the long-term use of nerve cuff recording electrodes for the control of functional electrical stimulation systems and neural prostheses in human applications.

2.1. INTRODUCTION

Recent results with functional electrical stimulation (FES) systems have indicated that closed-loop control of FES is both desirable and necessary for returning more efficient and useful function to paralyzed extremities (Crago et al., 1991; Stein, 1992; Popovic et al., 1993; Hoffer et al., 1996). External sensors can be used to provide force and position feedback for neural prostheses systems, yet external devices require frequent calibration and are often inaccurate and difficult to position without external support (Webster, 1992). An attractive approach of providing feedback to FES systems is to utilize the natural sensors available in the extremities to retrieve contact, force, and position information from peripheral nerve recordings (Hoffer and Haugland, 1992; Sinkjær et al., 1992; Haugland et al., 1994; Riso et al., 1995; Haugland et al., 1995).

Our overall objective is to identify reliable sources of neural control signals and extract features, such as contact and slip information, that may be applied in closed-loop FES systems for restoring voluntary use of paralyzed muscles in humans (Hoffer, 1988; Popovic et al., 1993; Haugland and Hoffer, 1994).

In order for natural sensory signals to be utilized as feedback in closed-loop control of FES systems, the nerves must not be damaged by chronic instrumentation and the signals recorded from these nerves must be stable and invariant over long periods of time. In this study we address the question of stability of recorded signals from cutaneous nerves in the cat forelimb that were chronically implanted with stimulating and recording nerve cuffs over periods of at least six months. We implanted fourteen cats, eight in a first series with conventional nerve recording cuffs closed with sutures (Hoffer, 1990), and six in a second series in which a new closing mechanism for the recording cuffs was implemented (Kallesøe et al., 1996).

It is important to highlight that in this study the cats were group-housed and free to move about their holding room. In their daily activities the cats frequently climbed and jumped up and down steps and shelves up to heights of 1.5 m. The implanted nerves and devices were thus exposed to a severe endurance test, possibly exceeding the conditions expected in clinical applications of similar implanted electrodes in disabled humans.

Preliminary aspects of this research have been published in abstract form (Strange et. al., 1995).

2.2. BACKGROUND

2.2.1. The Cat Forelimb as a Model of The Human Limb

The forelimb of the cat was selected as the experimental model in which to investigate the long-term stability of implanted recording nerve cuffs because cutaneous nerve dimensions are comparable to many human forearm and hand nerves, surgical accessibility of nerves and muscles is similar, and the temperament of the animal is suited for chronic experiments. In further studies, described in a companion paper (Strange and Hoffer, 1996, in preparation), we recorded electroneurogram (ENG) and electromyogram (EMG) signals during voluntary tasks. Cats were also the animal of choice for this research because of their trainability and ease of handling for locomotion and reaching tasks.

2.2.2. Anatomy and Physiology

Figure 2.1 provides medial and lateral views of the Median, Ulnar, and Radial nerves in the cat forelimb. The branches of these nerves distal to the elbow mainly innervate the glabrous and hairy portions of the cat's paw as well as the intrinsic digit muscles.

Just distal to the elbow, the Median nerve sends branches to the main wrist and digit flexor muscles, including Palmaris Longus and Flexor Digitorum Profundus. Midway along the distal forelimb the Median nerve largely contains cutaneous afferent axons The Median branches in the palmar side of the paw mainly innervate mechanoreceptors in the glabrous skin pads on the I (thumb), II, III, and IV digits as well as the centre pad of the paw. The Median nerve in the distal forelimb is typically 1.5 to 2 mm in diameter, and can be dissected free over a length suitable for instrumentation of up to 20 or 25 mm. The length of nerve available is generally determined by the pattern of nerve branches leaving the main nerve, the network of longitudinal and transverse blood vessels that run parallel to and supply the nerves, and the distance to the nearest joints. Implanted nerve cuffs should not interrupt blood supply to the nerve, and should not be subject to physical stress resulting from movement at the joint (Hoffer, 1990).

The Ulnar nerve provides innervation to wrist muscles located in the lateral forelimb, including Flexor Carpi Ulnaris and Extensor Carpi Ulnaris, and the distal Ulnar branches (Palmar and Dorsal Cutaneous) normally innervate the glabrous skin pads on the IV and V digits and sometimes the I digit. The Ulnar nerve above the split (see Fig. 1A) is typically 1.5 to 2.0 mm in diameter, while each of its distal branches are normally 1.2 to 1.5 mm in diameter. The Ulnar nerve distal to the elbow can normally be surgically mobilized for a length of 15 to 20 mm.

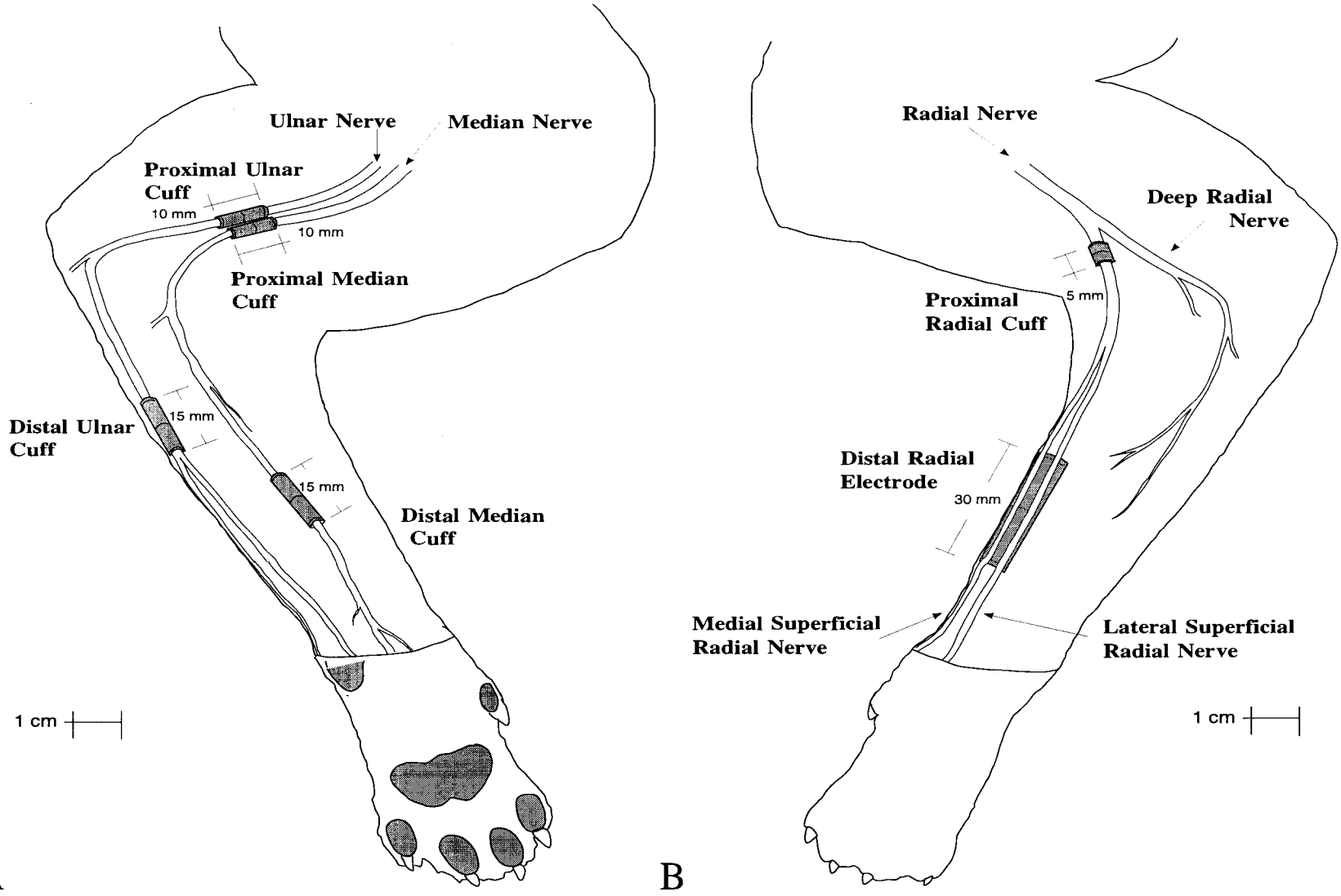

Figure 2.1: A. Medial view of cat left forelimb, showing Ulnar and Median nerves and approximate locations of implanted nerve cuff electrodes. B. Lateral view of cat left forelimb, showing Radial nerve branches and approximate locations of implanted nerve cuffs and ENG patch electrodes.

The Deep Radial nerve primarily innervates wrist and digit extensor muscles, including Extensor Digitorum Lateralis and Extensor Digitorum Communis, while the Superficial Radial nerve branches innervate the dorsal skin surfaces of the paw and digits. The Superficial Radial branches are typically 1.0 to 1.5 mm in diameter and can be freed over lengths of up to 30 or 35 mm below the elbow (Fig. 2.1B).

2.3. METHODS

2.3.1. Anesthesia and Analgesia Protocols

Halothane gas anesthesia was used during the implant surgery which normally lasted 10 to 12 hours. A premedication dose of intramuscular ketamine/acepromazine/atropine (5mg/kg/0.05mg/kg/0.02mg/kg) followed by intravenous ketamine/valium (5mg/kg/0.2mg/kg) was administered to facilitate intubation. Expired CO_2, respiration rate and heart rate were continuously monitored. A post-operative analgesic of torbugesic (0.2mg/kg) or temgesic (0.01mg/kg) was administered at the end of the surgery and maintained for 24 hours. Derapen or Cefadrops antibiotics were given for seven days following the implant surgery.

For each subsequent recording session that occurred approximately every two weeks, the cat was administered an intramuscular ketamine/acepromazine/atropine premedication followed by intravenous ketamine/valium, intubated, and maintained on halothane gas anesthesia for the duration of the experiment.

All surgical and experimental protocols met the guidelines set by the Canadian Council of Animal Care and were approved by the University Animal Ethics Committee. All anesthesia and analgesia procedures were performed by a certified veterinary technician.

2.3.2. Implanted Devices and Transducers

Two tripolar nerve cuffs were implanted on each of two nerves in the left forelimb of fourteen cats, instrumenting two of the Ulnar, Median, and/or Radial nerves. Each nerve was instrumented with a proximal stimulating cuff above the elbow, and a distal recording cuff located below the elbow. Recording cuffs were typically 15 or 20 mm in length, while the stimulating cuffs were typically 5 or 10 mm in length. Figure 2.1B shows a tripolar patch ENG electrode (consisting of a 10 x 30 mm silicone sheet, 0.13 - 0.25 mm thick) that was implanted in two cats (NIH 13 and 14) on the Radial nerve instead of a nerve cuff due to the superficial and fragile nature of the nerve branches (Hoffer, 1990). The patch electrode was sewn onto the inside surface of the skin and contacted the nerves without need for dissecting the nerves free from adjacent blood vessels.

In the first series of eight cats we implanted traditional recording nerve cuffs that had non-absorbable sutures to hold the cuff closed (Hoffer, 1990). In the second series of six cats we implanted recording cuffs that featured a new closing method, shown in Fig. 2.2. Cuffs were manufactured from segments of silicone tubing and three de-insulated wires (AS 631 Teflon-coated Cooner wire) were sewn into the cuff wall to provide three near-circumferential electrical contacts with the nerve (Hoffer, 1990). The middle electrode provided a signal that was differentially recorded with respect to two outer electrodes which were connected together (outer electrode wires of cuffs used in the first series were connected together external to the body, and outer electrodes used in the second series were connected at the cuff). The exit points of the electrodes were sealed with silicone adhesive to improve their isolation from sources of electrical noise (such as muscle activity) external to the cuff. Secure closing was provided by a baton-shaped closing member inserted through a series of interdigitated tubes attached to the edges of the longitudinal slit in the cuff wall (Kallesøe et al., 1996).

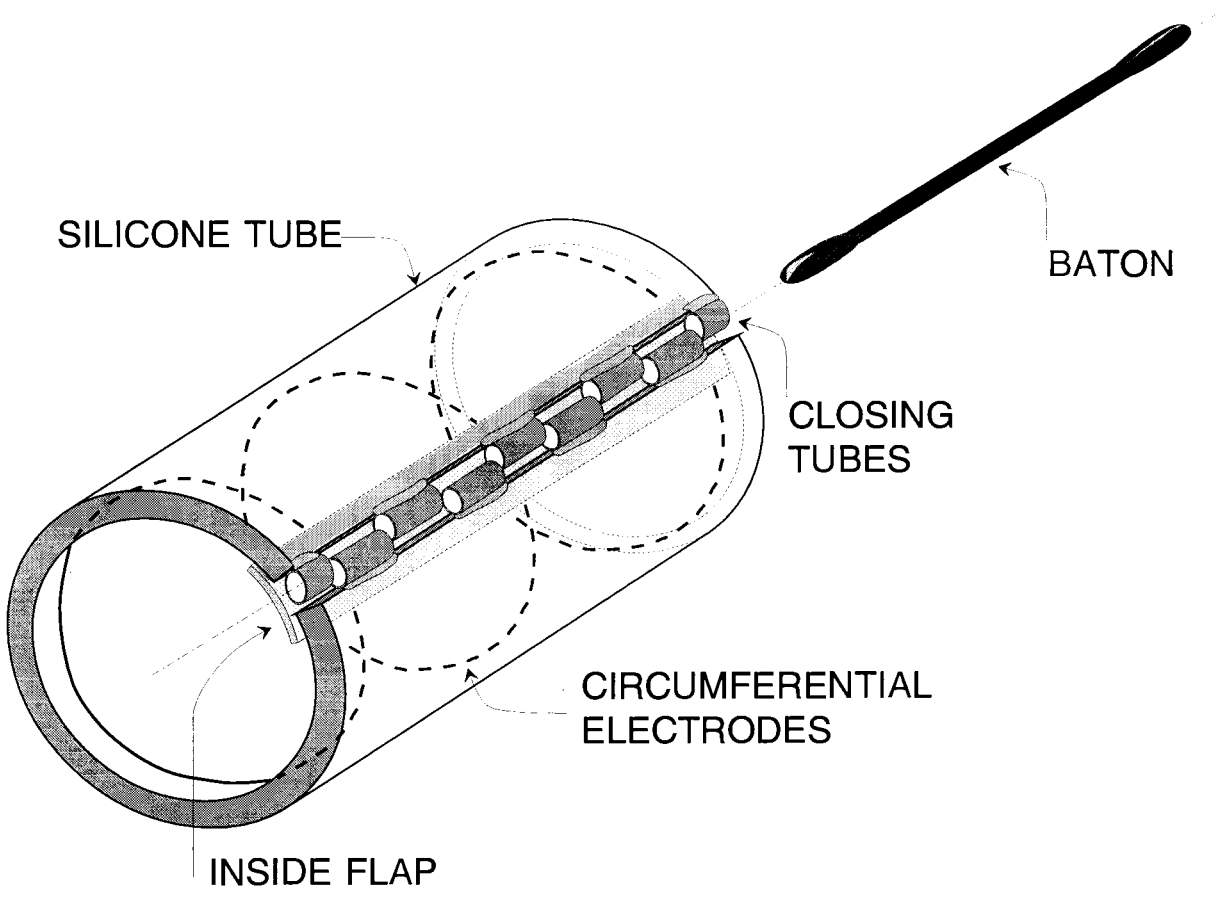

Figure 2.2: Implantable tripolar recording nerve cuff, showing an improved method of closing the cuff consisting of inserting a baton-shaped rod through a series of interdigitated closing tubes attached to the edges of the cuff (Kallesøe et al., 1996). The locations of circumferential electrodes sewn into the cuff wall are designated by the dashed lines, and the electrode exit point and lead wires have been omitted.

Each cuff was opened along a longitudinal slit and the nerve was introduced as shown in Fig. 2.3. The flexible cuff tubing was opened by pulling apart temporary sutures located through the tubes on the edges of the slit, and the nerve was allowed to gently drop into the interior of the cuff. The temporary opening sutures were then removed and the baton was carefully inserted through the series of interdigitated tubes, thus closing the cuff. By virtue of this design, the cuffs remained closed and maintained their original circumference.

In the implant surgery the inside diameter of each cuff was selected to exceed the nerve diameter by approximately 20% to allow for post-surgery inflammation of the nerve. Inside diameters for the distal recording cuffs in the second series of implants were typically 2.3 or 2.8 mm, while slightly smaller diameter cuffs (2.0 or 2.5 mm) were used in the first series. The difference was equal to the outside diameter of the closing tubes introduced in the longitudinal slit of the new cuff design. The proximal stimulating nerve cuffs were typically larger in diameter than the distal recording nerve cuffs in all implants.

In the first series we instrumented the Palmaris Longus muscle with intramuscular EMG electrodes. In the second series we implanted intramuscular EMG electrodes in two wrist flexors, Palmaris Longus and Flexor Carpi Ulnaris, and two wrist extensors, Extensor Carpi Ulnaris and Abductor Pollicis Longus, in order to monitor muscle activity during tasks such as walking on a treadmill (Strange and Hoffer, 1995, 1996).

A thermistor (Yellow Springs Instruments Inc., Model 44004, embedded in silicone) was implanted deep inside the proximal forelimb to monitor limb temperature during recording sessions under anesthesia. Body temperature was maintained near normal during experiments under anesthesia, to ensure that temperature did not adversely affect conduction velocity in the forelimb nerves.

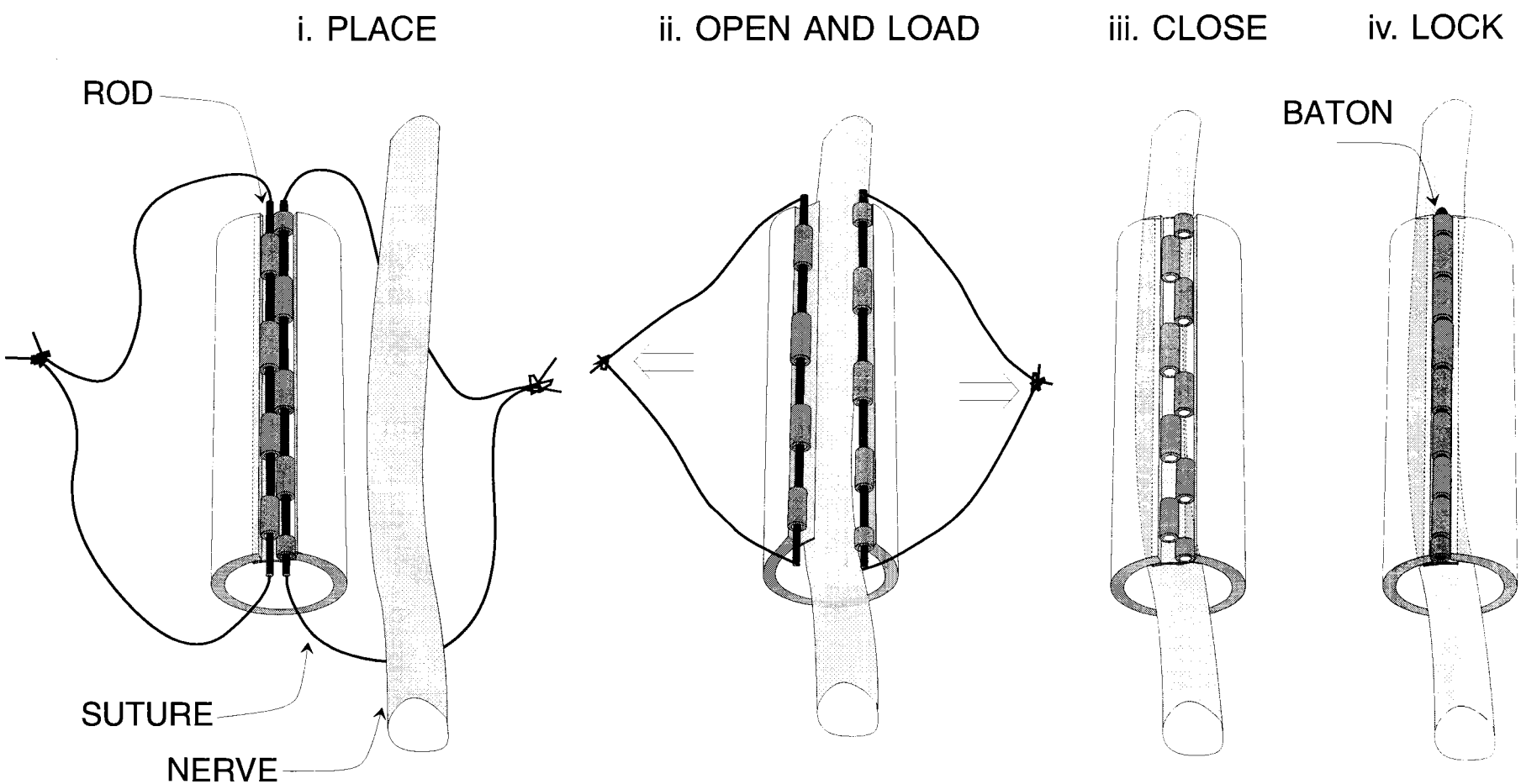

Figure 2.3: Implantation and closing technique for the nerve cuffs used in the second series of implants in this study. (i) the cuff is positioned beneath the isolated nerve of interest, (ii) the cuff is opened by pulling the cuff edges apart with sutures pre-installed through the closing tubes, allowing the nerve to carefully drop into the cuff, (iii) the elastic properties of the silicone cuff close the cuff, the opening sutures are removed, and the closing tubes are aligned, and (iv) a baton-shaped closing member is inserted through the set of interdigitated closing tubes, locking the cuff and fixing its circumference (Kallesøe et al., 1996).

All device leadout wires were routed to a common percutaneous exit point and attached to a specially designed backpack containing a printed circuit board and a 40-pin connector. The backpack was sutured to the back of the cat using sutures (No. 5 Ethibond) which were passed through skin and fascia and deeply around the L1-L2 and L4-L5 intervertebral ligaments. As some local infection problems were encountered in the early implants, in the second series of implants the backpack sutures were encased in silicone tubing (Dow Corning, Model 602-205). This reduced wicking of foreign materials into the body and subsequent tissue reaction. The backpack was covered with a contoured aluminum cover that restricted access to the device wires. In the second series, a fabric band encircled the belly and this further reduced access and damage to the wires. In clinical human experiments, it is expected that voluntary pulling and breaking of device wires will not be a problem.

2.3.3. Receptive Field Recording Protocols

The receptive fields of the instrumented cutaneous nerves were routinely examined following surgery to verify that the nerves remained viable and that afferent activity could be recorded in the distal cuffs during palpation of the skin in the paw. The ENG signals were amplified ($x10^5$; Leaf Electronics Ltd., Model QT-5A; Bak Electronics Inc., Model MDA-1), bandpass filtered (500-10kHz, Bak Electronics Inc., Model MDA-1) and fed into a Paynter Filter (Bak Electronics Inc., Model PF-1) that provided a rectified, smoothed envelope of the input signal. Both the raw cuff signal and the envelope were displayed on an oscilloscope. As the frequencies of the afferent signals occur in the audible range, an amplifier and speaker were used for auditory monitoring of afferent activity during palpation of cutaneous fields.

2.3.4. Compound Action Potential Recording Protocols

Under halothane gas anesthesia, the condition of the nerves and implanted cuffs was periodically monitored by stimulating through the proximal nerve cuffs and recording the evoked compound action potentials (CAPs) resulting in the distal cuffs. The peak-peak amplitude of the CAP and the latency or conduction time between cuffs were measured, both of which were indicative of the health of the instrumented nerve and stability of the nerve-cuff interface (Davis et al., 1978). During each recording session the temperature in the limb was monitored and maintained between 33 and 37°C through the use of a heated table and a radiant heat lamp. The CAPs in each of the 14 cats were followed for at least 180 days, with a longest implant period of 300 days.

The impedances of the four tripolar cuffs were monitored using an Electrode Impedance Tester (Bak Electronics Inc., model Imp-1, at 1 kHz) periodically over the duration of the chronic studies. The impedance between the centre and outer electrodes indicated the condition of cuff electrodes and determined the stimulation currents required to recruit nerve fibers, as well as the amplitude of the neural signals recorded with the cuff electrodes (Stein et al., 1978; Hoffer et al., 1981).

During stimulation, biphasic charge-balanced waveforms were generated with a pulse generator (Bak Electronics Inc., Model BPG-2) which controlled a constant current stimulator. The first pulse was negative with the amplitude determined by the constant current generator and a 50 μs pulse width. The second pulse was positive and was one-tenth the amplitude and ten times the duration of the negative pulse which was insufficient for stimulation but assured charge balancing (Mortimer, 1981). The waveform was applied to the centre electrode of the tripolar stimulation cuff using the outer electrodes as the reference. The typical stimulus repetition rate was 1 Hz.

Evoked CAP signals were measured at the centre electrode of the recording cuff using the two outer electrodes as reference. The signals were amplified (typically by 10^3 - 10^4) using low-noise

preamplifiers (Leaf Electronics Ltd., Model QT-5A) and amplifiers (Bak Electronics Inc., Model MDA-1). A 20 channel FM tape recorder (Honeywell, Model 96; 10 kHz/channel) was used to record all of the CAP signals, as well as evoked EMG signals from the instrumented muscles, a stimulus synchronization signal, a stimulus intensity signal, and a time code signal (Datum Time Code Generator, Model 9300).

The electrical threshold of the nerve was determined by increasing the stimulation intensity until a small CAP could be detected from the distal cuff. The supramaximal stimulation intensity was then determined by increasing the intensity until the CAP at the distal cuff reached its maximum amplitude. Threshold currents were typically between 100 and 300 μA and supramaximal stimulation currents were typically less than 2 mA.

Figure 2.4 shows as an example the triphasic neural CAP recorded from cat NIH-2 at the distal ulnar nerve cuff. The neural CAP began just before 1 ms, and the EMG pickup signal caused by muscle activity evoked by stimulation began after 2 ms. The EMG signal normally began at longer latency than the nerve CAP but it could distort the second positive peak of the CAP or even the negative peak, depending on the cuff location in the distal forelimb and its distance to the surrounding muscles. The conduction latencies and amplitudes of maximum positive and negative peak values of the ENG and EMG components of the CAP were monitored and approximately 25 stimulations of the supramaximal CAP were recorded on FM tape for later analysis. The actual signal amplitudes were determined from the calibrated amplifier gains.

Changes in the EMG pickup amplitude and in the ENG-to-EMG signal-to-noise ratio over the duration of the study give an indication of changes in EMG rejection by the recording cuff and its possible causes, e.g., gradual opening of the cuff and connective tissue invasion. The EMG pickup in the distal cuff on the other cuffed, non-stimulated nerve was also recorded during stimulation, to monitor the EMG pickup/rejection properties in a cuff placed on a non-stimulated nerve.

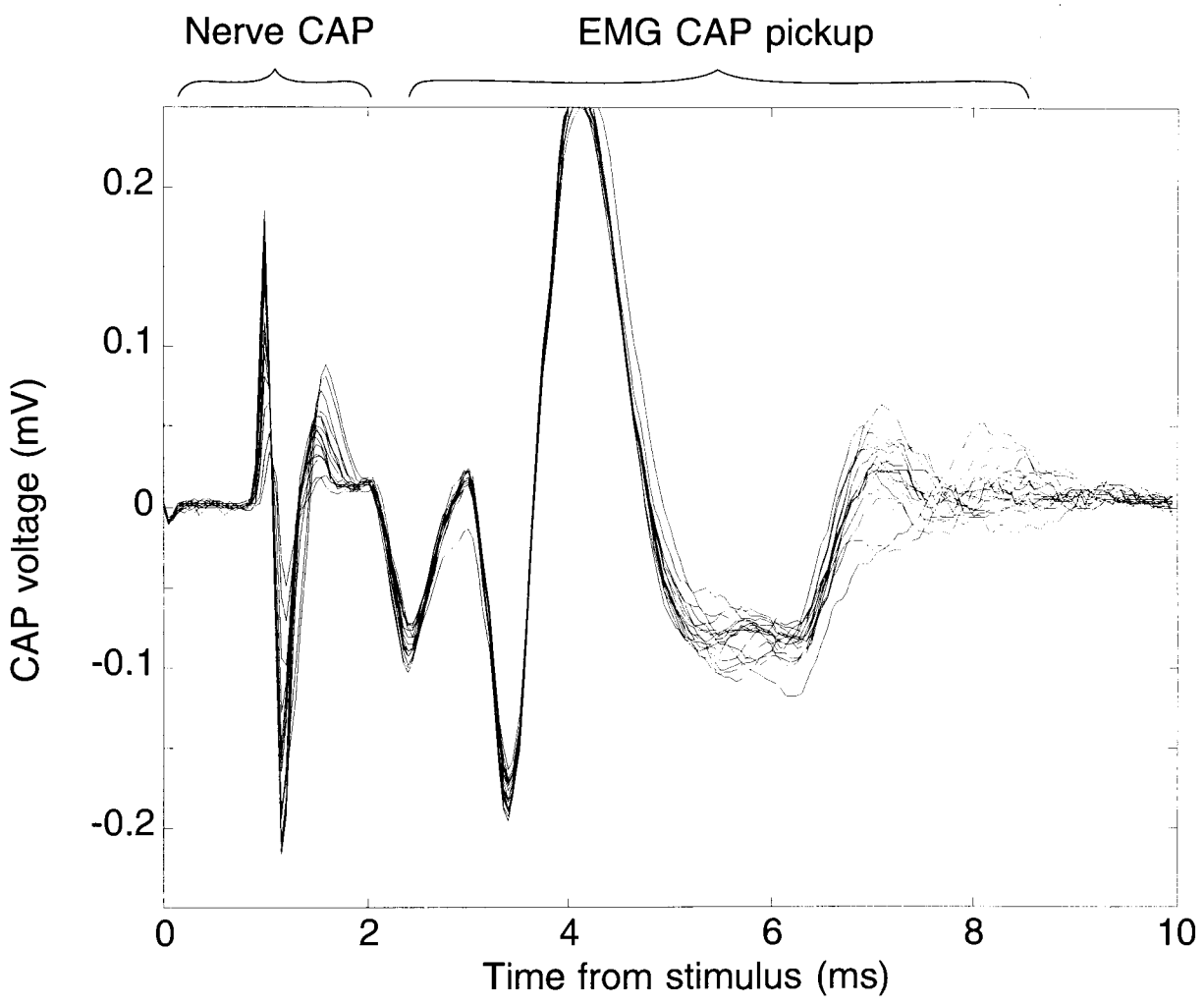

Figure 2.4: Compound action potential (CAP) recorded in the distal Ulnar nerve cuff of NIH-2. The nerve CAP and EMG CAP are of comparable amplitude, but the EMG CAP has a longer latency due to slower conduction velocity through muscle. This figure shows the superposition of approximately 20 consecutive recorded CAPs from the Ulnar nerve.

As a check during each recording session, we repeated the stimulation procedure but reversed the roles of the cuffs, i.e., stimulated the distal cuff and recorded the CAP in the proximal cuff. The CAP signal recorded at the proximal cuff was, predictably, smaller in amplitude and essentially free of EMG contamination. The proximal nerve CAP verified conduction times between the proximal and distal cuffs if there was uncertainty concerning EMG contamination of the distal CAP.

2.3.5. Data Analysis Protocols

Impedance, CAP amplitude and conduction latency (to the first positive peak of the CAP) data were processed using Excel (Microsoft Corporation). The gains used during each CAP recording session were accounted for and the data were interpolated to 30 day intervals in order to compare results from each of the implanted cats over a 180 day period. Impedance and CAP data with anomalies that were obviously caused by pulled or broken wires were removed from the data set.

To compare the data from all 14 implanted cats, the CAP data for each nerve were normalized with respect to the original CAP amplitude and conduction latency recorded on the day of surgery. Geometric means of the CAP data from the two series of implants were calculated to summarize the stability of all instrumented cutaneous nerves that were monitored for at least 180 days.

2.3.6. Final Surgery

All implanted devices were explanted at the end of the experiment, and the nerve cuffs were inspected for connective tissue growth into and around the cuffs and any evidence of electrode

breakdown. The closing mechanisms of the two cuff designs were evaluated in terms of connective tissue growth around the cuff and local tissue reactions. The distance between stimulating and recording cuffs was measured and used to calibrate the conduction velocity of the CAPs, and control and experimental nerve samples were taken to histologically evaluate any resulting nerve damage.

2.4. RESULTS

2.4.1. Compound Action Potentials: Results of first series of implants

Table 2.1 presents a summary of the first series of 16 nerves implanted in 8 cats, including the total days implanted for each cat, any observed mechanical problems with the implanted cuffs, and an evaluation of the nerve CAPs on the last recording day. The final nerve CAP amplitudes are reported as a percentage of the initial CAP amplitudes recorded on day 0, giving a quantitative indication of the CAP stability and the nerve-cuff integrity over the entire implant period.

In the first series there were several instances of pulled wires that caused the early termination of some experiments (see below). A total of 9 nerves out of the 16 implanted reached the milestone of 180 days (56%; shown in grey in Table 2.1). The Median nerve cuffs in NIH-1 were removed on day 7 following clear evidence of severe nerve compression. The average duration of the implants that lasted the full term (n = 9) was 193 days and the average distal nerve CAP amplitude on the final day of recording was 69% of the average day 0 amplitude.

For 5 other nerves in 4 cats in the first series, the cuff wires were snagged by the cats at their skin-connector interface and broken prior to day 180. The Median nerve of NIH-5 was included in spite of wire breakage after day 180, given the stability of the CAP amplitude documented up to

Table 2.1: Summary of first series of eight implants, showing total days implanted, any observed device problems including pulled and broken wires, and final distal CAP amplitude as a percent of the amplitude recorded on the day of surgery. Nerves that were recorded from for at least 180 days are shaded.

Subject	**Total Days implanted**	**Problems with Implanted Cuffs**		**Final Distal Nerve CAP Amplitude**	
		Ulnar	**Median**	**Ulnar**	**Median**
				% day 0, last day	% day 0, last day
NIH-1	101	prox wires broken after day 63	Cuff leads were too short. Cuffs removed on day 7	51%, 63	N/A
NIH-2	212			73%, 212	90%, 212
NIH-3	202			117%, 202	24%, 202
NIH-4	189		prox wires broken after day 75	71%, 189	100%, 29
NIH-5	203	prox wires broken on day 135	prox wires broken on day 182	131%, 132	100%, 160
NIH-6	190			84%, 190	56%, 190
NIH-7	204	prox and dist wires broken on day 151	prox wires broken on day 39, cuffs removed on day 71	90%, 142	173%, 33
NIH-8	180			5%, 180	14%, 94

day 160. Only one nerve showed a severe decline in CAP amplitude that could not be attributed to a wire pull problem: the Median nerve on NIH-8. A subclinical infection affecting the distal portions of both Median and Ulnar nerves was the presumed cause for the observed decline in signal amplitude.

2.4.2. Compound Action Potentials: Results of second series of implants

In the second series of 12 nerves implanted in 6 cats there were four incidences of cuff related problems: one involved nerve compression, one cuff had electrodes that deteriorated, and two involved pulled or broken wires, as detailed in Table 2.2.

In NIH-9 the proximal Median cuff was too tight and induced a compression injury that caused a rapid, large decline in CAP amplitude. It was removed on day 35, a larger diameter replacement cuff was implanted in its place, and by the end of the 300-day implant period, the nerve CAP recovered to 100% of the amplitude on day 0.

In NIH-11, the proximal Median cuff showed a large increase in impedance after 180 days and it was no longer possible to either record from or stimulate the nerve. During the final acute on NIH-11, the wires to the proximal Median cuff were observed to have broken approximately 0.5 cm from the cuff. We speculate that the cable was likely subjected to excessive movement or bending at that point and the wires broke due to metal fatigue.

The final section of Table 2.2 details the final CAP amplitudes for all implanted nerves. Boxes shaded in grey represent instrumented nerves that gave successful recordings for at least 180 days (11 out of 12, or 92%). The average duration of successful implants until voluntary termination was 251 days. The average (n = 11) distal nerve CAP amplitude on the final day of recording was 86% of the average amplitude at day 0.

Table 2.2: Summary of second series of six implants, showing total days implanted, any observed device problems including pulled and broken wires, and final distal CAP amplitude as a percent of the amplitude recorded on the day of surgery. Nerves that were recorded from for at least 180 days are shaded.

Subject	**Total Days Imp.**	**Problems with Implanted Cuffs** Median	Ulnar	Radial	**Final Nerve CAP Amplitude** Median %, last day	Ulnar %, last day	Radial %, last day
NIH-9	300	prox cuff replaced on day 35 due to nerve injury			100%, 300	76%, 300	
NIH-10	204				108%, 204	117%, 204	
NIH-11	281	large increase in prox cuff impedance after day 180			116%, 180	23%, 281	
NIH-12	289			prox wires broken after day 75	31%, 289		prox wires broken after day 75 106%, 75
NIH-13	180					87%, 180	89%, 180
NIH-14	254			dist wires broken on day 199		130%, 254	70%, 191

Figure 2.5 shows the normalized amplitudes and conduction latencies of CAP recordings in the second series of implants. Each of the 11 data traces (the wires to the proximal Radial nerve cuff in one cat were broken after day 75, see Table 2) is interpolated to 30 day intervals from the original recording days, which occured approximately every two weeks and continued for at least 180 days.

In Fig. 2.5A, the normalized CAP amplitude data show variability in the first 90 days followed by considerable stability in the final 90 days. This is consistent with early connective tissue growth around and inside the cuffs and subsequent stabilization of the cuff impedances (Stein et al., 1978). In Fig. 2.5B, the normalized latency data, which indicate the condition of the largest, fastest conducting fibres in the nerve, show a high degree of stability throughout the entire implant period. Figure 2.5 suggests that the population of largest fibres may show some partial decline after the nerve is implanted, as evidenced by decreasing CAP amplitudes, but the constancy in conduction latency indicates that at least some of the largest axons remained unaffected.

The Median nerve in NIH-9, believed to have suffered a compression injury, is represented by the small squares in Fig. 2.5A. Its CAP amplitude showed a drastic decline in the first 30 days and a slow recovery up to day 180. The proximal Median cuff in NIH-9 was replaced with a larger diameter cuff on day 35 and this allowed the nerve to gradually recover over the remainder of the implant period. This animal was followed for a total of 300 days and recordings after day 180 showed further recovery, such that the CAP amplitude reached 100% at day 300 as shown in Table 2.2. This trend was mirrored in the latency data of Fig. 2.5B which showed an increase in latency in the first month and then a slow improvement to original levels at the end of the implant period.

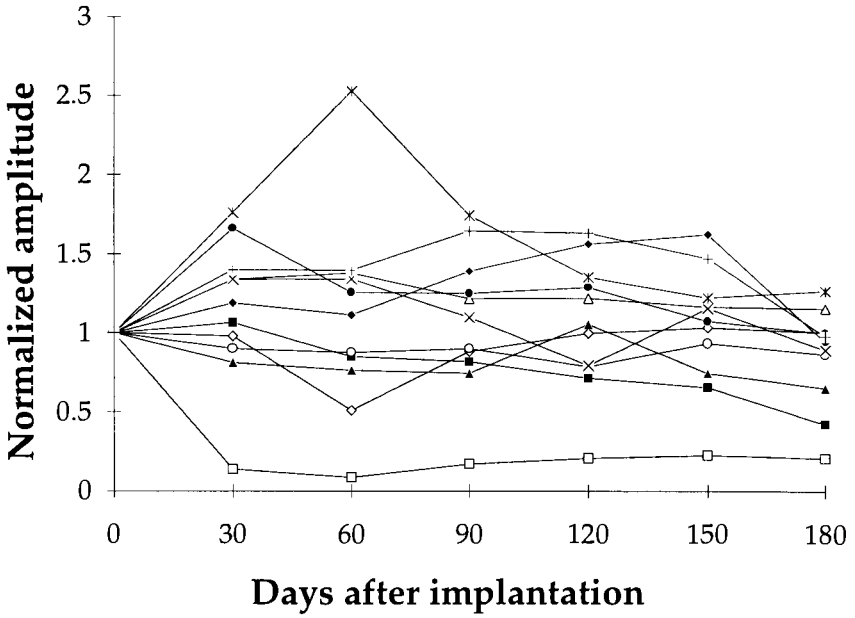

A

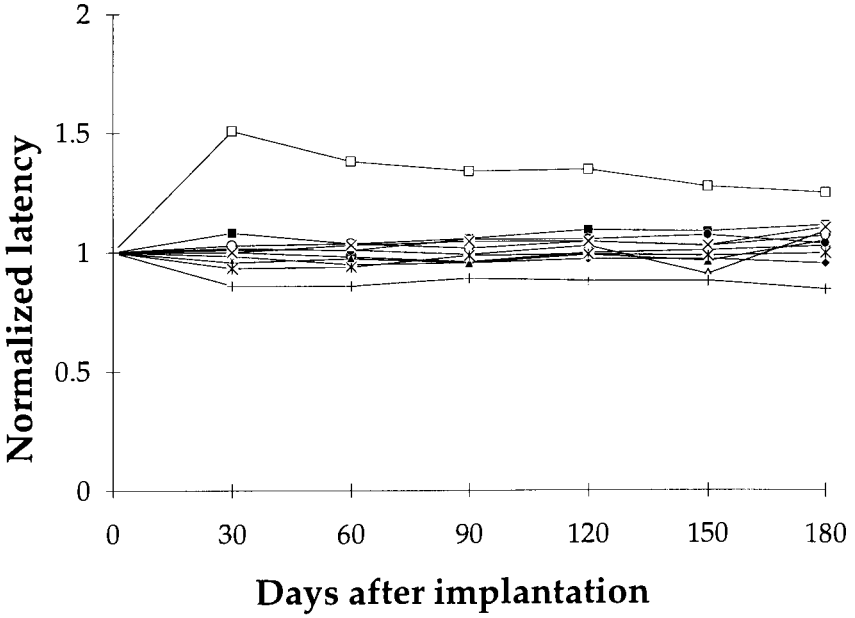

B

Figure 2.5: A. Normalized peak-to-peak amplitudes and B. conduction latencies of CAPs recorded from the second series of implants over 180 days. Data from original recording days have been interpolated to 30 day intervals. Data is from Median, Ulnar, and Radial nerves from cats 9 - 14 (n = 11, shaded in Table 2.2).

Figure 2.6 presents the geometric means of the CAP amplitude and latency data from the second series of six implants (NIH 9-14; n = 10) after the data representing the Median nerve in NIH-9, which suffered a compression injury, was removed from the data set.

In the ten unaffected nerves in the second series shown in Fig. 2.6, the geometric mean of the CAP amplitude was very stable, with a final amplitude of 88% (±27%) of day 0, and a maximum standard deviation of 50% (at day 60). As expected from Fig. 2.5B, the mean conduction latency showed an even higher degree of stability, with a final latency of 103% (±8%) of day 0, and a maximum standard deviation of 8% (at day 180).

By comparison, in the nine unaffected nerves of the first series (see Table 2.1), the geometric mean of the CAP amplitude was less stable, with a lower final amplitude of 67% (±73%) of day 0 and a larger maximum standard deviation of 69% (at day 90). Similarly, the average conduction latency showed lower stability, with a final latency of 107% (±28%) of day 0 and a maximum standard deviation of 34% (at day 150).

2.4.3. Recording Cuff Impedances

Figure 2.7 shows the geometric means of distal cuff impedances for the first (n=14, out of 16 implanted) and second (n=10, out of 12 implanted) series of implants respectively. Anomalous distal cuff impedance values that occurred after observed instances of pulled wires were removed. Impedance data for patch electrodes implanted on two Radial nerves in the second series were omitted from this analysis in order to compare only cuff electrodes.

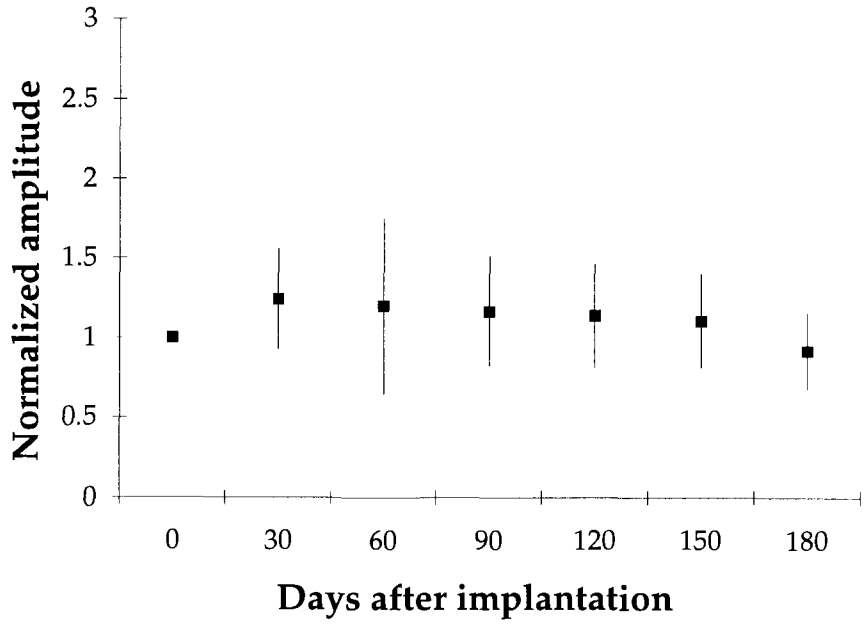

A

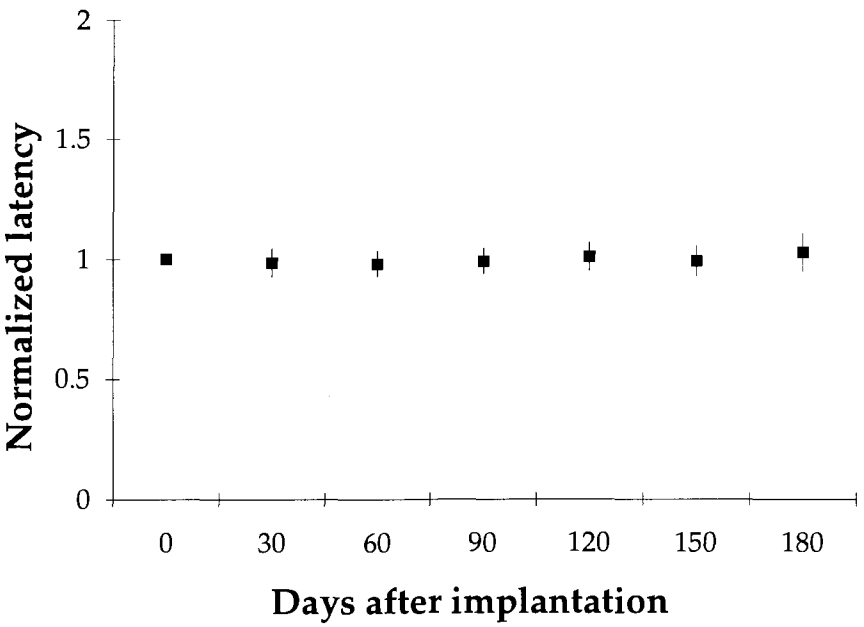

B

Figure 2.6: A. Geometric mean of normalized CAP amplitudes and B. CAP conduction latencies over 180 days, with error bars representing ±1SD. Data from original recording days have been interpolated to 30 day intervals. Data is from Median, Ulnar, and Radial nerves from cats 9 - 14 (n = 10, shaded in Table 2.2 minus NIH-9 Median).

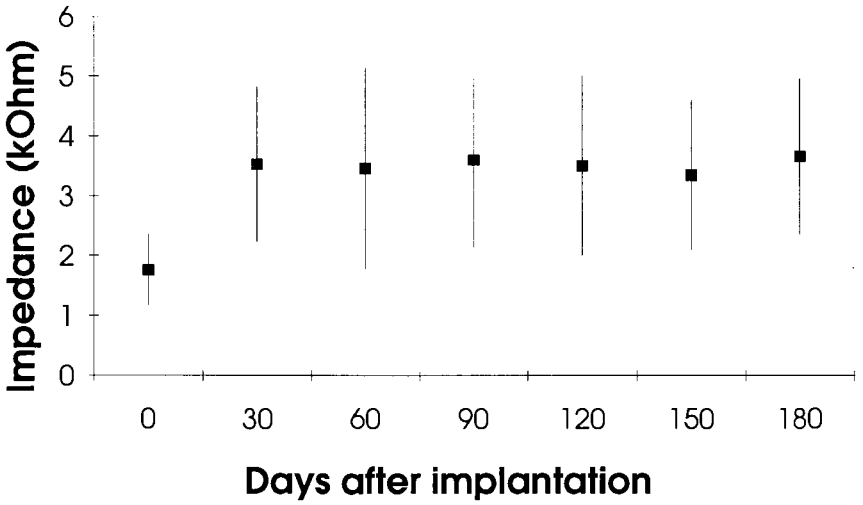

A

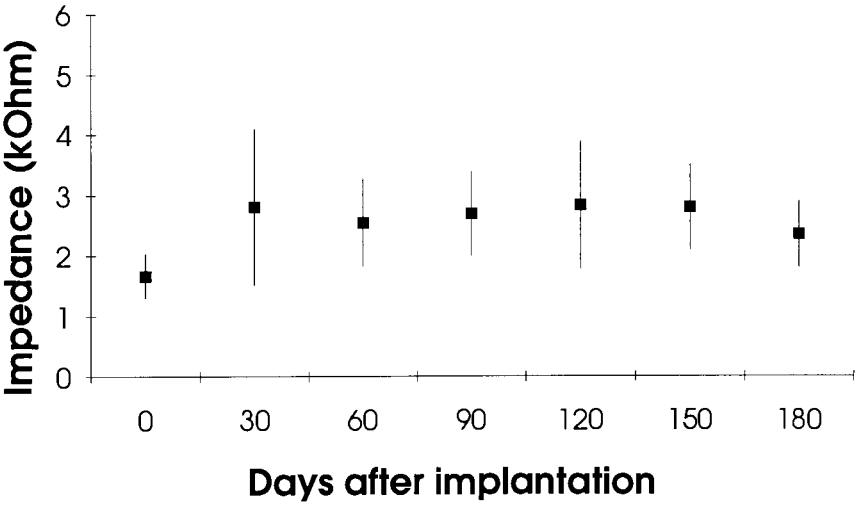

B

Figure 2.7: A. Geometric mean of distal nerve cuff impedances from first series of implants over 180 days (data is from cats 2 - 7; n = 14) and B. from second series of implants over 180 days (data is from cats 9 - 14; n = 10). Error bars represent ±1SD.

The data from both series of implants exhibited a characteristic increase in impedance in the first 30 days and then reached a steady-state, as expected from previous studies (Stein et al., 1978). The data also show that cuffs used in the second series of implants which implemented the new closing technique exhibited lower overall and more stable impedances than the suture-type cuffs used in the first series.

2.4.4. Survival of Other Implanted Electrodes

While the cuffs implanted on distal nerves generally displayed excellent electrical and mechanical stability in implants up to 300 days, particularly in the second series, other implanted devices did not survive equally well the long term chronic implants. The shorter, larger diameter stimulation cuffs implanted in proximal locations above the elbow in all six cats of the second series exhibited poor recording qualities, large impedance increases, and required progressively larger currents (5-10 mA) to stimulate the nerves. In some cats the proximal cuff electrode wires were degraded and could no longer be used to stimulate after some time (e.g. NIH-11).

In addition, many of the intramuscular EMG electrodes implanted in the forelimb muscles broke down with repetitive movement after implant periods of a few months, indicating that the 631 Cooner wire used to manufacture the EMG electrodes was not suitable for long term chronic intramuscular implants.

2.5. DISCUSSION

In this study comprising 14 implanted cats, the viability of the instrumented nerves and the status of the nerve cuffs were monitored for periods of at least six months. Compound action potentials (CAPs) and electrode impedances were followed throughout the implant period. Both indicators demonstrated stability of the nerve interface after a period of two to four weeks as connective tissue grew in and around the nerve cuffs (Stein et al., 1980). In the implant that was followed for the longest period (NIH-9), the signals were stable for up to 300 days and demonstrated a full recovery of the CAP in the Median nerve following an initial compression injury.

The CAP recording technique proved to be an accurate and valuable indicator of the viability of the nerves and the CAP data were used to calibrate neural recordings during voluntary tasks such as walking on a treadmill (Strange and Hoffer, 1996). The CAP amplitudes in the second series of implants exhibited improved stability, with a higher mean at 180 days of 88% (±27%) of the amplitude on the day of implantation. The low standard deviation of the CAP amplitudes indicated that the population of large axons in most of the instrumented nerves were essentially unaffected by the implant procedure.

In those nerves that experienced a decline in amplitude as a result of compression injury or pulled wires, a particular point of interest from the CAP data is the differential changes in amplitude and latency. The peak-to-peak CAP amplitude typically declined in these situations, sometimes quite drastically, although the minimum conduction latency increased only marginally. Compression injuries normally affect larger fibres first (Sunderland, 1968). A hypothesis to explain these observations is that only some of the large fibres in the nerve were affected by compression, accounting for a decrease in CAP amplitude (especially the first peak in the CAP which is determined by the largest fibres in the nerve), but other large fibres remained unaffected and continued to conduct at near normal velocities. These observations suggest that the CAP

amplitude is a more valid indicator than minimum conduction latency to monitor the status of chronically instrumented nerves.

The impedances of the implanted nerve cuffs showed that the devices were quite stable, following an increase in impedance in the first four weeks after implantation, similar to earlier studies (Stein et al., 1978). The nerve cuffs in the second series exhibited lower overall impedances and a higher degree of stability throughout the implant period, due to shorting the reference electrodes together at the cuff, implementing a new closing technique for the nerve cuffs, and fewer instances of pulled wires.

The results from this study of 28 implanted recording nerve cuffs and patch electrodes in the forelimbs of 14 cats suggest that recording nerve cuffs can be left implanted in unrestrained cats for periods of at least six months without inflicting significant damage to the large axons in nerves and without experiencing mechanical or electrical breakdown. Several conditions are necessary for successful chronic instrumentation of peripheral nerves with recording nerve cuffs: 1) the implantable devices must be designed to be physically compatible with the nerve and surrounding tissues, 2) care must be taken when surgically accessing and manipulating the nerve and installing the cuff, and 3) provisions must be taken to prevent pulling and breaking of wires. In the second series of implants, the second and third conditions were better met by the improved cuff closing technique which required less manipulation of the nerve, and by the use of coated backpack sutures which reduced the possibility of local infections and irritation at the backpack and a fabric band around the backpack which restricted access to the backpack connector and device lead wires exiting the body.

Improved design features of the recording nerve cuffs used in the second series of implants included connecting the outside reference electrodes together at the cuff, thus reducing the impedance of the device and the number of lead wires to the device to two, and fixing the diameter of the implanted nerve cuffs by holding the cuff edges together with the new closing technique

(Kallesøe et al., 1996). Holding the cuff closed and fixing its circumference eliminates the possibility of the cuff opening and providing a shunt from the inside of the cuff to extracellular fluid, which would markedly reduce the recording capabilities of the cuff. By hermetically sealing the cuff, the recording characteristics of the device are ensured provided that the nerve remains healthy and the electrodes do not break down. The new cuff design eliminates the need for sutures to be tied around the cuff to keep the cuff closed (Hoffer, 1990). Sutures, even non-absorbable versions, can initiate local tissue reactions and cannot prevent the edges of the cuff from slipping past one another allowing the cuff to spiral in on itself and compressing the nerve, a type of failure that has been observed in previous studies (Stein et al., 1980). The new cuff closing mechanism prevents these failure modes by pulling the edges together and fixing the circumference of the cuff.

The present study supports and expands on previous findings that, by implanting nerve cuffs whose inside diameters are 20% larger than the nerve diameters and fixing the cuff circumference, stable nerve interfaces are achievable with little or no damage to the instrumented nerves (Hoffer, 1990).

The main drawback of the current cuff electrodes are the lead wires. The main improvement that is desirable for successful clinical systems implementing recording nerve cuffs will be to utilize telemetry. This will avoid the use of wires that can pull on the cuffs or break inside the body or at percutaneous connectors and will minimize mechanical loading of the instrumented nerves and nerve trauma.

Chapter 3:

Sensory signals from cat paw receptors during walking: applicability as controller feedback for FES

Summary

In this study we recorded natural sensory nerve signals of primarily cutaneous origin in the forelimbs of cats during walking on a motorized treadmill, using chronically implanted nerve cuff or patch electrodes on the Median, Ulnar, and Radial nerves. EMG activity from four forelimb muscles, Palmaris Longus, Flexor Carpi Ulnaris, Extensor Carpi Ulnaris, and Abductor Pollicis Longus, was also recorded during walking to correlate sensory ENG activity with EMG activity during the step cycle. Features in the ENGs that were related to paw contact and lift-off were detected by a finite state controller model and used to predict the timing of the activity of a forelimb muscle for a variety of walking conditions. The accuracy with which EMG timing information could be predicted from the cutaneous ENG signals recorded during walking suggests that natural sensory signals may be implemented as a source of feedback for closed-loop control of functional electrical stimulation (FES).

3.1. INTRODUCTION

A necessity for strategies for closed-loop control of functional electrical stimulation (FES) of paralyzed muscles has developed in the last decade based on investigations of natural control systems (Stein, 1992) and the results of clinical applications of FES (Hambrecht, 1992). Neural signals generated by natural sensors in the extremities may be recorded with nerve cuff electrodes and used to extract contact, force, and position information useful for closed-loop control of FES (Hoffer, 1988; Hoffer and Haugland, 1992; Hoffer et al., 1996).

In a companion study, we investigated the long-term stability of chronic recording nerve cuff signals by recording evoked compound action potentials (Strange et al., 1996, submitted concurrently). We showed that nerve signals recorded with cuff electrodes remained very stable over periods of six months and longer.

Recently, a clinical trial of a closed-loop functional electrical stimulation (FES) system to correct for drop-foot in a stroke patient implemented the use of cutaneous activity recorded from the Sural nerve with a chronically implanted nerve cuff as a feedback source (Sinkjær et al., 1992; Haugland and Sinkjær, 1995). In that application the sensory nerve information was used as a simple switch to trigger the end of stimulation of foot dorsiflexor muscles at foot contact. That study confirmed that there is a need to identify reliable sources of neural control signals and extract features, such as ground contact and slip information, that may be applied in closed-loop FES systems for restoring voluntary use of paralyzed muscles in humans, in particular for the upper limb (Popovic et al. 1993; Haugland and Hoffer, 1994).

In this study we examined the feasibility of extracting electroneurogram (ENG) features from chronic nerve cuff recordings from sensory nerves in the cat forelimb. We present data recorded from chronically implanted cats during walking on a level treadmill at a single speed. Features of

the ENGs that correspond with external events such as paw contact and lift-off may be used to replicate natural electromyogram (EMG) patterns in a closed-loop FES system. A model of an FES state controller is presented that predicts the timing of muscle activity based on ENG signals recorded from the cat forelimb during walking.

Preliminary aspects of this research have been published in abstract form (Strange and Hoffer, 1995a; Strange and Hoffer, 1995b).

3.2. BACKGROUND

3.2.1. Cat Forelimb as Model of Human Limb

We selected the forelimb of the cat as an experimental model in which to investigate the feasibility of extracting sensory ENG information during a voluntary task and to examine the applicability of such sensory information for closed-loop control of FES. The selection criteria included sensory nerve dimensions comparable to human forearm and hand nerves, surgical accessibility of nerves and muscles in the animal, and ease of trainability of the animals for stereotyped motor tasks.

3.2.2. Anatomy and Physiology

The anatomy and physiology of the cutaneous nerves in the forelimb of the cat were discussed in detail in a companion paper (Strange et al., 1996, in preparation). Briefly, the receptor field of the Median nerve includes the glabrous skin pads on the I (thumb), II, III, and IV digits as well as the main centre pad of the paw, the Ulnar nerve innervates the glabrous skin pads on the I, IV and V

digits, and the Superficial Radial nerve branches innervate mechano- and hair receptors in the dorsal surface of the paw and digits. The pattern of innervation of cutaneous fields normally show some variation from cat to cat as well as some overlapping of cutaneous receptor fields for the three main cutaneous nerves in the forelimb.

Two sets of antagonist muscle pairs were selected for instrumentation in this study, based on muscle function during movement and surgical accessibility of each muscle and an antagonist. The first pair consisted of Flexor Carpi Ulnaris (FCU) and Extensor Carpi Ulnaris (ECU), and the second pair included Palmaris Longus (PalL) and Abductor Pollicis Longus (APL). Figure 3.1 illustrates the locations of the four muscles in the forelimb of the cat.

The FCU is a superficial muscle innervated by the Ulnar nerve and inserts on the ulnar portion of the wrist, producing paw flexion and adduction movements. The ECU is also superficial and also innervated by the Ulnar nerve but inserts on the lateral side of the V digit and produces extension and adduction movements.

The PalL and APL form a less specific antagonist pair. The PalL is a large superficial muscle innervated by the Median nerve whose tendon inserts on all of the digits in the paw, producing paw and digit flexion. The APL is a deep extensor muscle whose tendon crosses the radial side of the wrist and inserts on the I digit, extending the paw and abducting the I digit.

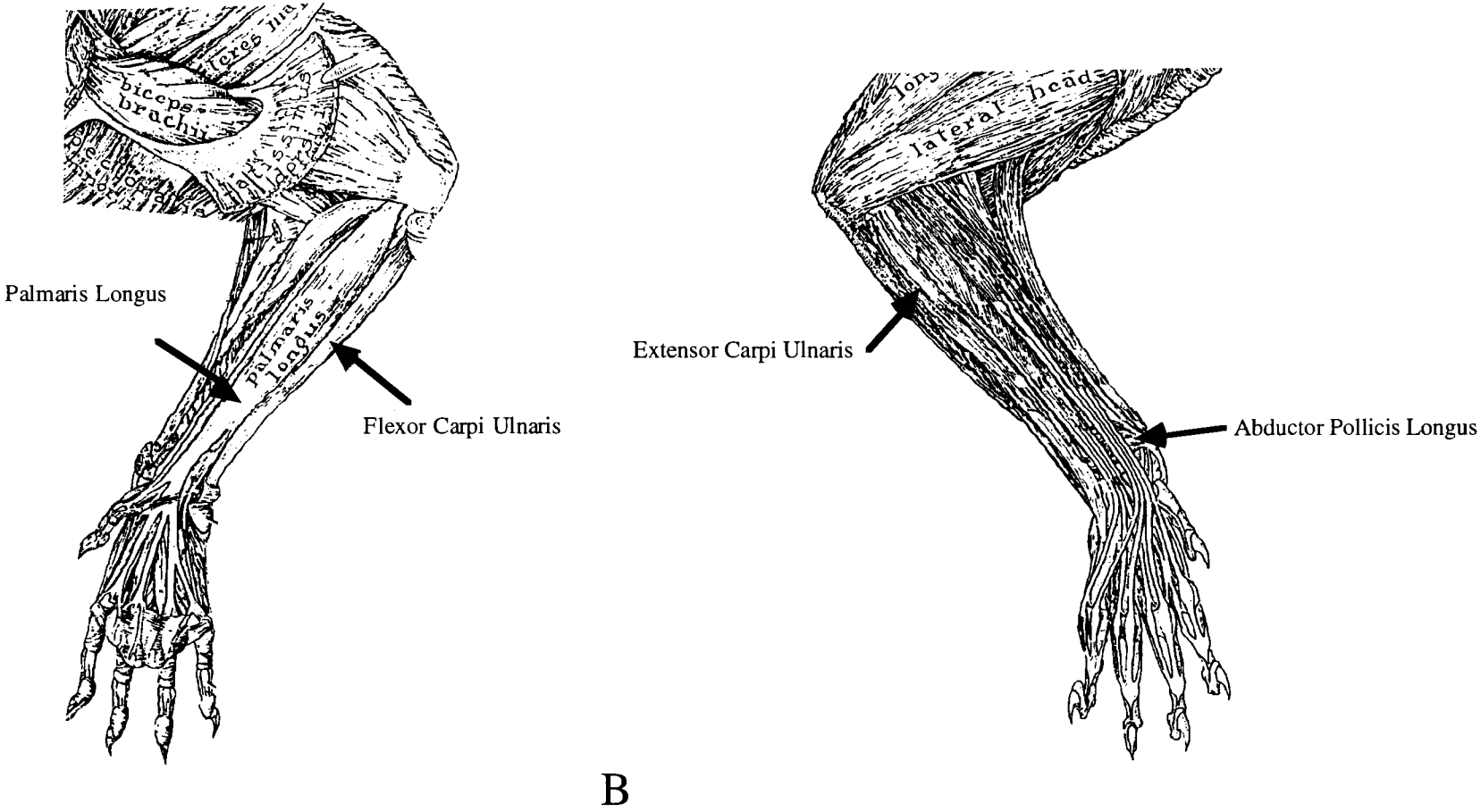

Figure 3.1: A. Medial view of superficial flexor muscles in the cat right forelimb, showing locations of Palmaris Longus and Flexor Carpi Ulnaris. B. Lateral view of superficial extensor muscles in the cat right forelimb, showing locations of Extensor Carpi Ulnaris and Abductor Pollicis Longus (Crouch, 1969).

3.3. METHODS

3.3.1. Anesthesia and Analgesia Protocols

Halothane gas anesthesia was used during the implant surgery for each cat which normally lasted 10 to 12 hours. A premedication dose of intramuscular ketamine/acepromazine/atropine followed by intravenous ketamine/valium was administered prior to anesthesia. Expired CO2 concentration, respiration rate and heart rate were continuously monitored. A post-operative analgesic (torbugesic or temgesic) was administered prior to the end of the anesthetic and maintained for 24 hours. Derapen or Cefadrops antibiotics were given daily for seven days following the implant surgery.

Our surgical and experimental protocols met the guidelines set by the Canadian Council of Animal Care and were approved by the University Animal Ethics Committee. All anesthesia and analgesia protocols were performed by a certified veterinary technician.

3.3.2. Implanted Devices and Transducers

Two tripolar nerve cuffs were implanted on each of two nerves in the left forelimb of each of six cats, instrumenting two of the Ulnar, Median, and/or Radial nerves. The first three cats were instrumented on the Ulnar and Median nerves, the fourth on the Median and Radial nerves, and the final two on the Ulnar and Radial nerves.

The placement of each implanted cuff depended on the local anatomy in the forelimb including available free length along the nerve which could be dissected without compromising nerve branches or blood supply. Each nerve was instrumented with a proximal stimulating cuff above the elbow, and a distal recording cuff located below the elbow (Strange et al., 1996). The distal location of the recording cuffs ensured that ENG signals recorded in the awake cat primarily consisted of cutaneous sensory activity and contained little efferent activity. Stimulation of the implanted distal cuffs resulted confirmed the sensory nature of the cutaneous nerve locations.

The recording nerve cuffs implanted in this study were manufactured from a segment of silicone tubing, typically 2.0 to 2.5 mm I.D. (Hoffer, 1990). Three de-insulated wires (AS 631 Teflon-coated Cooner wire) were sewn into the cuff wall to provide three near-circumferential electrical contacts with the nerve. During recording, the middle electrode provided the signal while the outer two electrodes were connected together at the cuff as a reference. The nerve cuff closing mechanism (Kallesøe et al., 1996) and implant procedure are detailed in a companion paper (Strange et al., 1996). Recording cuffs were typically 15 or 20 mm in length, depending on available free length in the forelimb, which provided a length to inside diameter ratio of typically 7.5 to 10, necessary for nerve cuff recordings (Hoffer, 1990). A patch ENG electrode (10 X 30 mm) was used on the Radial nerve in the final two cats of this series instead of a recording cuff to take advantage of the superficial location of the nerve branches (Hoffer, 1990). The patch electrode covered the nerves and adjacent blood vessels and was sewn onto the inside surface of the skin.

The intramuscular EMG electrodes were fabricated from 631 Teflon-coated Cooner wire, with 5 to 7 mm insulation stripped and the bared end implanted in the muscle belly and held in place with a segment of 3-0 non-absorbable suture (Hoffer, 1990). Two intramuscular electrodes were implanted in the muscle belly, separated by 5 to 10 mm to provide differential EMG signals. A thermistor (Yellow Springs Instruments Inc., Model 44004, embedded in silicone tubing) was implanted above the elbow to monitor the limb temperature during recording under anesthesia.

All device leadout wires were routed to a common percutaneous exit point and attached to a specially designed backpack as detailed in a companion paper (Strange et al., 1996).

3.3.3. Awake Recordings on the Motorized Treadmill

Prior to the implant surgery, each animal was trained daily to walk at various speeds and slopes. During a recording session the cat was connected to the recording station via a ribbon cable passed through a slot at the top of the treadmill. Food rewards and positive reinforcement were used to ensure that the cat felt comfortable and walked with a steady gait near the front of the treadmill.

At the beginning of each recording session, the impedances of all implanted devices were measured and compared to previous recording sessions under anesthesia to verify that the devices had stable properties (Strange et al., 1996). The value of nerve cuff impedances affects the amplitude of the neural signals recorded with the cuff electrodes, thus making variability in impedance undesirable (Stein et al., 1978; Hoffer et al., 1981). Typical recording nerve cuff impedances were under 5 kΩ, measured at 1 kHz (Bak Electronics, Inc. Electrode Impedance Tester, Model Imp-1), and typical intramuscular EMG electrode impedances were 1 kΩ.

Each nerve cuff signal was amplified (typically by 10^4 - 10^5) using a low-noise preamplifier (Leaf Electronics Ltd., Model QT-5A, 65 Hz high pass-filter) and AC-amplifier (Bak Electronics Inc., Model MDA-1, 500 Hz - 10 kHz band-pass filter) and recorded on FM tape. The nerve cuff signals were also high-pass filtered (24 dB/octave, normally at 1 kHz; Ithaco 4302 Filter) with a gain of 1 or 10 and recorded on additional FM tape channels. The Ithaco filter cut-off frequency was determined for each recording nerve cuff in each session by comparing a Paynter filtered (Bak Instruments Inc., Model PF-1) envelope of the Ithaco output with EMG signals of muscles

surrounding the recording cuff and minimizing obvious correlation between the signals which was taken as an indication of excessive EMG pickup (Hoffer, 1990). In addition, the nerve cuff signals were amplified and played through a loudspeaker to assess the frequency content of the signal in reducing EMG contamination.

EMG signals were amplified (typically by 10^3) and filtered using a single amplifier (Bak Electronics Inc., Model MDA-2, 50 Hz - 1 kHz band-pass filter). A 20 channel FM tape recorder (Honeywell, Model 96; 10 kHz/channel) was used to record all of the physiological signals and a time code signal (Datum Time Code Generator, Model 9300).

The motions of the left forelimb were videotaped to correlate physiological data with discrete events and phases of the gait cycle during each recording session. The video screen display included the time code signal (Datum Time Code Generator, Model 9300) and on-line sampling of nerve cuff and EMG signals (Codas, Dataq Instruments, Inc.) were inserted in the video display to aid in analysis of recorded data.

3.3.4. Data Processing Protocols

Physiological signals were sampled from FM tape using DataSponge (Biosciences Analysis Software Ltd.), with sample rates of 10 kS/s and 1 kS/s for ENG and EMG signals respectively. The data were then imported into Matlab (The Math Works, Inc.) and digitally processed to produce figures for analysis. For each physiological signal, gains used during recording were removed to produce units of volts and dc components were removed. The signal was then rectified, bin-integrated to 10 ms bins (Haugland et al., 1994), and digitally smoothed by a balanced 3 point filter.

Model state controllers were designed in Matlab to predict the state of forelimb muscles, on or off, based on characteristics of the recorded ENG signals related to events in the step cycle. Hand-

crafted rules were developed to detect bursts of neural activity related to paw contact and lift-off and trigger the state transitions of the finite state machine. In FES state controller systems, natural sensory information from nerve cuffs may provide useful state information which can be used to control the timing of muscle stimulation (Haugland and Sinkjær, 1995).

3.4. RESULTS

3.4.1. ENG Activity Recorded During Walking

Figure 3.2 presents representative examples of ENG and EMG data recorded from cat NIH-9 walking on the treadmill on day 113 post-implant. The top two traces are the Ulnar and Median nerve cuff signals sampled at 10 kS/s, with peak amplitudes of ±15 and ±10 μV respectively. Both nerve signals showed systematic modulations with the step cycle and bursts of activity at paw contact, as shown on the bottom trace. Throughout the stance phase the two nerve signals displayed higher levels of activity, as expected when mechanoreceptors in the glabrous skin and paw firing were mechanically loaded. During the swing phase, the two nerves showed quieter periods of activity, as expected when the mechanoreceptors were largely unloaded. The Ulnar ENG peaked at paw contact and declined throughout stance, while the Median ENG peaked both at contact and at lift-off, indicating that the cutaneous nerves innervating the paw have a mixture of dynamic and static responses during the gait cycle.

The bottom four traces in Fig. 3.2 represent EMG data from the PalL, FCU, ECU, and APL respectively. The absolute amplitude of EMG recordings was dependent on distance between the electrodes and surgical placement of the electrodes with respect to the nerve entry point in the muscle. EMG signals from the paw plantar flexors PalL and FCU were highly modulated with

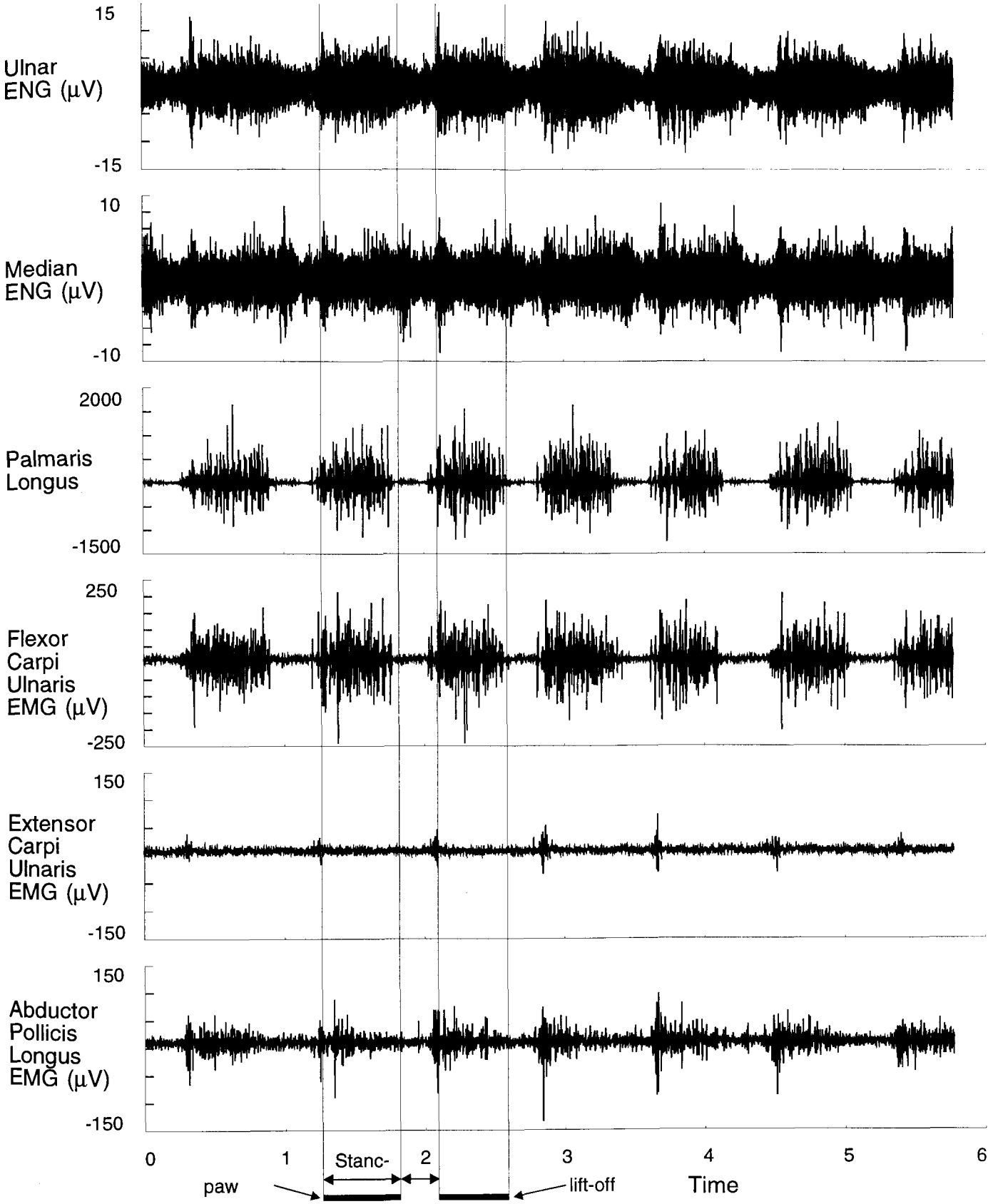

Figure 3.2: Physiological data recorded from NIH-9 (day 113 post implant) during walking on the level treadmill (0.5 m/s). All signals are shown in microvolts against a time scale of seconds. The top two traces show Ulnar and Median nerve ENG (sampled at 10 kS/s), and the bottom four traces show EMG activity from PalL, FCU, ECU, and APL respectively (sampled at 1 kS/s). Paw contact and lift-off are shown as light lines on the time scale, and the stance phase is signified by a heavy bar.

the step cycle, with large bursts of activity just prior to and during stance. The two extensors, ECU and APL, also showed modulations during the gait cycle, but at a much lower amplitude and only at paw contact, implying co-contraction of extensors to stiffen the wrist joint prior to load acceptance.

Figure 3.3 presents rectified, bin-integrated versions of the same data shown in Fig. 3.2. The trace order is the same as for Fig. 3.2, with the top two traces representing ENG signals and the bottom four representing EMG signals. The processed data show the trends as observed from the raw data, especially in terms of the Ulnar and Median ENG peaks at paw contact and Median ENG peaks at lift-off. The EMG data confirm that the plantar flexors were activated just prior to stance, and remained activated throughout stance until just prior to lift-off. The extensors showed little modulation during the step cycle other than brief bursts of activity prior to paw contact.

Figure 3.4 presents rectified, bin-integrated data recorded from another cat, NIH-14 on day 49. The top two traces show Ulnar and Radial nerve cuff signals, and the bottom four traces show EMG activity from PalL, FCU, ECU, and APL muscles respectively. The Ulnar ENG was modulated with the step cycle, with sharp bursts of activity at contact and phases of higher activity during stance. The Radial ENG also showed bursts of activity at foot contact, but showed even larger bursts of activity just following lift-off that resulted from paw extension at the beginning of the swing phase.

Figure 3.4 also shows that the EMG activity from the four implanted muscles was modulated with the step cycle. Once again, the two plantar flexors were highly modulated with greatest activity during the stance phase. The two extensors were also modulated with the step cycle, with the ECU showing activity that persisted during stance and APL showing bursts of activity during stance that could be highly variable from step to step.

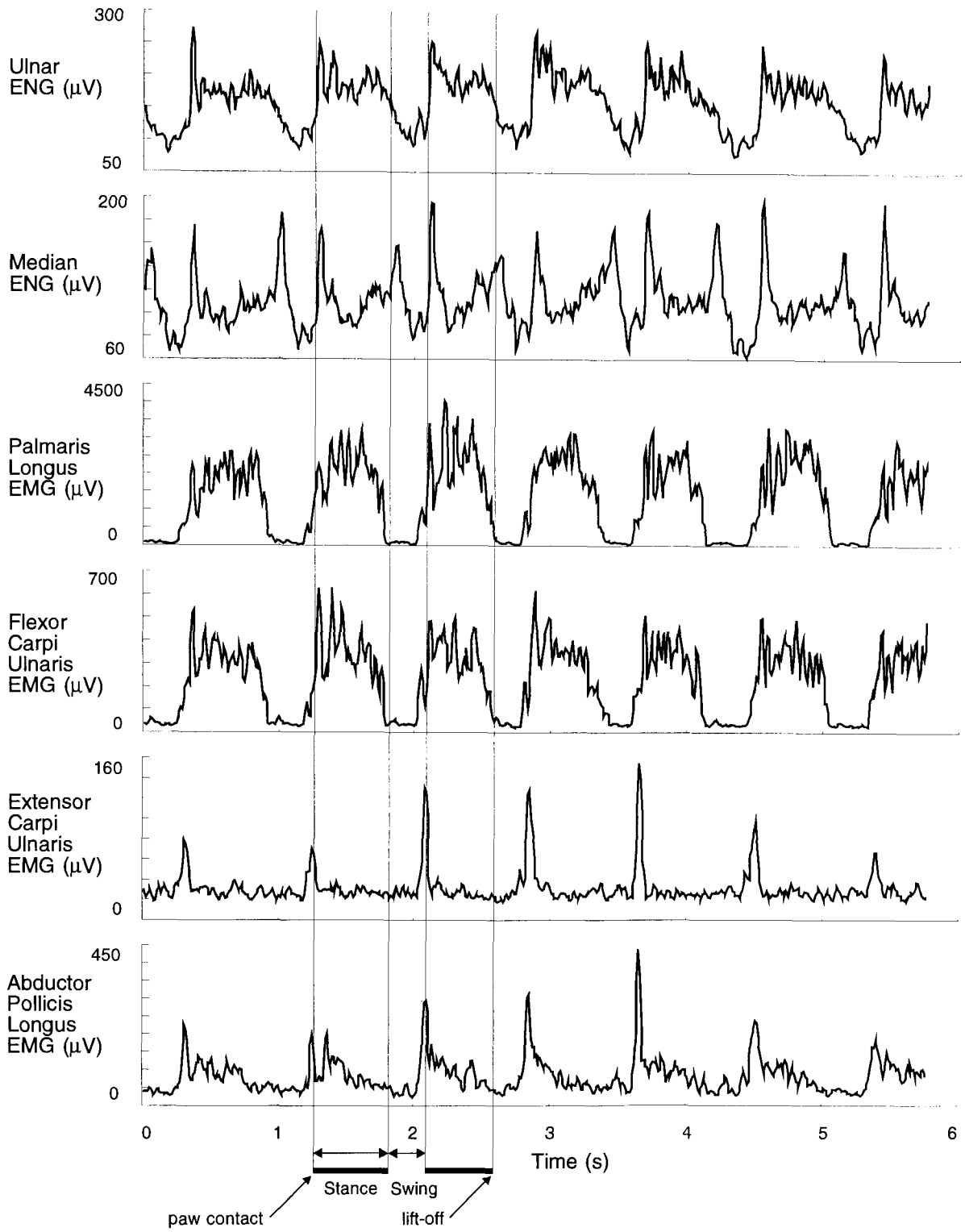

Figure 3.3: Rectified, bin-integrated data recorded from NIH-9 (day 113 post implant) during walking on the level treadmill (0.5 m/s). ENG and EMG signals were sampled at 10 kS/s and 1 kS/s respectively. All signals have been bin-integrated to 10 ms bins, and are shown in microvolts (omitting 10 ms binwidth) against a time scale of seconds. The top two traces show processed Ulnar and Median nerve ENG, and the bottom four traces show processed EMG activity from PalL, FCU, ECU, and APL respectively. Paw contact and lift-off are shown as light lines on the time scale, and the stance phase is signified by a heavy bar.

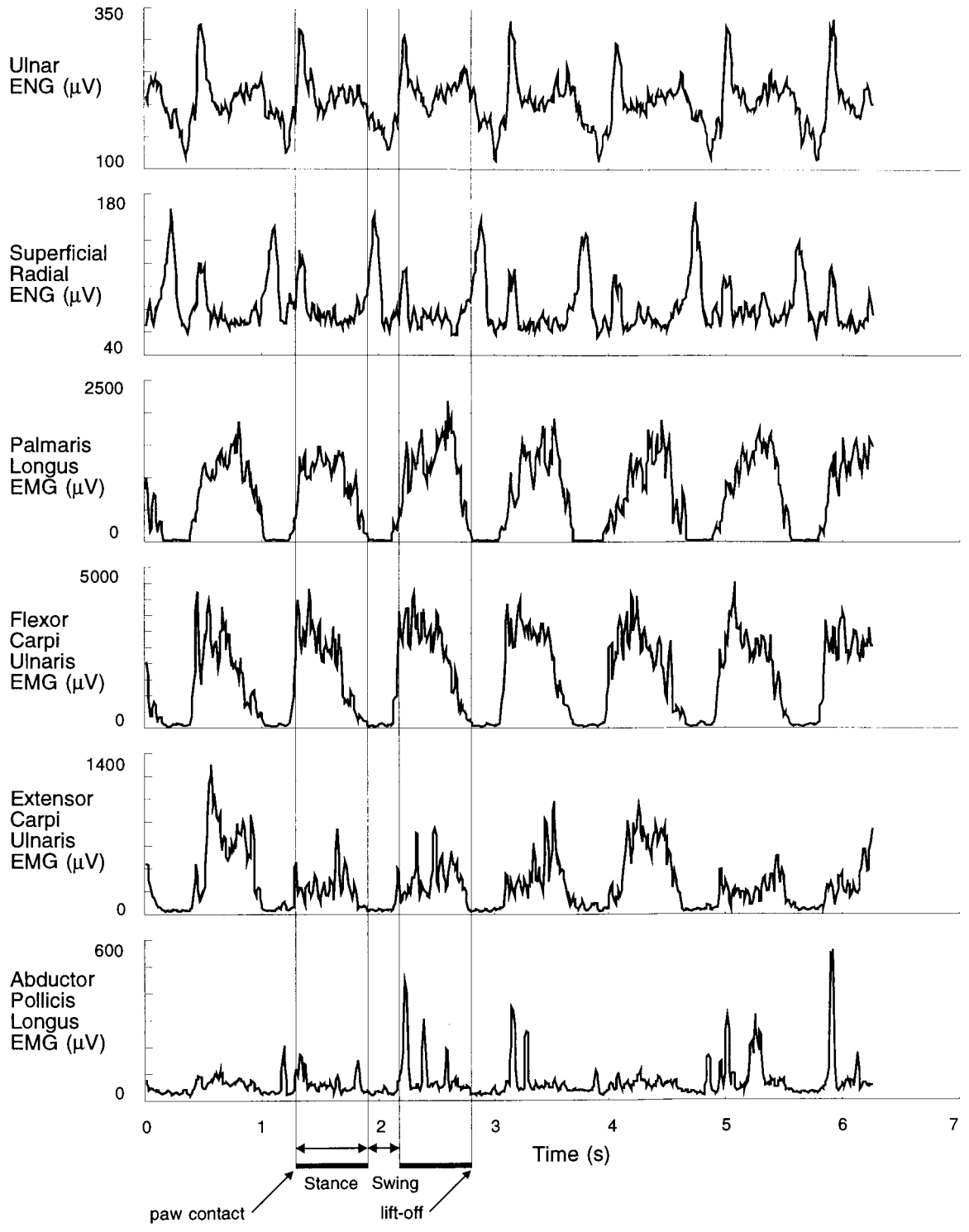

Figure 3.4: Rectified, bin-integrated data recorded from NIH-14 (day 49 post implant) during walking on the level treadmill (0.5 m/s). ENG and EMG signals were sampled at 10 kS/s and 1 kS/s respectively. All signals have been bin-integrated to 10 ms bins, and are shown in microvolts (omitting 10 ms binwidth) against a time scale of seconds. The top two traces show processed Ulnar and Superficial Radial nerve ENG, and the bottom four traces show processed EMG activity from PalL, FCU, ECU, and APL respectively. Paw contact and lift-off are shown as light lines on the time scale, and the stance phase is signified by a heavy bar.

Figures 3.3 and 3.4 show that there were fundamental similarities in the cutaneous ENG signals recorded from the two cats when walking on the treadmill, indicating that the gait pattern, characteristics of the implanted recording devices, and sensory neural signals from the cutaneous receptors in the paw were similar between these two cats.

The Ulnar, Median, and Radial neural signals recorded in the six cats showed characteristic bursts at paw contact, while the Median nerves showed bursts at lift-off, and the Radial nerves showed bursts following lift-off at the beginning of the swing phase. Video analysis showed that the gait patterns of all the cats were normal and did not vary after implantation. Gait features were similar in different cats, thus ensuring that the cutaneous receptors were receiving similar mechanical inputs during walking.

The plantar flexor muscle data shown in Figs. 3.3 and 3.4 also showed characteristic similarities, namely high levels of activity beginning at or just prior to foot contact, and lasting to near the end of the stance phase. All six cats showed similar patterns of flexor activity, with PalL being the most consistent from cat to cat. The paw and digit extensor EMG in Figs. 3.3 and 3.4 showed variation in activity between the two cats and even between successive steps in each cat. In addition, the extensor EMG signals were generally weak and less modulated with the step cycle when compared to the flexors, implying that these extensors played a secondary role during treadmill walking, perhaps mainly involved in correcting for unusual steps or conditions. The timing of recorded EMG during normal walking generally agreed with reports in the literature for forelimb muscles (English, 1976; Hoffman et al., 1985). EMG amplitude modulation data in the forelimb during walking have not been well reported in the literature to date.

3.4.2. EMG Contamination of ENG Signals

The presence and magnitude of EMG contamination was evaluated for all nerve cuff and patch electrode signals using data from the first recording session on the treadmill following implantation. The ENG signals were digitally sampled at 20 kHz and then imported into Matlab. The power spectral density was calculated using a 1024 point Fast Fourier Transform. The EMG portion of the spectrum was integrated from 0 Hz to 1 kHz and the ENG portion of the spectrum was integrated from 1 kHz to 10 kHz. The ratio of ENG/EMG signal-to-noise ratio (SNR) was calculated and used to evaluate the EMG rejection of the implanted cuffs and the secondary Ithaco filtering stages. Table 1 presents a summary of findings on EMG contamination of nerve cuff and patch electrode signals in the cat forelimb. The data from the Median nerve from NIH 9 were omitted due to a nerve compression injury, as discussed in a companion paper (Strange et al., 1996).

Table 3.1 shows that the ENG signals recorded from the Median, Ulnar, and Radial nerves in the cat forelimb typically exhibited an ENG/EMG SNR of about 16 after high pass filtering at 1 kHz with Ithaco filters. The average SNR was approximately 32 times larger following high pass filtering to reduce EMG rejection.

As an example of the spectral densities of the ENG signals, the spectra of the Median nerve ENG recorded from NIH-12 on day 34 are shown in Fig. 3.5. Figure 3.5A shows the signal spectrum before Ithaco filtering, and Fig. 3.5B shows the signal spectrum after Ithaco highpass filtering (24 dB/octave, 1 kHz; Ithaco 4302 Filter). Note that the EMG pickup component (under 1 kHz) in the signal was substantial in the nerve cuff signal but was markedly reduced by highpass filtering, such that the ENG/EMG SNR was improved from 0.24 to 8.89.

Table 3.1: Summary of EMG rejection characteristics of nerve cuffs and patch electrodes implanted on Median, Ulnar, and Radial nerves in the forelimb of six cats. The data shown is from the first recording day on the treadmill following the implant surgery. The table details the recording day, the ENG/EMG signal-to-noise ratio (SNR) prior to and following highpass filtering at 1 kHz with Ithaco filters, and gain in SNR due to Ithaco filtering.

Subject	Day	Nerve	ENG/EMG after Bak amplifier	ENG/EMG after Ithaco filter	Increase in ENG/EMG
NIH-9	15	Ulnar	0.04	1.58	38x
NIH-10	29	Ulnar Median	0.20 0.19	9.39 6.35	47x 33x
NIH-11	15	Ulnar Median	0.07 1.35	2.26 42.5	33x 31x
NIH-12	34	Median Radial	0.24 5.18	8.89 89.0	38x 17x
NIH-13	21	Ulnar Radial	0.07 0.21	2.39 4.78	36x 23x
NIH-14	14	Ulnar Radial	0.31 0.14	6.09 5.34	20x 38x
Geometric Mean			0.72	16.2	32x
Standard Deviation			1.52	26.7	8.8x

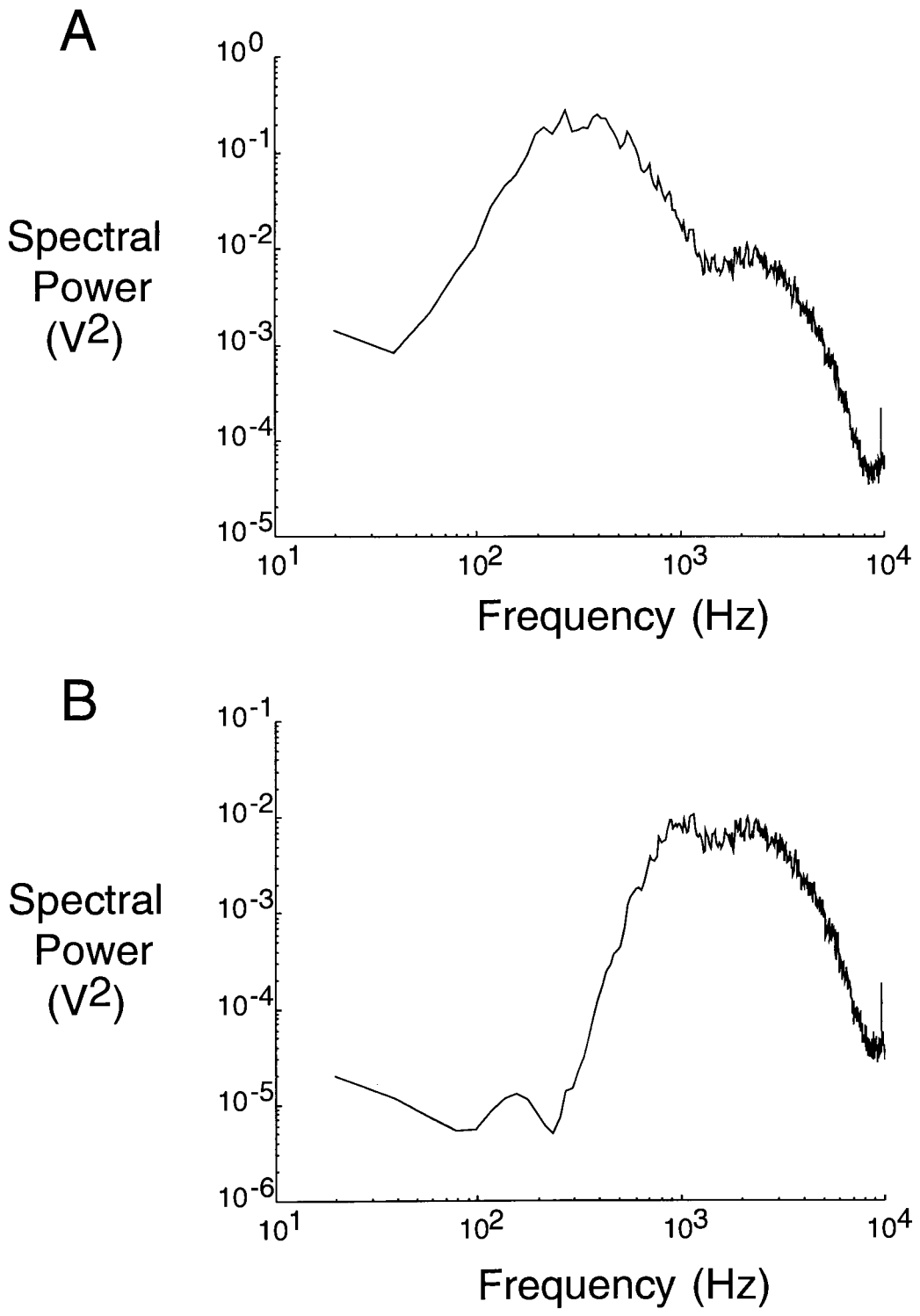

Figure 3.5: EMG contamination of nerve cuff signals recorded from the Median nerve in NIH-12 (day 34 post implant) during walking on the treadmill (0.5 m/s). Spectral power is shown in units of volts squared against a frequency scale in Hz. Panel A shows the Median cuff signal prior to high-pass filtering with considerable EMG content below 1 kHz (ENG/EMG SNR = 0.24), and panel B shows the same signal after high-pass filtering at 1 kHz with reduced EMG contamination (ENG/EMG SNR = 8.89).

3.4.3. Analysis of State Controller to Predict Timing of EMG Activity from ENG Signals

To model a closed-loop FES control system utilizing cutaneous ENG feedback, a state controller using hand-crafted rules to process signals recorded from the cat forelimb was designed in Matlab. Figure 6 shows a schematic diagram of the state controller including sources of neural feedback signals, possible uses for stimulation control signals, and derivation of controller output error signals. A detailed description of the design process and preliminary results of testing has been published by the authors (Strange and Hoffer, 1995a).

The model state controller was designed to use sensory cutaneous ENG signals as inputs in order to predict the timing of PalL EMG activity. Thresholds chosen for ENG (typically 60% of normalized signal peak) and EMG (typically 10% of peak, to detect presence or absence of muscle activity) were selected to identify discrete events and phases in the physiological signals and convert these signals to binary form. The model state controller was evaluated in terms of the output state error between the predicted muscle timing and the actual muscle activity for the test data, as shown in Fig. 3.6. Positive sign errors indicated that the predicted EMG activity occurred when the actual EMG was off, and negative errors indicated that the predicted activity did not occur when the actual EMG was on. Absolute errors were integrated over the entire data set and divided by the number of samples to give a percent state error, which indicated the percent of time during which the state controller gave an incorrect prediction of EMG activity. The state error can also be interpreted as the overall uncertainty in the prediction of the state controller model.

The two-state controller specifically detected the large spike of Median activity related to paw contact and the beginning of stance phase (Figs. 3.2 and 3.3) and the large spike of Radial activity generally related to lift-off and the initiation of swing phase (Fig. 3.4). The controller implemented a delay of 100 ms at state transitions to avoid noisy transition periods between states resulting from multiple threshold crossings.

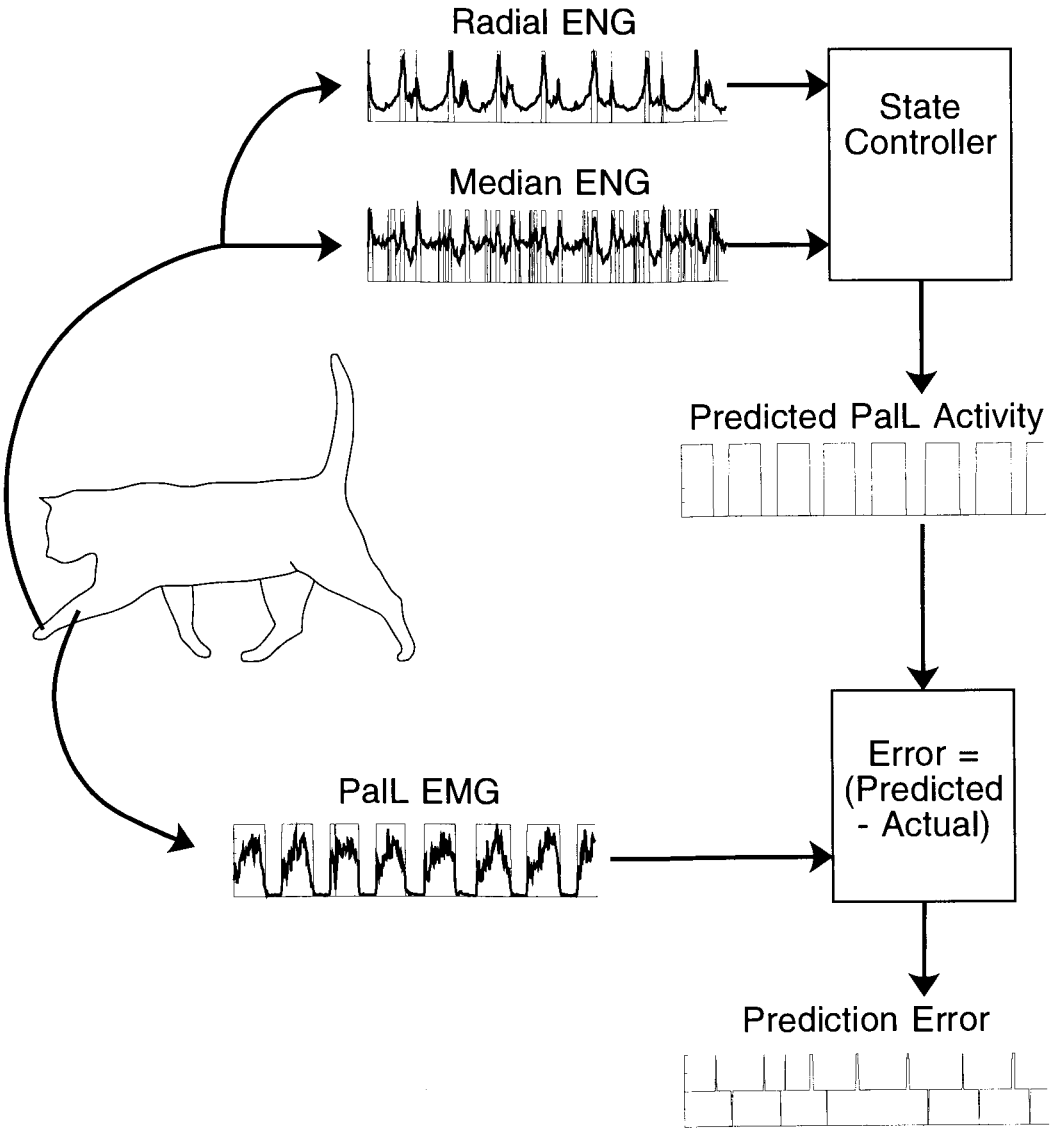

Figure 3.6: Schematic diagram of model state controller for proposed functional electrical stimulation applications. The state controller predicts the timing of PalL activity based on features in Radial and Median ENGs, and the actual binary PalL activity is subtracted from the predicted activity to produce a prediction error signal.

3.4.4. Reproducibility of Prediction Accuracy

Figure 3.7A shows normalized, processed nerve (top trace, Superficial Radial; second trace, Median) and muscle (third trace, PalL) signals with their corresponding binary levels of activity based on arbitrary thresholds (0.6, 0.6, 0.1 respectively), recorded in NIH-12 (day 85 post-implant) while walking on a level treadmill at 0.5 m/s. Figure 3.7A also shows the binary output of the state controller (fourth trace, predicted PalL activity), the error of the state controller output (fifth trace, equal to predicted minus actual EMG signals), and the output state of the controller (bottom trace). The state controller implemented two states, representing an active (stimulated) phase and a passive phase for the PalL. The output closely matched the recorded times of transitions in PalL activity, with a cumulative state error of 5.4% for the test data.

Figure 3.7B shows state controller results when tested on a different data epoch, recorded from NIH-12 in the same recording session and same conditions as Fig. 3.7A. The thresholds for neural inputs to the state controller remained at 60%. The cumulative error was 5.9% which was comparable to the error shown in Fig. 3.7A. Figure 3.7 shows that the state controller algorithm with fixed threshold parameters was robust in predicting the timing of PalL activity for different sets of data from the same recording session.

3.4.5. Performance for Different Days and Different Subjects

Figure 3.8 shows that application of the state controller algorithm to data obtained from the same cat on a different day, and to data from a different cat, produced consistent results. Figure 3.8A shows state controller results for data recorded from NIH-12 on an earlier day (day 34 post implant) for the same treadmill conditions (level, 0.5 m/s). Once again, the threshold parameters were fixed at 60% of the maximum of the neural signals. The cumulative state error was 3.8%.

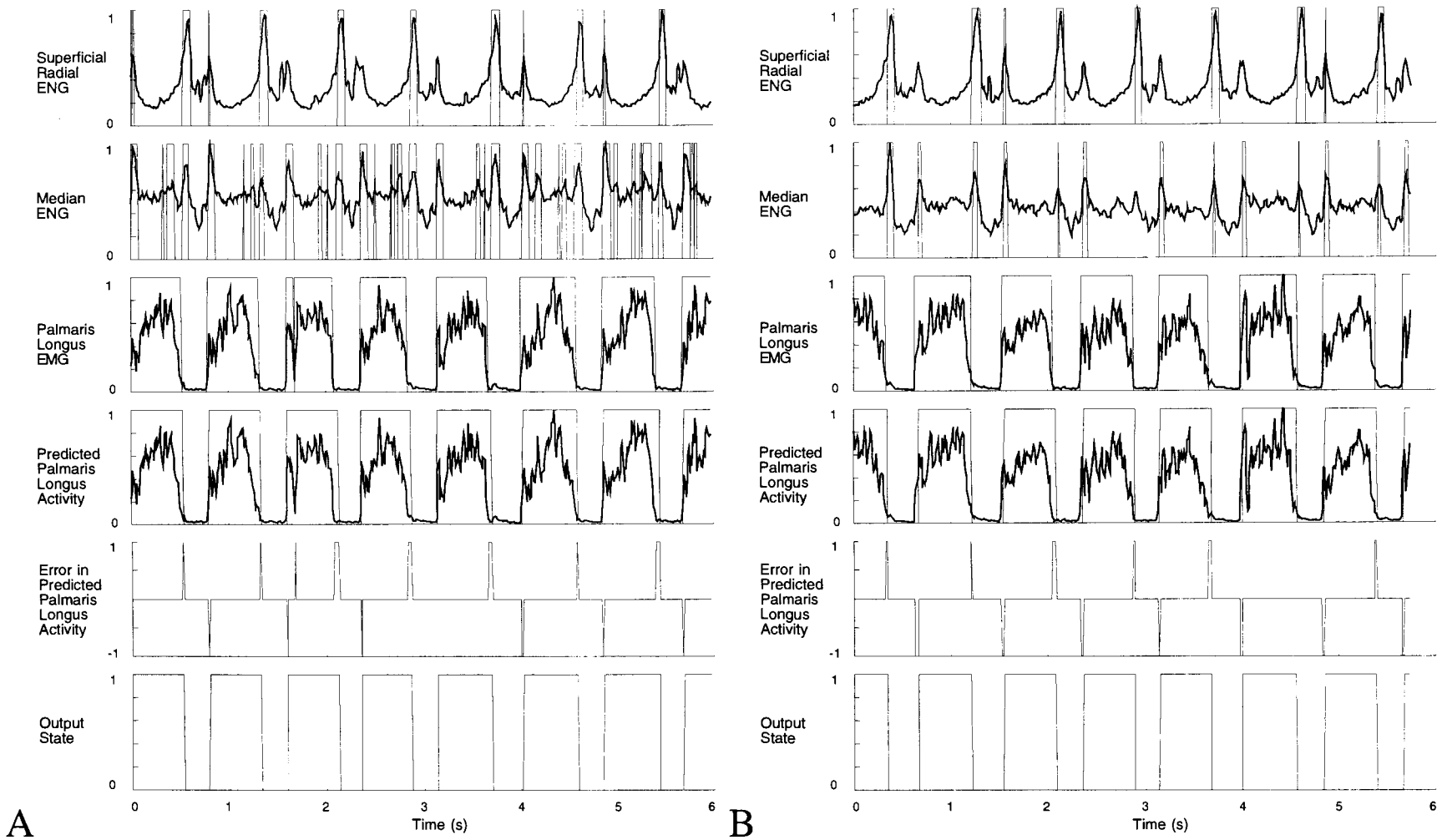

Figure 3.7: A. State controller output for normalized data recorded from NIH-12 (day 85a, 0.5m/s, level). Error = 5.4%. B. State controller output for a different data epoch recorded from NIH-12 in the same conditions as Fig. 7A (day 85b, 0.5m/s, level). Error = 5.9%.

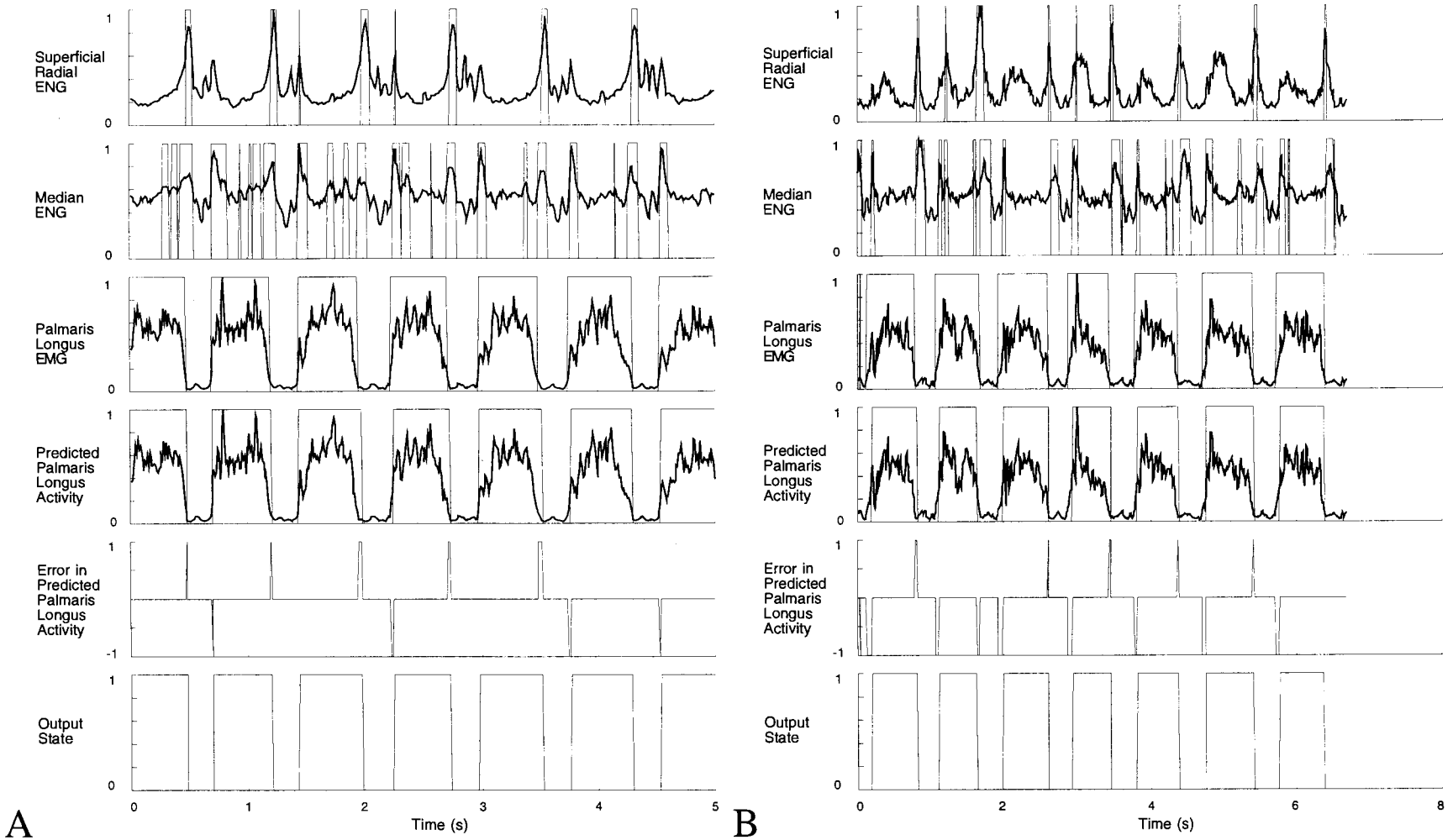

Figure 3.8: A. State controller output for normalized data recorded from NIH-12 on a different day (day 34a, 0.5m/s, level). Error = 3.8%. B. State controller output for normalized data recorded from NIH-15 (day 82a, 0.5m/s, level) in same walking conditions as NIH-12 in Fig. 7A. Error = 8.2%.

Figure 3.8B shows state controller results for data recorded from a different cat (NIH-15, day 82 post implant) for the same treadmill conditions (level, 0.5 m/s). The cumulative state error with fixed threshold parameters was 8.2%. The state controller approach with fixed parameters appeared accurate and robust in predicting PalL activity for constant walking speeds and slopes for data from different cats and different days.

3.4.6. Performance for Faster Speeds of Walking

Figure 3.9 shows state controller results for data recorded from NIH-12 (day 85 post implant) walking at a faster speed (1.0 m/s) on the level treadmill. With the 60% Median and Radial ENG threshold parameters, the state controller output error was 12.1% with greatest errors occurring prior to foot contact.

The relatively high error for a faster treadmill speed was a result of a natural phase advance of the actual PalL EMG activity to stiffen the forelimb prior to foot contact. The state controller looked for the Median nerve sensory burst resulting from foot contact and could not predict the phase advance of the PalL EMG. To compensate for this, the neural thresholds were lowered (Median to 35% of the highest peak in the data trace, and Radial to 50%), which advanced both the beginning and the end of the predicted PalL activity in each step and reduced the cumulative state error to 6.2%.

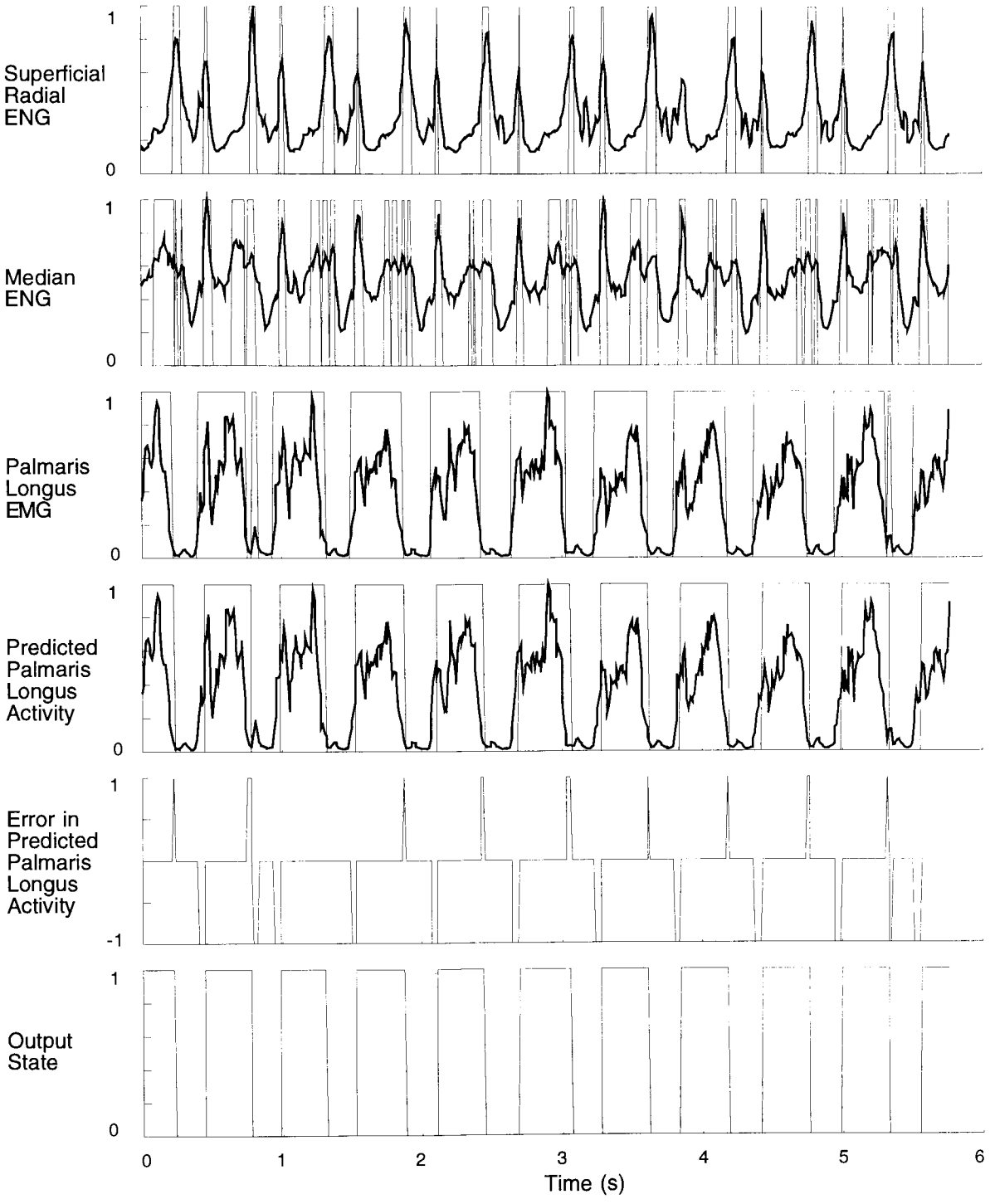

Figure 3.9: State controller output for normalized data recorded from NIH-12 at a higher walking speed (day 85c, 1.0m/s, level). Error = 12.1%.

3.4.7. Performance for Uphill and Downhill Walking

As a final step in testing the state controller with fixed parameters, the algorithm was tested on data recorded while walking at different slopes on the treadmill. Figures 3.10A and 3.10B show state controller results for NIH-12 (day 85 post implant) walking at 0.5 m/s uphill and downhill on a 10% slope respectively. The cumulative state error with fixed 60% neural thresholds was 5.4% for uphill walking and 8.5% for downhill walking, in the range of errors for all other walking conditions.

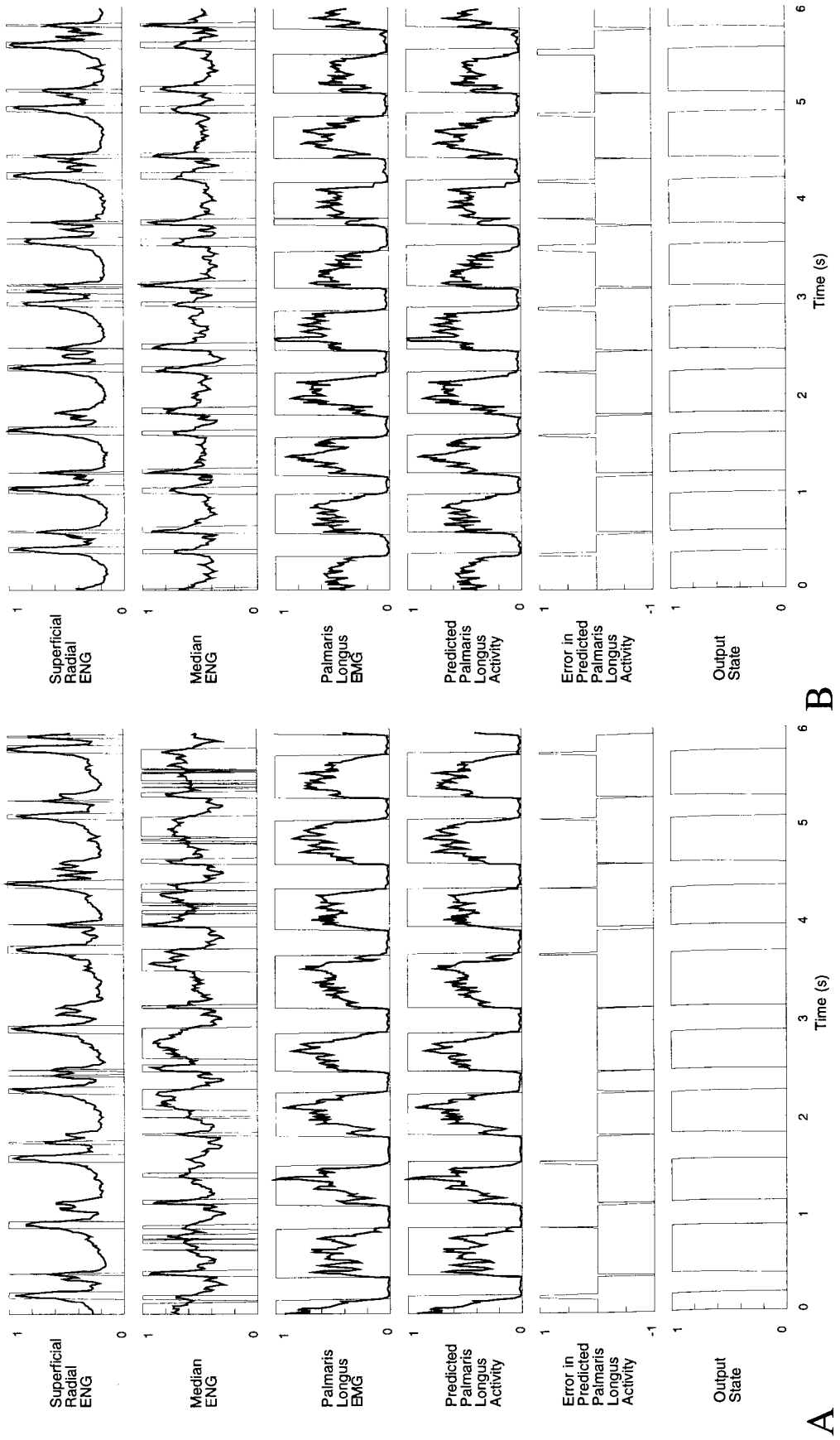

Figure 3.10: A. State controller output for normalized data recorded from NIH-12 walking uphill (day 85d, 0.5m/s, +10%). Error = 5.4%. B. State controller output for normalized data recorded from NIH-12 walking downhill (day 85e, 0.5m/s, -10%). Error = 8.5%.

3.5. DISCUSSION

This study suggests that it is feasible to predict with good accuracy the timing of onset and termination of EMG bursts, on the basis of features in sensory nerve signals recorded with chronically implanted nerve cuffs. The predominantly cutaneous sensory ENG signals from the Median, Ulnar, and Radial nerves that we monitored during walking on a treadmill showed characteristic features during the step cycle that were consistent from cat to cat and over the full duration of the implants, which lasted for up to 300 days. In one case in which we replaced a proximal nerve cuff on the Median nerve to relieve a compression injury, the compound action potential (CAP) dropped in amplitude to approximately 5% of the amplitude on the day of implant, and then slowly recovered to near 100% after 300 days (Strange et al., 1996, in preparation). During this time, awake recordings on the treadmill showed that the Median nerve continued to respond to mechanical loading and unloading of the paw during walking, although the signal showed lower peak amplitudes. Figures 3.2 and 3.3 present data from this implant at day 113 when the CAP was approximately 20% of the original amplitude, implying that even partially injured cutaneous sensory nerves continue to transmit relevant information.

A potentially significant issue in the use of nerve cuffs to record neural information is contamination of recorded ENG signals with EMG activity (stimulated or voluntary) from nearby muscles and stimulus artifacts in FES systems. We have been able to show in this study that, with proper design of recording cuffs and sharp high pass filtering, useful ENG signals with very little EMG contamination can be obtained. Thinking ahead to clinical applications utilizing recorded neural signals in closed-loop FES systems, the issue of EMG contamination becomes less predictable, depending on the nature of the injury, as voluntary control of limb muscles is removed and spasticity may be present.

During stimulation, evoked compound EMG signals will be present and stimulus artifacts may also contaminate neural recordings. The problems of stimulus artifact contamination become amplified as more channels of stimulation are added to FES systems and as stimulation rates are increased. Several solutions have been suggested and investigated, including selective omission of periods of stimulus artifact by blanking the recording channels during stimulation (Strange and Hoffer, 1996), and selective recording during periods with no stimulation (Haugland and Hoffer, 1994).

The nerve activity analyzed in this paper was predominantly of sensory origin but probably included contributions from a small number of efferent axons. The recording nerve cuffs were implanted distally on the cutaneous nerves to minimize the number of motor fibres present. Electrical stimulation through the recording cuffs normally resulted in very little muscle response or force generated at the paw and digits, which confirmed the largely sensory nature of the distal nerves. FES systems implemented in patients with complete and incomplete spinal cord injuries may require strategic placement of recording devices and investigation of the sensory and motor components of recorded ENG signals. The remaining motor ENG in the peripheral nerves may be due to residual motor control and spasticity.

As an example of a potential application of closed-loop control of FES utilizing natural sensory feedback, a state controller was designed to predict the activity in one muscle during walking on a treadmill. The features and patterns of ENG and EMG data were analyzed and hand-crafted rules were written so that the controller specifically detected features in the Median ENG related to paw contact at the beginning of stance and features in the Radial ENG related to paw lift-off at the beginning of swing. Transitions from stance to swing and swing to stance were detected for all walking speeds, and thus the controller was rate-independent (unlike previous FES systems that required counters to determine the duration of certain states (Sinkjaer et al., 1992; Upshaw et al., 1995, Haugland and Sinkjær, 1995).

Single threshold analysis of both ENG and EMG signals was implemented to convert input and output signals to binary form, and the state controller used binary logic to predict the timing of activity of PalL.

The state controller was specifically tuned using hand-crafted rules on test data as a demonstration of a potential use of cutaneous feedback in closed-loop control of FES. The limitations of applying the controller with hand-crafted rules to a variety of conditions (velocities, slopes, changes in neural signals over time) was investigated. With neural thresholds left constant at of 60% of maximum, output state errors were less than 12.1% for all the data presented in this paper, with the maximum error occurring for data at the highest velocity of 1.0 m/s. For treadmill velocities of 0.5 m/s, the state errors were in the range of 3.8 to 8.5% using fixed threshold parameters. The larger error at the higher velocity resulted from a phase advance in the recorded PalL EMG with respect to the step cycle and recorded Median nerve signal. By customizing the threshold parameters for those data, the output error of the controller was reduced to within the typical range.

The amplitudes of nerve cuff signals could vary from cat to cat and to a lesser extent from recording session to recording session, but the state controller approach was found to be robust and reliable when the neural thresholds were simply set as a percentage of the peak value for each particular data set. In real-time FES system applications, adaptive thresholds could be generated as percentages of the previous steps' ENG peaks or as percentages of the running average of the previous n peaks. The thresholds would then float and adjust for dynamic walking conditions and continue to accurately predict the timing of PalL activity.

Tuning simple controllers to minimize the error on one particular set of test data will usually create a tradeoff in generalization error with new sets of inputs and different conditions. Restricting the conditions or environment in which the FES system operates can make the state controller approach more viable. State machine controllers have been successfully implemented in clinical

FES systems in either open loop and closed-loops systems for upper and lower extremities (Andrews et al., 1989; Kirkwood and Andrews, 1989; Peckham and Keith, 1992; Popovic, 1992; Kobetic and Marsolais, 1994;) where the range of motion, surfaces, patterns of motion and other variables were controlled.

Although the present approach of implementing sensory feedback is limited to predicting the timing of muscle activation for basic walking conditions, more complex controllers involving machine learning techniques, pattern recognition, and adaptive control may accommodate a wider range of input conditions such as rate and slope changes, changes in surface characteristics, muscle fatigue, and spasticity (Veltink et al., 1990; Chizeck, 1992; Popovic et al., 1993; Kostov et al., 1993, 1994, 1995a,b,c). These systems implement automatic rule generation and one particular technique involving adaptive logic networks has shown that, when trained on one set of data recorded from the cat forelimb, the system can accurately predict both the timing and continuously varying levels of muscle activity for test data from the same cat recorded in the same recording session as the training data and data recorded on different days (Kostov et al., 1996). Using these advanced approaches, FES controllers implementing neural feedback should result in clinical applications of FES with increased functionality, accuracy and robustness.

3.6. CONCLUSIONS

In this study natural sensory signals from cutaneous nerves were recorded in the forelimbs of six cats during walking on a motorized treadmill, using chronically implanted nerve cuffs and patch electrodes. The cutaneous ENG signals recorded from the Median, Ulnar, and Radial nerves suggest that natural sensory signals may be implemented as a reliable source of feedback in closed-loop control of FES. Future directions include characterizing the neural signals resulting from different environments and conditions, investigating recording techniques in the presence of

EMG and stimulus artifact contamination, and implementing sensory neural signals as feedback in models of closed-loop control of FES.

Chapter 4:

Forelimb sensory nerve signals provide reliable state controller feedback for FES during cat walking.

Summary

A real-time FES state controller was designed that utilized sensory nerve cuff signals from the cat forelimb to control the timing of stimulation of the Palmaris Longus (PalL) muscle during walking on the treadmill. Sensory nerve signals from the Median and Superficial Radial nerves provided accurate, reliable feedback related to foot contact and lift-off which, when analyzed with single threshold Schmitt triggers, produces valuable state information regarding the step cycle. The study involved three experiments: prediction of the timing of muscle activity in an open-loop configuration with no stimulation, prediction of the timing of muscle activity in a closed-loop configuration that included stimulation of the muscle over natural PalL EMG, and temporary paralysis of selected forelimb muscles coupled with the use of the state controller to stimulate the PalL in order to return function to the anesthetized limb. The FES state controller was tested in a variety of walking conditions, including different treadmill speeds and slopes. The results obtained in these conditions with the animal model demonstrate that nerve cuff signals may provide a reliable source of feedback to FES systems used for restoration of movement in humans.

4.1. INTRODUCTION

Nerve cuff recordings may provide useful and robust feedback signals for control of functional electrical stimulation (FES) systems (Hoffer, 1988; Haugland et al., 1994, Hoffer et al., 1996). Natural nerve signals generated by external forces applied to the skin may be recorded with nerve cuff electrodes and used to extract contact, force, and position information useful for closed-loop control of FES of paralyzed muscles (Hoffer and Haugland, 1992; Sinkjær et al., 1992; Popovic et al., 1993; Haugland and Hoffer, 1994a,b; Upshaw et al., 1995; Haugland and Sinkjær, 1995; Hoffer et al., 1996).

In a companion study (Strange et al., 1996, submitted concurrently) we investigated the long-term stability of chronically recorded nerve cuff signals by measuring the amplitude and latency of electrically evoked nerve compound action potentials (CAPs). Signals recorded with cuff electrodes generally remained very stable over periods of six months and longer (Strange et al., 1995).

In a second companion study (Strange and Hoffer, 1996, submitted concurrently) we identified gait-related features in the electroneurogram (ENG) signals recorded with nerve cuffs from sensory nerves in the cat forelimb. ENG features that corresponded with events such as paw contact and lift-off were used by a model state controller to predict the phases of the step cycle and the timing of activation of forelimb muscles. The timing prediction of the model was accurate to within 12% of the actual timing of EMG from the Palmaris Longus for a variety of walking conditions at different treadmill speeds and slopes when constant percentage thresholds where applied to the ENG signals.

In this study, we report on the implementation of a real-time FES state controller that was designed to use sensory nerve cuff signals to control the timing of activation with FES of the

Palmaris Longus muscle during walking on the treadmill. This FES state controller was tested in three conditions: 1) prediction of the timing of muscle activity in an open-loop configuration with no stimulation, 2) prediction of the timing of muscle activity in a closed-loop configuration with stimulation of the muscle over natural EMG, and 3) prediction of the timing of muscle activity in a closed-loop configuration with stimulation of the muscle to return function to the wrist during temporary paralysis of the wrist plantar flexors innervated by the Median nerve.

The FES state controller was tested in a variety of walking conditions. The accurate, reliable results obtained in these different conditions demonstrate that nerve cuff signals can provide a reliable source of feedback to FES systems used for restoration of movement.

4.2. METHODS

4.2.1. Implanted Devices and Transducers:

In this study, we implanted two nerve cuffs on the Median nerve and two nerve cuffs on the Radial nerve of the left forelimb of each of two cats (NIH-15 and NIH-16). The approximate locations of the implanted devices for NIH 16 are shown in Fig. 4.1.

In subject NIH-15, the Radial nerve was instrumented with a 5 mm long, 3.7 mm ID, stimulation nerve cuff proximal to the branching of the Deep and Superficial Radial branches, and with a 10x30 mm recording patch electrode enveloping both branches of the Superficial Radial Nerve (Strange and Hoffer, 1996, submitted). The Radial nerve was instrumented proximal to the split so that stimulation of the cuff resulted in recruitment of motor fibres to some wrist extensor muscles.

In subject NIH-16, the Radial nerve was instrumented with a 10 mm long, 2.8 mm ID, stimulation nerve cuff distal to the branching of the Deep and Superficial Radial branches, and with a 15 mm long, 1.9 mm ID, recording nerve cuff on the Lateral Superficial Radial Nerve. The Superficial Radial Nerve is mostly afferent in nature and stimulation of the proximal cuff did not result in any motor recruitment.

The Median nerves in both cats were instrumented with proximal stimulating and distal recording cuffs in the locations detailed in Fig. 4.1. In NIH-15, the proximal cuff was 5 mm long and 2.8 mm ID, and the distal cuff was 20 mm long and 2.3 mm ID. In NIH-16, the proximal cuff was 10 mm long, 3.7 mm ID and included a reservoir around the nerve to contain anesthetic agents introduced through the catheter that temporarily blocked conduction of the nerve (Hoffer, 1990). It also included two stimulating electrodes in the proximal portion of the cuff that were used to periodically monitor the CAP throughout the implant period and assess the condition of the nerve and implanted devices (Strange et al., 1996, submitted).

All of the implanted cuffs were constructed in the lab from silicone tubing and wire electrodes (AS 631 Teflon-coated Cooner wire) (Hoffer, 1990; Kallesøe et al., 1996; Strange et al., 1996).

The placement of each cuff depended on the local anatomy of nerve branches and blood supply in the forelimb. Recording cuffs were placed as distally as possible to ensure that ENG signals would primarily consist of cutaneous sensory activity and contain little efferent activity.

Four forelimb muscles were instrumented with bipolar EMG patch electrodes constructed from silicone sheeting with wire electrodes (AS 634 Teflon-coated Cooner wire). The patch electrodes were sewn to the muscle belly near the nerve entry point for each of the Palmaris Longus (PalL), Flexor Digitorum Profundus (FDP - 5th head), Extensor Digitorum Communis (EDC), and Extensor Digitorum Lateralis (EDL). These muscles were selected based on surgical accessibility and their function during walking as observed in earlier experiments (Strange and Hoffer, 1996).

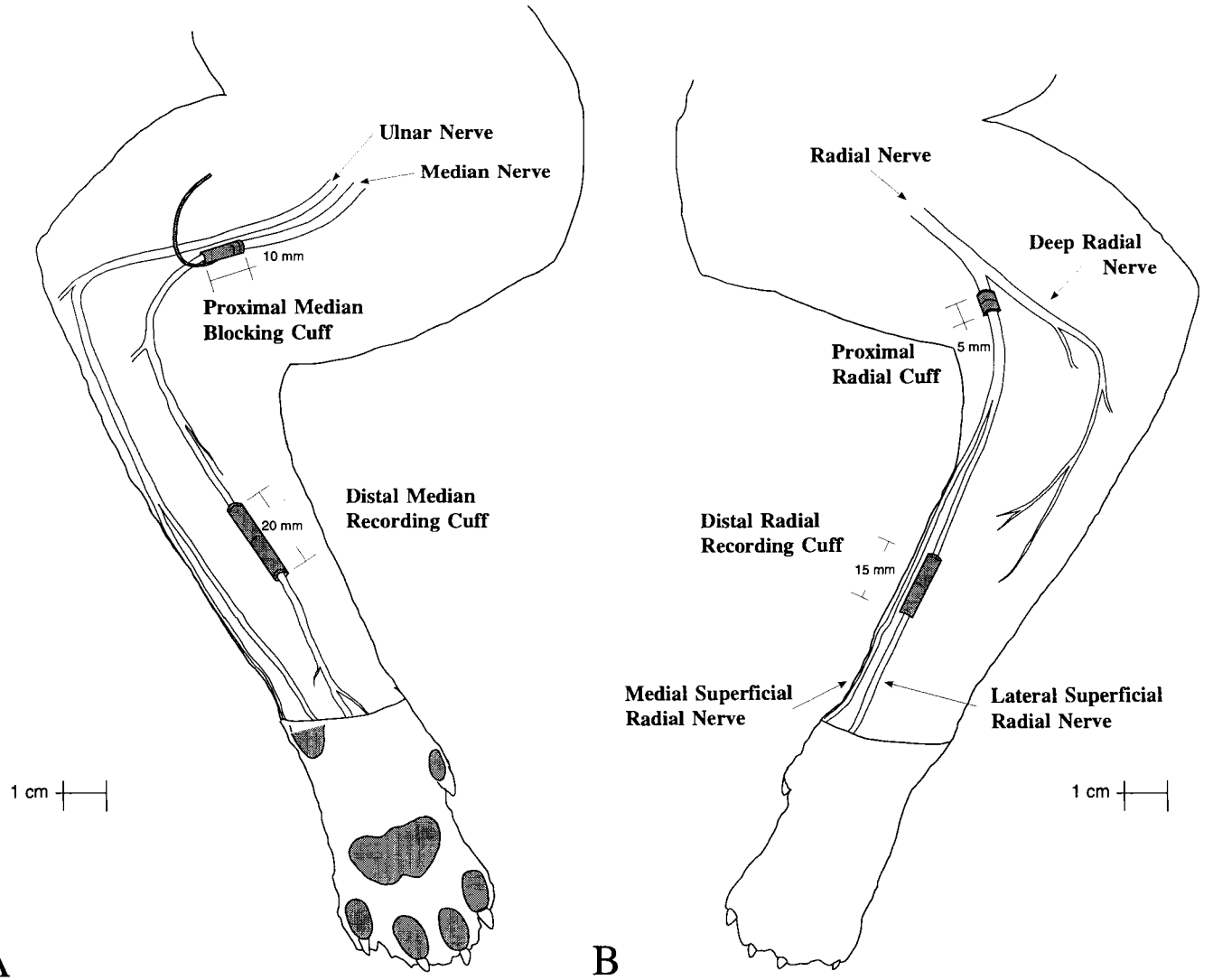

Figure 4.1: A. Medial view of cat left forelimb, showing instrumentation of the Median nerve implanted in NIH-16, including a proximal Median blocking cuff (with catheter to allow injection of local anesthetic agent to block nerve conduction) and a distal Median recording cuff. B. Lateral view of cat left forelimb, with implanted proximal stimulating cuff and distal recording cuff on the Superficial Radial nerve.

A thermistor (Yellow Springs Instruments Inc., Model 44004), embedded in silicone, was implanted above the elbow to monitor limb temperature during experiments under anesthesia. Ground wires were implanted at the elbow and at the wrist. All device leadout wires were routed to a common percutaneous exit point and attached to a specially designed backpack as detailed in a companion paper (Strange et al., 1996). The backpack included a 40-pin connector which was attached to the recording station with a flexible ribbon cable during experiments.

Our surgical and experimental protocols met the guidelines set by the Canadian Council of Animal Care and were approved by the University Animal Ethics Committee. All anesthesia and analgesia protocols were performed by a certified veterinary technician.

4.2.2. Nerve Cuff Signals During Walking

Prior to the implant surgery, each animal was trained on a daily basis to walk at various speeds and slopes on a motorized treadmill. Food rewards and positive reinforcement were used to ensure that the cat was comfortable and walked with a confident and steady gait close to the front of the treadmill.

At the beginning of each recording session, the impedances of all implanted devices were measured as described by Strange and Hoffer (1996). Typical recording nerve cuff impedances were under 5 kΩ measured at 1 kHz (Bak Electronics, Inc. Electrode Impedance Tester, Model Imp-1). Typical EMG electrode impedances were 1 kΩ.

During recording sessions when the cat was walking on the treadmill, a 20 channel FM tape recorder (Honeywell, Model 96; 10 kHz/channel) was used to record all of the physiological and processed signals and a time code signal (Datum Time Code Generator, Model 9300).

Nerve cuff signals were amplified (typically by 10^4 - 10^5) using low-noise preamplifiers (Leaf Electronics Ltd., Model QT-5A, 65 Hz high pass-filter) and amplifiers (Bak Electronics Inc., Model MDA-1, 500 Hz - 10 kHz band-pass filter) to a level so as not exceed ±2 V p-p to avoid being clipped when recorded on FM tape. The nerve cuff signals were then high-pass filtered (normally at 1 kHz) with an analog filter (Ithaco 4302 dual 24 dB/octave Filter) with a gain of 1 or 10. The filtered nerve cuff signals were then rectified and integrated with sample and hold circuits (Bak Electronics Inc., Model PSI-1) with the sample time set at 10 ms to provide useful envelopes of the neural activity. In addition, the amplified nerve cuff signals were played through a loudspeaker to assess the frequency content of the signal and assess EMG contamination. Filtered and integrated neural signals were recorded on additional FM channels in parallel with the raw nerve cuff signals.

EMG signals from the PalL were amplified (typically by 10^3) and filtered using a differential amplifier (Bak Electronics Inc., Model MDA-2, 50 Hz - 1 kHz band-pass filter).

The motions of the left forelimb were videotaped to correlate physiological data with discrete events and phases of the gait cycle during each recording session. The video screen display included the time code signal and on-line sampling of nerve cuff and EMG signals (Codas, Dataq Instruments, Inc.) in a separate window to aid in on-line analysis of nerve and muscle activity.

4.2.3. State Controller

A FES state controller was developed in hardware to reproduce the results in real-time of the model FES state controllers discussed in Strange and Hoffer (1995a,6). The model state controllers were designed to predict the timing of activation of the PalL during walking based on

the neural activity recorded from the Median and Superficial Radial nerves in the cat forelimb, as shown in Fig 4.2. The model identified bursts of Median and Radial ENG activity related to foot contact and lift-off by using threshold detectors and produced a binary PalL activation signal for a range of treadmill speeds and slopes.

Figure 4.3 shows a schematic diagram of the real-time FES state controller. The Median and Radial nerve cuff signals were amplified, filtered, and then integrated to provide clean envelopes of neural activity during walking. Schmitt triggers were used as threshold detectors to identify bursts and phases of neural activity, and the TTL level outputs were used as inputs to a JK-type flip-flop with a feedback delay circuit to minimize erroneous state transitions resulting from noise around the neural threshold levels. The Q output of the flip-flop represented the binary nature of the PalL muscle (also the stance phase), and was connected to the gate input of a biphasic pulse generator (BPG; Bak Instruments Inc., Model BPG-2). The pulse generator output controlled the stimulation of the PalL using biphasic constant current pulses (described in section 4.2.4) applied to the implanted patch electrode on the muscle belly.

The nerve cuff signals passed through custom-built switching circuitry designed to remove stimulus artifacts from the ENG during stimulation of the PalL. The switching circuitry was designed using JFET analog multiplexers and is described in more detail in the next section.

The Schmitt trigger circuits were custom-built to include variable threshold hysteresis to reduce erroneous transitions. The integrated nerve cuff signals were amplified to utilize the maximum range of input stage of the battery-powered Schmitt triggers, which was approximately 4 V. The input stage consisted of an active subtraction circuit (LF353) to remove the threshold level from the input signal. The resulting signal was then sent to a comparator (LF353) with variable hysteresis, whose output supplied an inverter (CD4049) and then a current amplifier (LH0002CN) output stage.

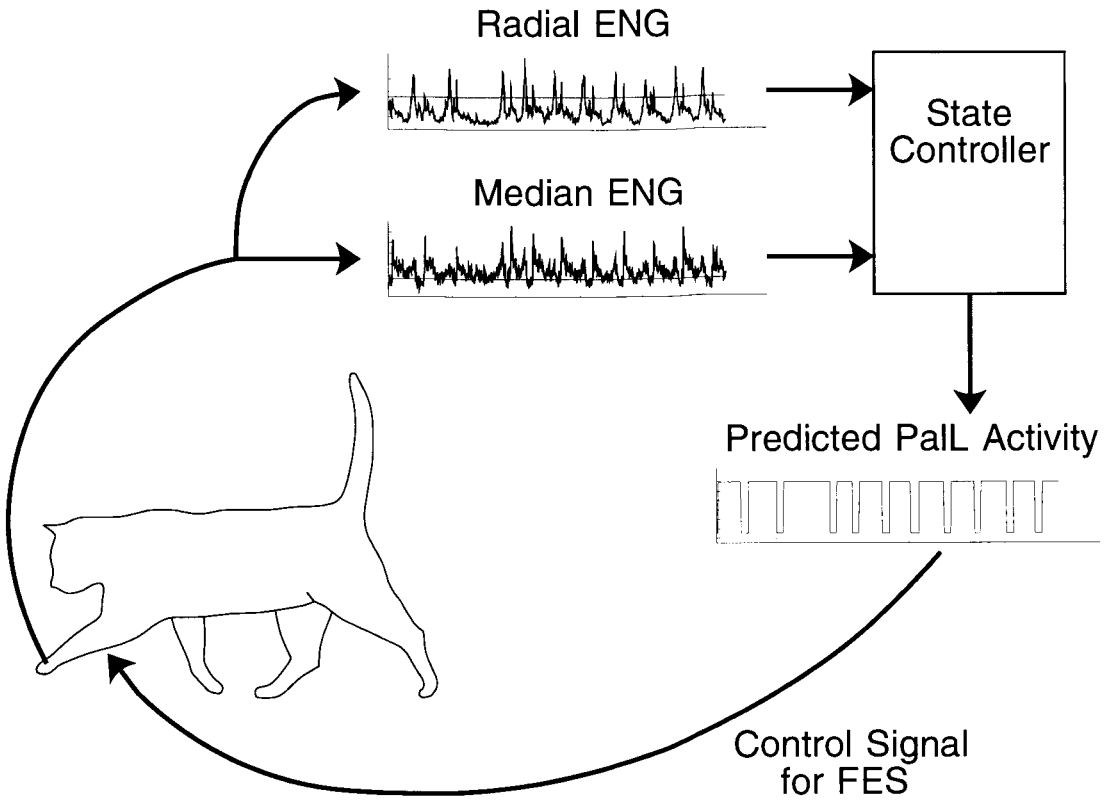

Figure 4.2: Schematic diagram of closed-loop state controller for functional electrical stimulation in the cat forelimb during walking. The state controller predicts the timing of PalL activity (ON or OFF) based on features in Radial and Median ENGs related to foot contact and lift-off, and the predicted PalL activity signal is used to control stimulation of the PalL during walking. Data from NIH-16, day 62d, -10% downhill walking at 0.5 m/s. Note step-to-step variability in Radial and Median ENGs which is accommodated by the state controller in predicting PalL activity.

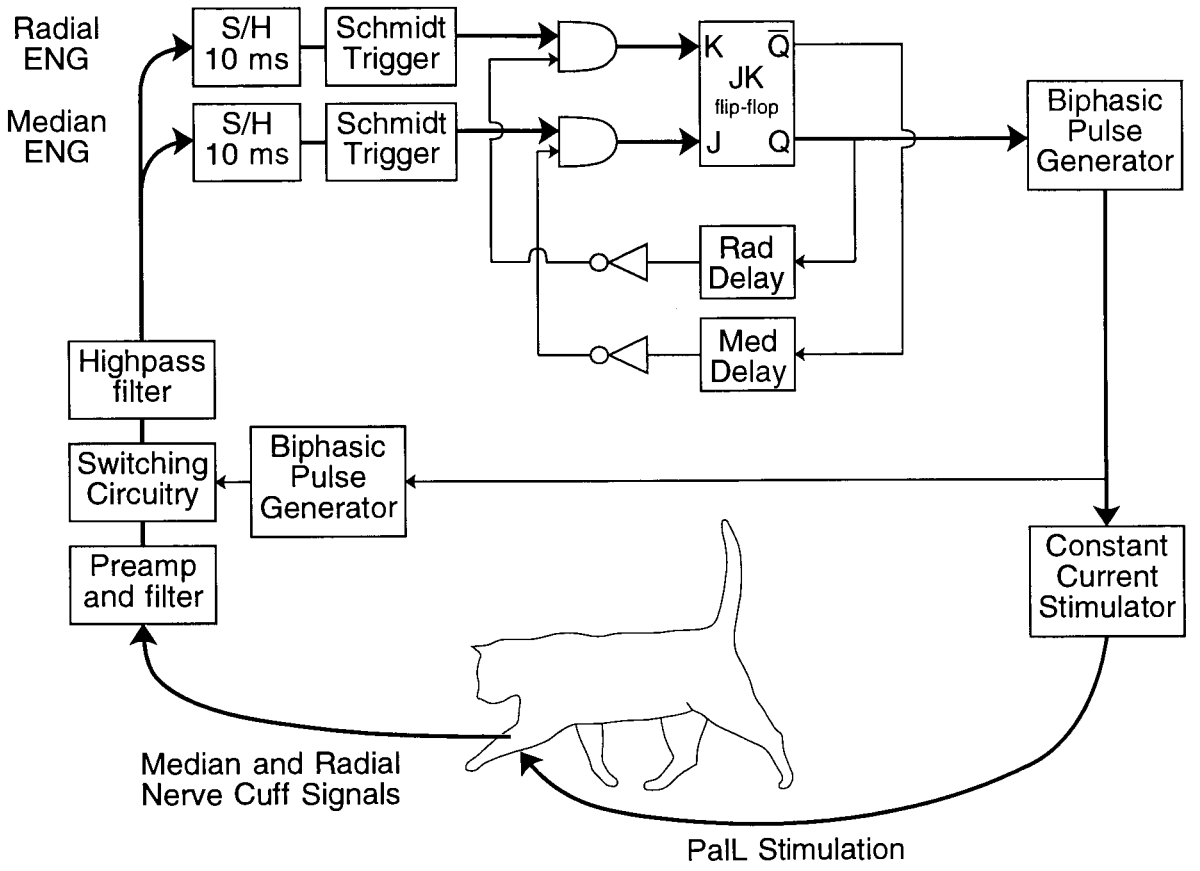

Figure 4.3: Detailed schematic of FES state controller. ENG signals are amplified and filtered, switching circuitry is used to omit stimulus artifacts, highpass filters are used to eliminate evoked or natural EMG from cuff signals, sample-and-hold circuits are used to generate envelopes of ENG signals, and Schmitt triggers are used as threshold detectors to identify activity in the ENG signals. A JK-type flip-flop is used to generate the output state of the state controller (PalL ON or OFF), and digital counters are used as feedback delays in the flip-flop circuit to avoid erroneous state transitions due to multiple threshold crossings. The output of the state controller is gated to a biphasic pulse generator which sets the stimulation frequency and timing of each pulse, which in turn drives a constant current stimulator. The stimulation pulses are applied to the PalL muscle belly.

The thresholds and hysteresis levels of the Schmitt triggers were adjusted at the beginning of experiments during on-line visual comparisons of predicted and actual PalL activity. These parameters were then held constant for the duration of the experiment.

The digital circuitry shown in Fig. 4.3 was designed using a digital controller (Bak Instruments Inc., Model DC-1) and patching the logic gates together. The delay feedback lines utilized separate counters and could be adjusted on-line if necessary. The TTL outputs of the delay counters were inverted and combined with the outputs of the Median and Radial Schmitt triggers using AND logic gates to determine if a state transition was possible. For example, if the Median nerve signal was above threshold and if a minimum time had elapsed since the last flip-flop transition from high to low (set by Median Delay), then the output of the Median AND gate went high and the flip-flop changed state to high. Similarly, state transitions from high to low utilized the Radial nerve signal and the Radial Delay counter.

The Q output of the flip-flop was used as the gate input to the BPG, and a train of stimuli was supplied to the constant current stimulator as long as the gate input was high. The overall function of the state controller was to determine when the PalL should be active from the two neural signals, and then supply a stimulation control signal which could be visually compared to existing PalL EMG and applied to the muscle.

4.2.4. PalL Stimulation and Stimulus Artifact Rejection

The stimulation current range required for PalL stimulation was determined during CAP recordings under anesthesia (Strange et al, 1996; Strange and Hoffer, 1996). Biphasic current pulses were used to minimize patch electrode breakdown (Mortimer, 1981), and consisted of a short, high-amplitude depolarizing pulse followed by a longer, low-amplitude charge balancing

pulse. A biphasic pulse is shown schematically in the top trace of Fig. 4.4. Typically, the depolarizing pulse was 5 to 10 mA and 50 to 100 μs in duration, and the charge balancing pulse was ten times smaller in amplitude and ten times longer in duration. Stimulation repetition rates ranged from 25 to 33 Hz. The repetition rate and stimulation pulse amplitude and duration parameters were preset based on observations of PalL muscle force output in experiments under anesthesia, but were adjusted during the state controller experiments if necessary.

Stimulus artifacts were clearly observable in nerve cuff signals during stimulation of the PalL. The stimulus artifact normally resembled a filtered stimulation pulse, as shown in the second trace in Fig. 4.4. The artifact amplitude depended on distance from the stimulation point to the recording nerve cuff and on the common mode rejection properties of the nerve cuff. The artifact decay characteristics depended on the stimulus pulse amplitude and duration and tissue conduction properties.

Stimulus artifact rejection circuitry was designed utilizing JFET analog multiplexers (Precision Monolithics, Inc., MUX-24), with two inputs to each switch: the nerve cuff signal or ground. During each stimulation pulse, the nerve cuff recording channel was switched to ground for a short period to avoid recording the stimulus artifact. The main BPG generated a synchronization pulse with each stimulus which triggered a second BPG to control the duration of the blanking pulse, which was normally 2-3 ms. A 50 μs delay between the synchronization signal and the biphasic pulse output of the main BPG ensured that the channel would be blanked prior to stimulus delivery. The output of switching circuits were low-pass filtered at 10 kHz to reduce switching noise.

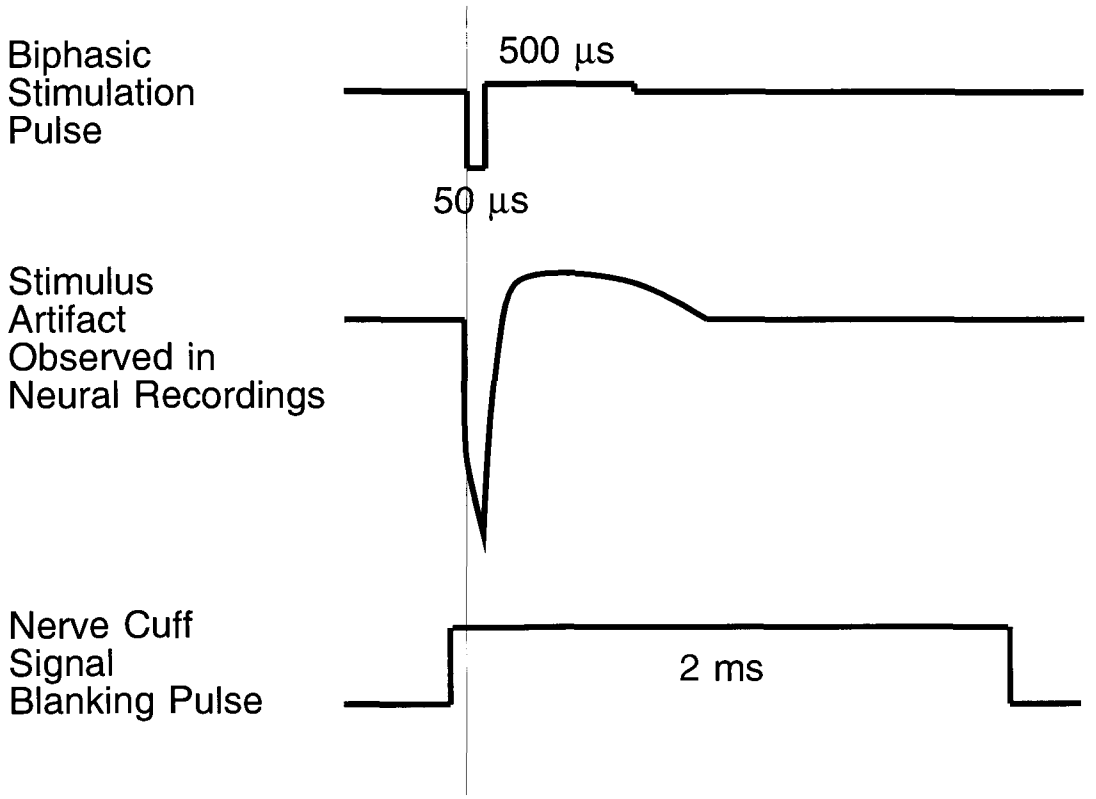

Figure 4.4: Typical biphasic stimulation pulse and expected stimulus artifact observed in nerve cuff recordings. Stimulus artifact rejection was achieved by using a blanking pulse to ground the ENG signal for the period where stimulus artifacts are expected. The start of the blanking pulse preceded the stimulation pulse to minimize initial artifact in the neural signals, and the duration of the blanking pulse was set independently of the stimulation pulse to omit the entire stimulus artifact.

Figure 4.5 shows a typical recording of the Median ENG from the cat forelimb during walking on the treadmill. The top panel in Figure 4.5 shows the nerve cuff signal sampled at 10 kS/s with stimulus artifacts resulting from tonic 25 Hz stimulation of the PalL with 5 mA depolarizing pulses. The bottom panel shows the nerve cuff signal when a blanking pulse lasting 2 ms was used during tonic stimulation of the PalL.

Blanking the nerve cuff signal effectively reduced the integrated signal amplitude by the duration of the blanking pulse multiplied by the stimulus repetition rate, and this should be taken into consideration in multi-channel FES systems where many muscles are being phasically stimulated at higher rates. Other stimulus artifact reduction techniques may be required for these types of systems (e.g. Haugland and Hoffer, 1994b).

4.2.5. Anesthetic Block of the Median Nerve

During the blocking experiments, 2% Lidocaine solution was injected through the catheter into the proximal Median blocking cuff to cause a conduction block of the nerve. The goal was to temporarily remove voluntary control of wrist flexor muscles, including the PalL. Typically, an initial injection of 0.6 ml was followed with smaller doses of 0.1 or 0.2 ml every minute until the PalL EMG was reduced and a yield about the wrist was observable during walking on the treadmill. The block of the proximal Median nerve affected all of the innervated wrist muscles and resulted in a large yield in wrist and paw flexors. During the block, the cat walked with its wrist on or near the treadmill belt rather than walking on its toes with its wrist 1 to 2 cm above the belt.

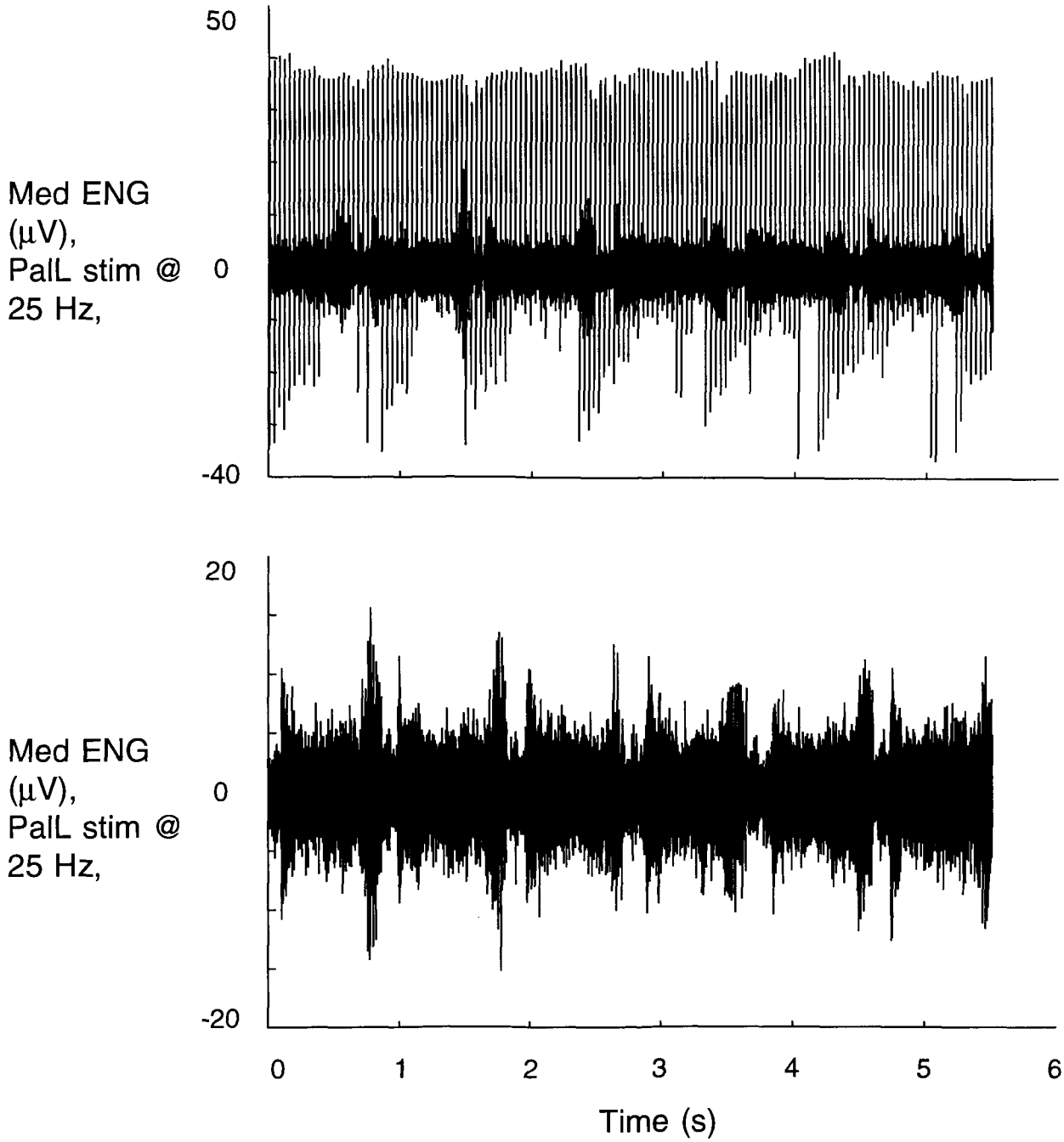

Figure 4.5: Typical nerve cuff recordings (sampled at 10 kS/s) from the Median nerve during walking on the level treadmill at 0.5 m/s (NIH-15, day 106). The top panel shows Median ENG contaminated with stimulus artifact resulting from tonic 25 Hz stimulation of the PalL. The bottom panel shows the results of blanking the Median nerve cuff channel to ground for each stimulus pulse to eliminate the stimulus artifact and produce a clean ENG signal.

4.2.6. Evaluation of FES State Controller and PalL Stimulation

In Strange and Hoffer (1996), the PalL activity prediction errors of the model state controllers were analyzed in terms of percentage timing errors between predicted PalL activity and recorded activity. In the experiments discussed in this paper, the PalL activity predicted by the real-time state controller was calibrated on-line by visually comparing the timing of the stimulation control signal with the PalL EMG. The timing of the stimulation (using a bright LED triggered by the stimulation pulses) was also displayed in the video of the cat walking to correlate stimulation with the step cycle.

Median and Radial ENG thresholds were calibrated to produce the best prediction of PalL timing at the beginning of each experiment for normal walking on the treadmill. The neural thresholds were then held constant during the rest of the recording session, including the stimulation and blocking experiments in different walking conditions. Physiological data and stimulation control signals were collected on-line during the experiments, with all signals digitally sampled at 1 kHz per channel using DataSponge (Biosciences Analysis Software, Ltd.). The prediction error of timing of PalL activity for non-stimulation experiments was estimated by comparing off-line the stimulation control signal to the recorded PalL EMG (Strange and Hoffer, 1996). In experiments with PalL stimulation, the natural PalL EMG was unavailable.

Video recordings of the cat were analyzed off-line to evaluate the effect of the Median nerve conduction block and the effect of the stimulation applied to the PalL. The elevation of the wrist, as monitored by a marker attached to the wrist, and hence the yield in the wrist muscles at foot contact and during stance was measured directly from the monitor screen for three conditions: walking normally prior to nerve block, walking with the nerve blocked, and walking with the nerve blocked and with stimulation of the PalL.

4.3. RESULTS

4.3.1. On-line Prediction of Timing of PalL Activity During Walking

Figure 4.6 presents representative results of on-line prediction of the timing of PalL activity for NIH-16 during walking on the level treadmill at 0.5 m/s. The bin-integrated Radial and Median nerve cuff signals (inputs to Schmitt triggers) are shown in the top two panels respectively, along with the thresholds used by the Schmitt trigger circuits. The output of the state controller is shown in the bottom panel, superimposed onto the actual PalL EMG.

In Figs. 4.6-9, the PalL EMG has been bin-integrated to 10 ms bins and the neural, threshold, and state controller signals have been decimated to a sampling rate of 100 Hz to reduce the amount of data. The signal amplitudes in the top two panels of Figs. 4.6-9 are the voltage levels seen at the inputs of the Schmitt triggers after amplifier gains of 10^5 or 10^6. The PalL EMG envelope resulted from an amplifier gain of 10^3 and integration gain of 10 (sampling rate of 1 kS/s bin-integrated to 10 ms bins). The predicted PalL activity pulse is a TTL level signal scaled off-line to correspond with the level of the EMG.

Figure 4.6 shows that the state controller accurately detected the neural spikes resulting from foot contact and lift-off and accurately predicted the start and end times of PalL activity. The state controller turned ON at foot contact when the Median ENG signal surpassed the Median threshold (middle panel; level = 1.32 V), and the state controller turned OFF at lift-off as the Radial ENG rose above the Radial threshold (top panel; level = 0.92 V).

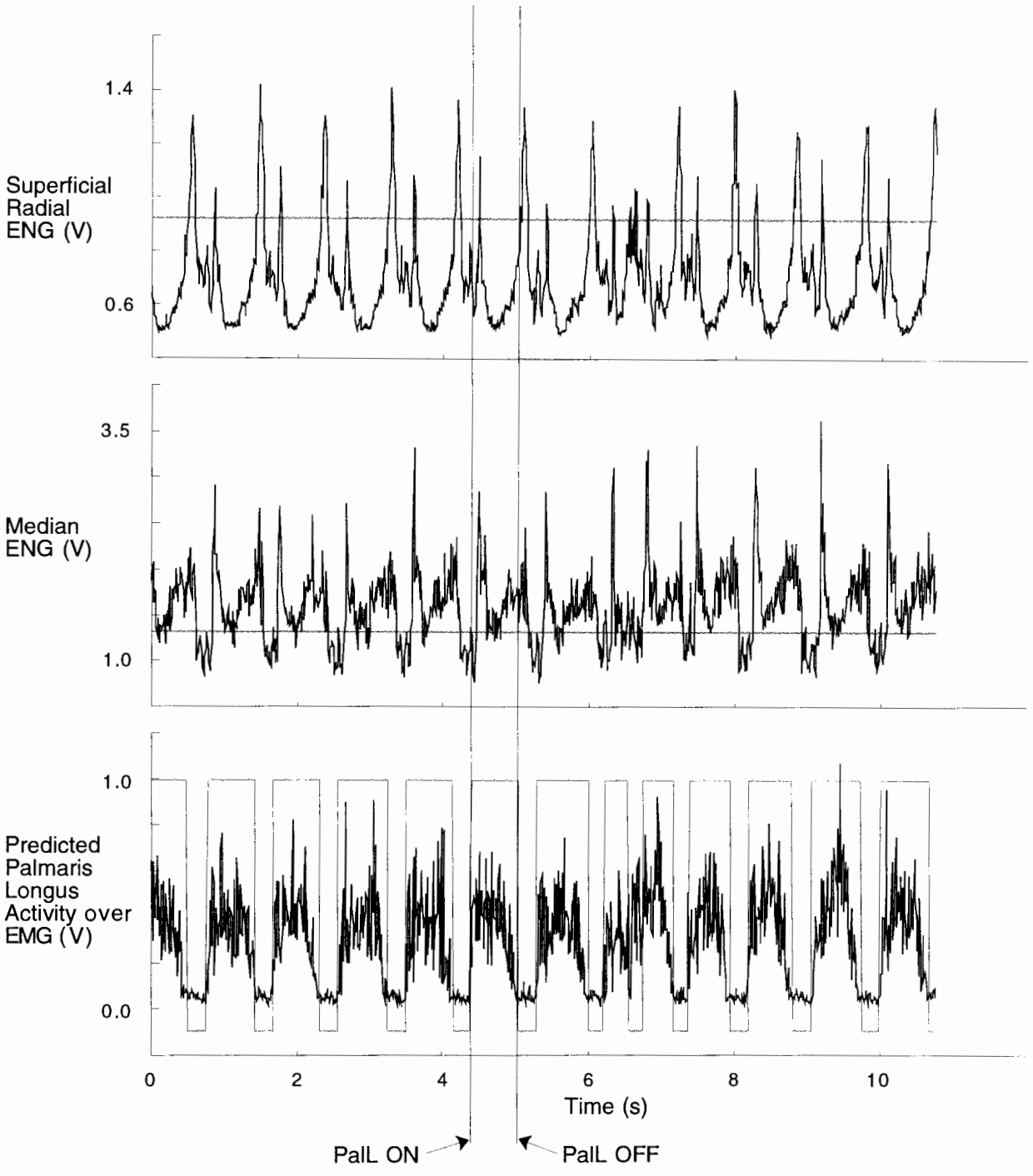

Figure 4.6: Results of open-loop state controller experiments for level walking at 0.5 m/s (NIH-16, day 62a). In the open-loop experiments, the PalL was not stimulated. The top panel shows the amplified envelope of Superficial Radial ENG supplied to the Schmitt trigger with a threshold of 0.92 V. The middle panel shows the envelope of the Median ENG supplied to the Schmitt trigger with a threshold of 1.32 V. The bottom panel shows the predicted PalL activity superimposed on the recorded PalL EMG.

The hardware state controller accurately predicted PalL activity for all steps, of either normal or abnormal duration, with transition errors similar to those found during simulations of the state controller reported in a companion paper (Strange and Hoffer, 1996). In the case of a hesitation step, which occurred at 6 s in Fig. 4.6 when the cat began to lift the foot but stepped down on it again, the state controller regained the correct state in 200 ms (the minimum transition delay set by Radial and Median delay in Fig. 4.3). The state controller accurately predicted the next normal step following the hesitation step.

4.3.2. On-line Prediction During Walking at Different Treadmill Velocities

The state controller performance was tested as the cat walked at different treadmill velocities up to 1.0 m/s. Figures 4.7A and 4.7B show representative results of state controller prediction of PalL activity for treadmill velocities of 0.75 and 1.0 m/s respectively.

The state controller accurately predicted the timing of PalL activity for every step (15 steps at 0.75 m/s, and 19 steps at 1.0 m/s are shown in Fig. 4.7), with small error between the predicted and actual PalL activity. Step-to-step variation in each trial, as observed in the variations in timing and amplitude of the neural and muscle signals, were successfully accommodated by the state controller. The Median ENG peak amplitudes increased with treadmill speed as the stance phase duration decreased and the force of foot contact increased, as shown in Figs. 4.6 and 4.7, yet the Radial ENG peaks remained similar for all velocities tested for subject NIH 16. PalL EMG also increased with increasing treadmill velocities, which agreed with earlier recordings from the cat forelimb reported in a companion paper (Strange and Hoffer, 1996).

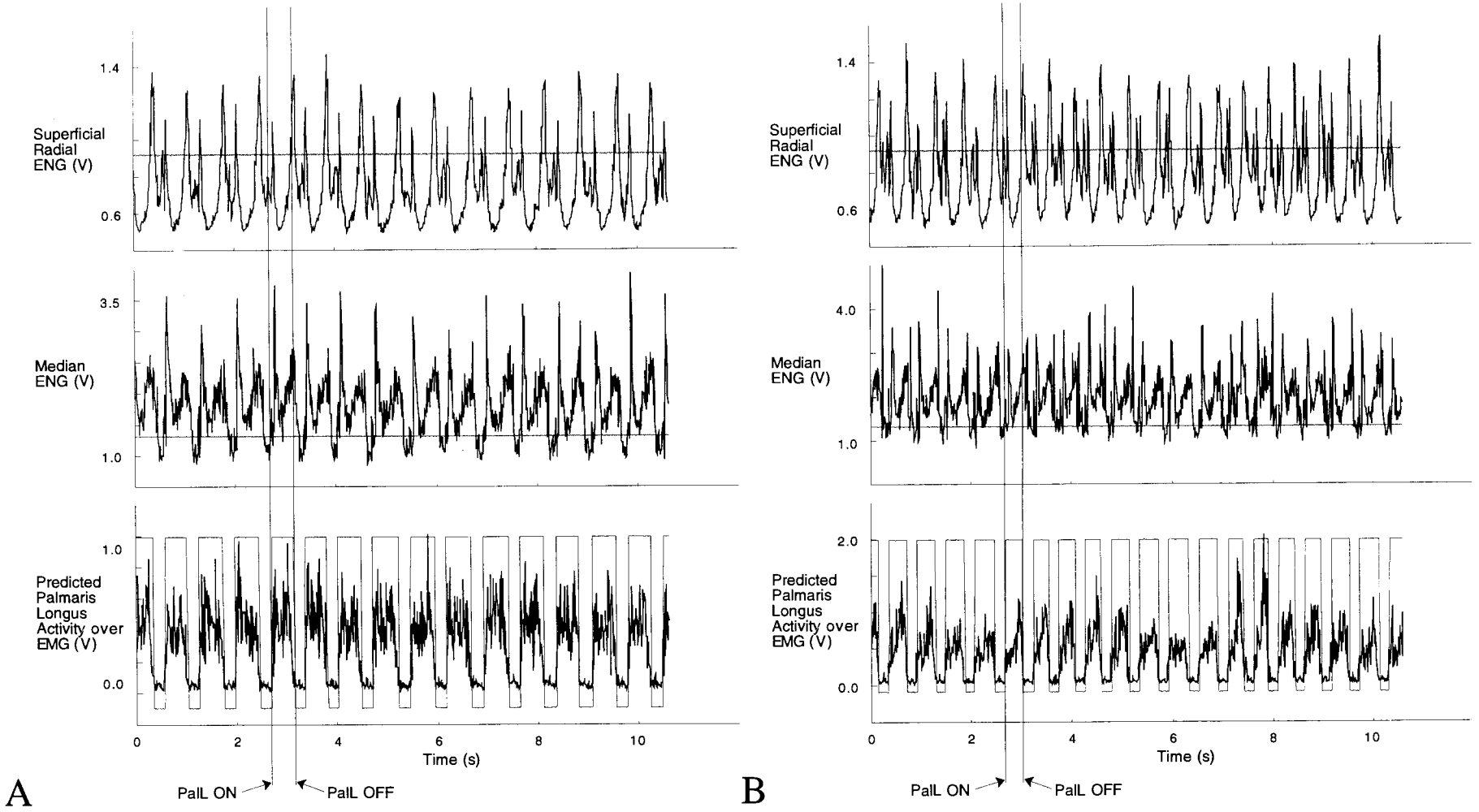

Figure 4.7: A. Results of open-loop state controller experiments for level walking at 0.75 m/s (NIH-16, day 62e). B. Results of open-loop state controller experiments for level walking at 1.0 m/s (NIH-16, day 62b). In the open-loop experiments, the PalL was not stimulated. The top panels show the amplified envelope of Superficial Radial ENG supplied to the Schmitt trigger with a threshold of 0.92 V. The middle panels show the envelope of the Median ENG supplied to the Schmitt trigger with a threshold of 1.32 V. The bottom panels show the predicted PalL activity superimposed on the recorded PalL EMG.

4.3.3. On-line Prediction During Walking at Different Treadmill Slopes

The state controller was also tested as the cat walked at different slopes on the treadmill. Figures 4.8A and 4.8B present data recorded as the cat walked at 0.5 m/s uphill and downhill at ±10% grades, respectively. The state controller accurately predicted the timing of PalL activity for all normal steps.

Figure 4.8A shows that the state controller predicted every step for the first 9 s of uphill walking at 0.5 m/s, up until the cat did a hesitation step: he started to lift his paw at the end of stance but then delayed and actually stepped down harder, as evidenced by the increased Median ENG and increased PalL EMG. However, the state controller detected a peak in the Radial ENG signifying the end of stance, and entered the OFF state. The continued high level of Median ENG initiated a false next ON state after the appropriate delay and the controller was now in the wrong state for the next real step. The controller adjusted to the second from last step and returned to the correct state for the last step shown in Fig. 4.8A.

Figure 4.8B shows that the state controller accurately predicted every step during downhill walking at 0.5 m/s, including a relatively long duration step at 2 s and the next relatively short duration step at 4 s. These steps, while varying greatly in stance phase duration, were normal steps and exhibited step-to-step variation that should be expected and accounted for by FES controllers.

4.3.4. State Controller Results With Stimulation Over Natural PalL EMG

In the second set of experiments, the FES state controller was tested in trials where the PalL was stimulated against a background of naturally occurring EMG. Results from trials recorded at

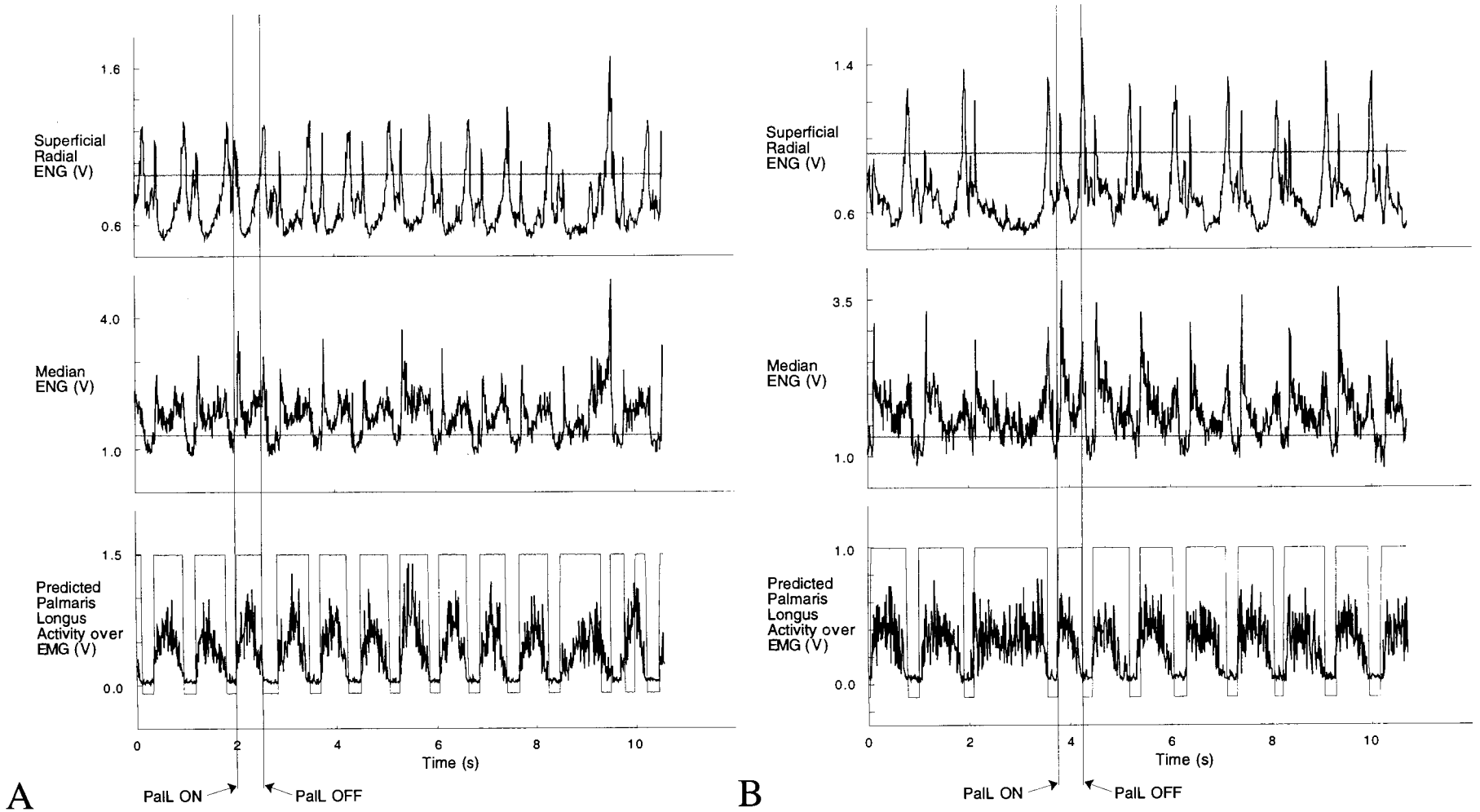

Figure 4.8: A. Results of open-loop state controller experiments for +10% uphill walking at 0.5 m/s (NIH-16, day 62c). B. Results of open-loop state controller experiments for -10% downhill walking at 0.5 m/s (NIH-16, day 62d). In the open-loop experiments, the PalL was not stimulated. The top panels show the amplified envelope of Superficial Radial ENG supplied to the Schmitt trigger with a threshold of 0.92 V. The middle panels show the envelope of the Median ENG supplied to the Schmitt trigger with a threshold of 1.32 V. The bottom panels show the predicted PalL activity superimposed on the recorded PalL EMG.

different treadmill velocities are shown in Fig. 4.9. Figures 4.9A and 4.9B show data recorded from the state controller as the cat walked on the level treadmill at 0.5 and 1.0 m/s respectively. The PalL was phasically stimulated with bursts of 25 Hz biphasic pulses during the PalL ON states, using depolarizing pulses 5 mA in amplitude and 50 μs in duration and charge balancing pulses -0.5 mA in amplitude and 0.5 ms in duration. These current levels and burst rates were determined to produce reasonable wrist flexion in experiments under anesthesia and were expected to provide sufficient wrist function during walking.

The Radial and Median ENG signals in Fig. 4.9 show very similar patterns as those recorded in trials without stimulation, although some noise was present in the Median ENG (stimulus artifact and switching noise), and the overall amplitude of both signals is slightly lower than in trials where stimulus artifact blanking circuits were not used. A possible reason for the observed noise pickup in the Median ENG signal was the close proximity of the stimulating patch electrode on the PalL to the recording cuff on the Median nerve (approximately 3 cm).

Even with the observed stimulus artifacts, the state controller accurately predicted every step at both treadmill velocities shown in Fig. 4.9. The gait pattern showed considerable variation from step to step, especially at the higher treadmill velocity, and the state controller successfully predicted the state transitions at foot contact and lift-off.

During these trials, there was no PalL EMG to record and to compare with the state controller output, so the challenge was to determine if stimulation affected the step cycle or gait pattern. Video recordings were analyzed and it was determined that stimulating the PalL at these current levels and repetition rates over the natural EMG did not appreciably add to the wrist flexion during the stance phase and did not elevate the wrist higher than in non-stimulated walking. The cat did not appear to sense the stimulation and walked normally.

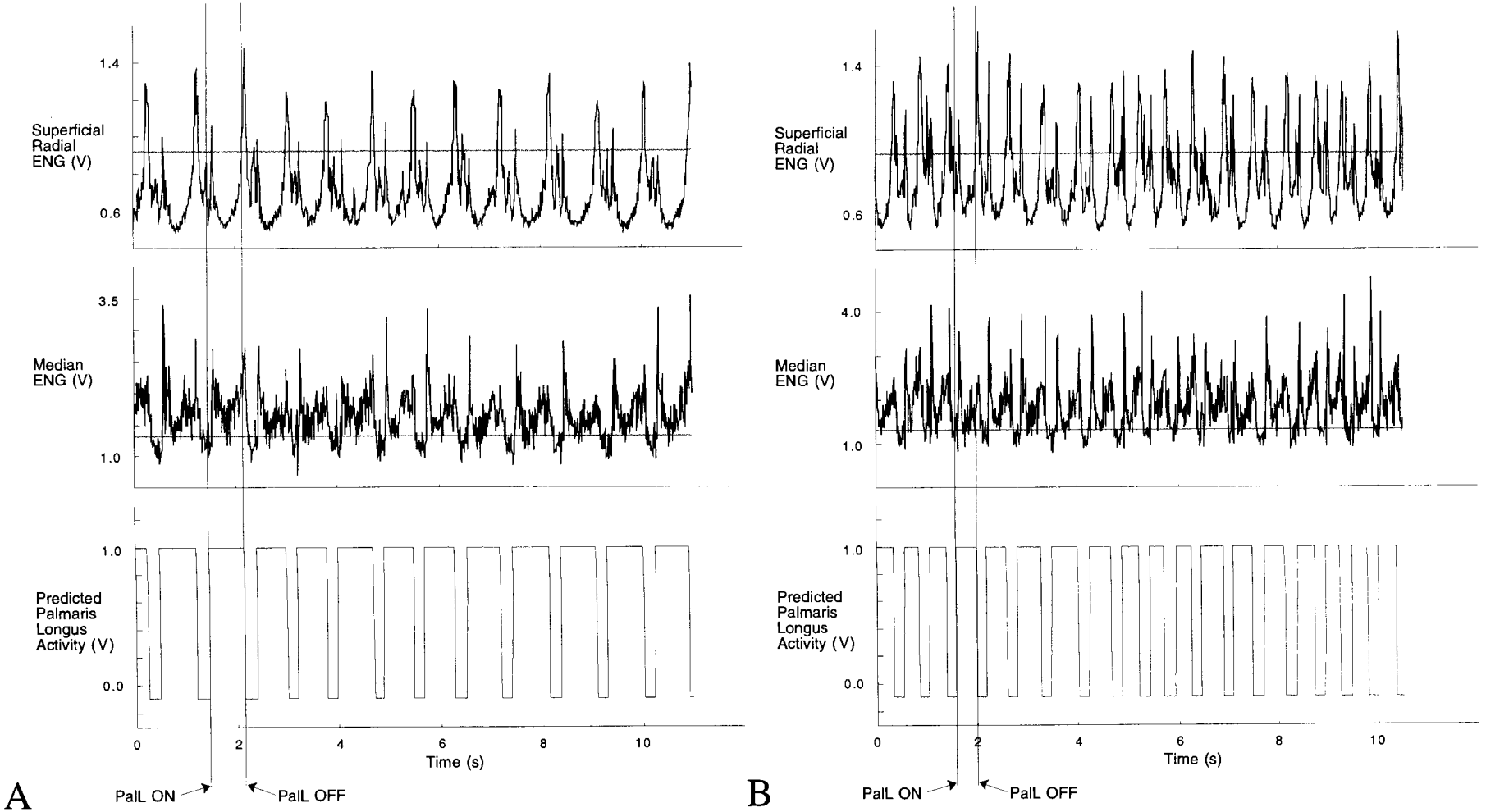

Figure 4.9: A. Results of closed-loop state controller experiments for level walking at 0.5 m/s (NIH-16, day 62f). B. Results of closed-loop state controller experiments for level walking at 1.0 m/s (NIH-16, day 62h). The top panels show the amplified envelope of Superficial Radial ENG supplied to the Schmitt trigger with a threshold of 0.92 V. The middle panels show the envelope of the Median ENG supplied to the Schmitt trigger with a threshold of 1.32 V. The bottom panels show the predicted PalL activity (note no PalL EMG recorded here).

4.3.5. Functional Recovery with FES State Controller During Reversible Paralysis

The final test for the state controller was to temporarily paralyze the PalL and determine if the FES system could return function to the wrist through electrical stimulation. The Median nerve conduction block was tested under anesthesia in CAP recording sessions, where the evoked Median CAP and PalL EMG could be reduced to zero with an initial dose of 0.6 ml Lidocaine was followed by 0.1 to 0.2 ml doses every minute for approximately 20 minutes. To replicate these conditions in the recording sessions with the awake cat, 2% Lidocaine solution was introduced into the proximal Median blocking cuff as the cat sat quietly on the treadmill. In the blocking trials with stimulation, the block was initiated immediately after calibrating the state controller during normal walking to reduce the time for the overall experiment.

It was important to determine if the cat walked normally and if the Radial and Median ENG patterns remained similar during the blocking trials, to determine if the feedback signals for the state controller still contained useful information. Figure 4.10 presents representative cutaneous nerve ENG recordings and state controller output during the Median nerve conduction block for level walking at 0.5 m/s (NIH-16, day 62r). The top two panels show amplified envelopes of Superficial Radial and Median nerve cuff signals, along with the associated thresholds used by the Schmitt triggers (the thresholds were the same for the entire recording session on that day, as shown in Figs. 4.6 - 4.9). The ENG patterns during the nerve block were very similar in both timing and amplitude to those signals recorded during normal walking as shown in Figs. 4.6 - 4.8. The Median nerve ENG showed bursts of activity at paw contact, and the Radial nerve ENG showed bursts of activity at paw lift-off, which suggested that the cat was walking normally even with the loss of sensation of paw contact and reduced motor control of the wrist plantar flexors. Video analysis of the gait patterns during the Median nerve conduction block also suggested that the cat walked with a steady gait and did not favour one forelimb over the other.

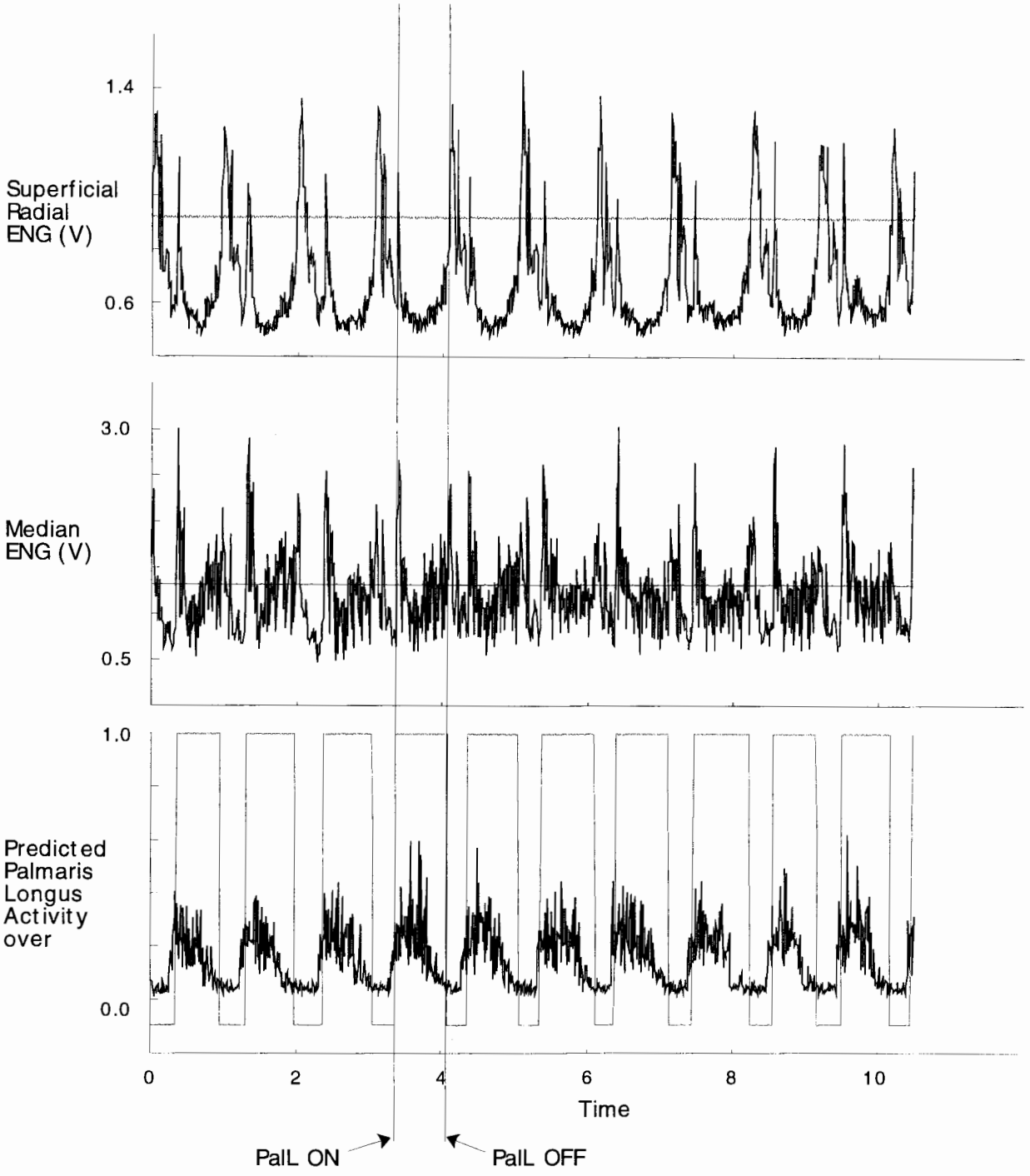

Figure 4.10: Cutaneous nerve recordings and state controller prediction during Median nerve conduction block for level walking at 0.5 m/s (NIH-16, day 62r). In this trial the PalL was not stimulated. The top panel shows the amplified envelope of Superficial Radial ENG supplied to the Schmitt trigger with a threshold of 0.92 V. The middle panel shows the envelope of the Median ENG supplied to the Schmitt trigger with a threshold of 1.32 V. The bottom panel shows the predicted PalL activity superimposed on the remaining PalL EMG which was still evident during the nerve conduction block.

The bottom panel of Fig. 4.10 shows the state controller output superimposed onto the remaining PalL EMG during walking with the Median nerve block. The timing of the output closely agreed with the timing of the step cycle and the associated PalL activity, although the PalL EMG data suggests an overall decrease in amplitude and a slight phase advance in PalL onset prior to paw contact. The changes in the PalL EMG patterns during the Median nerve conduction block suggested that the block was not complete and that PalL was less active during walking.

Blocking the Median nerve above the elbow affected several muscles, not just the PalL. Motor function was reduced in the FDP as well as all of the wrist flexor muscles innervated by the Median nerve. During walking on the level treadmill at 0.5 m/s, a noticeable yield occurred in the wrist flexor muscles as the cat supported its weight on its wrist rather than on its toes, as shown schematically in Fig. 4.11. The paw positions shown in Fig. 4.11 represent four positions during the stance phase: foot contact, one video frame (34 ms) after contact, the time at which the forelimb below the elbow was orthogonal to the treadmill belt, and the last video frame prior to foot lift-off. The trajectory of the marker on the wrist and the wrist elevation are displayed with the dotted line for both normal walking (top panel) and walking during Median nerve conduction block (bottom panel).

Figure 4.12 shows the wrist elevation measured during trials of normal walking, walking with a partially blocked Median nerve, and walking with a partially blocked Median nerve assisted by electrical stimulation of the PalL with bursts of 33 Hz biphasic pulses (depolarizing pulse was 10 mA and 400 us). Each data trace represents an average of 10 consecutive steps, recorded in NIH-16 (day 78) walking on the level treadmill at 0.5 m/s.

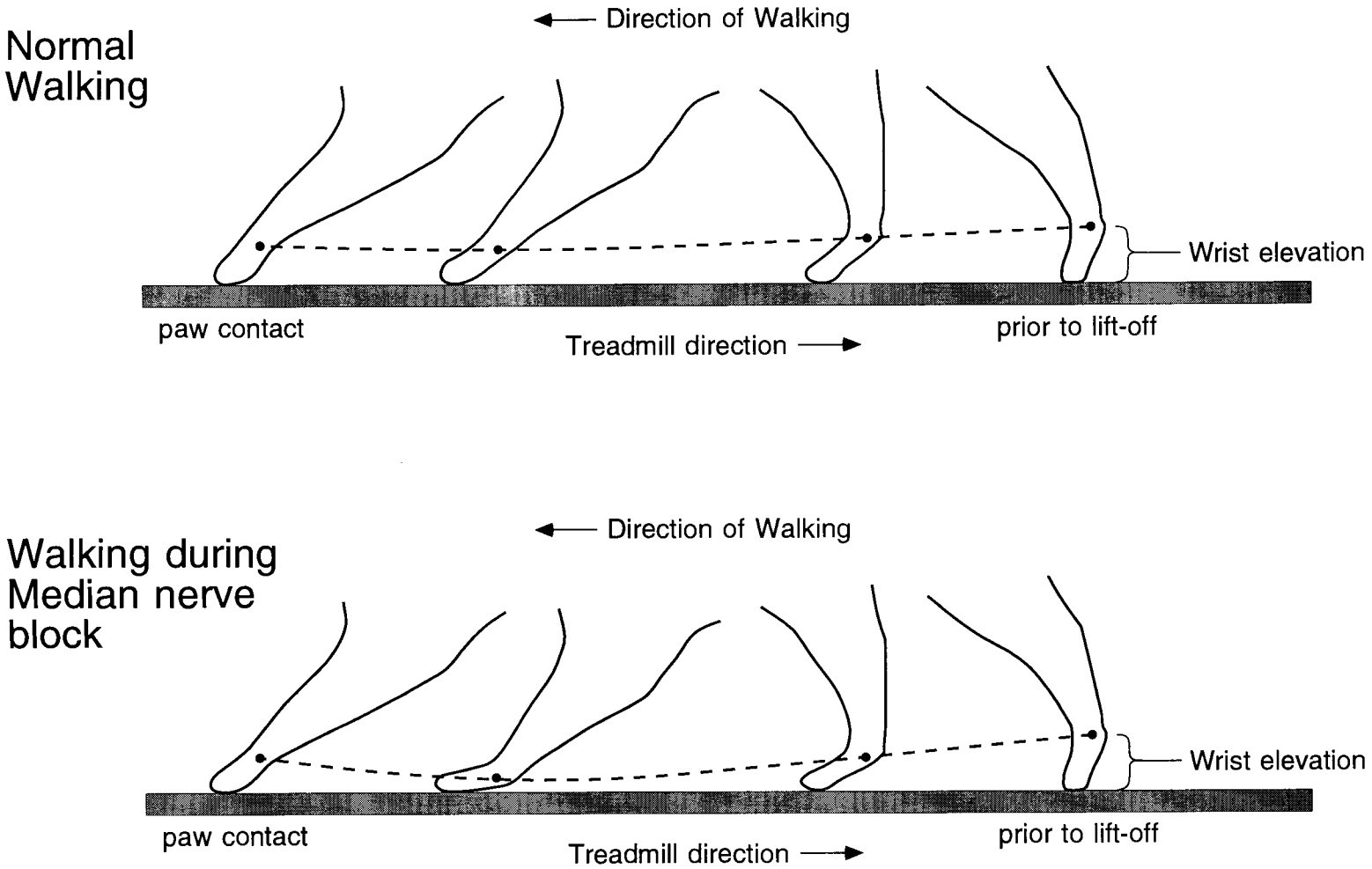

Figure 4.11: Schematic diagram of effects of Median nerve conduction block. Both panels show the left forelimb in four positions in the stance phase, from paw contact on the left to just prior to lift-off on the right. The wrist elevation was measured directly from video taken during the blocking experiments by recording the distance from the treadmill belt to the middle of the marker. The top panel shows the wrist elevation during normal walking where the cat walks on its toes and the wrist is relatively stiff. The bottom panel shows the typical wrist elevation when the Median nerve is blocked, where there is more yield in the wrist flexor muscles following contact and throughout the stance phase.

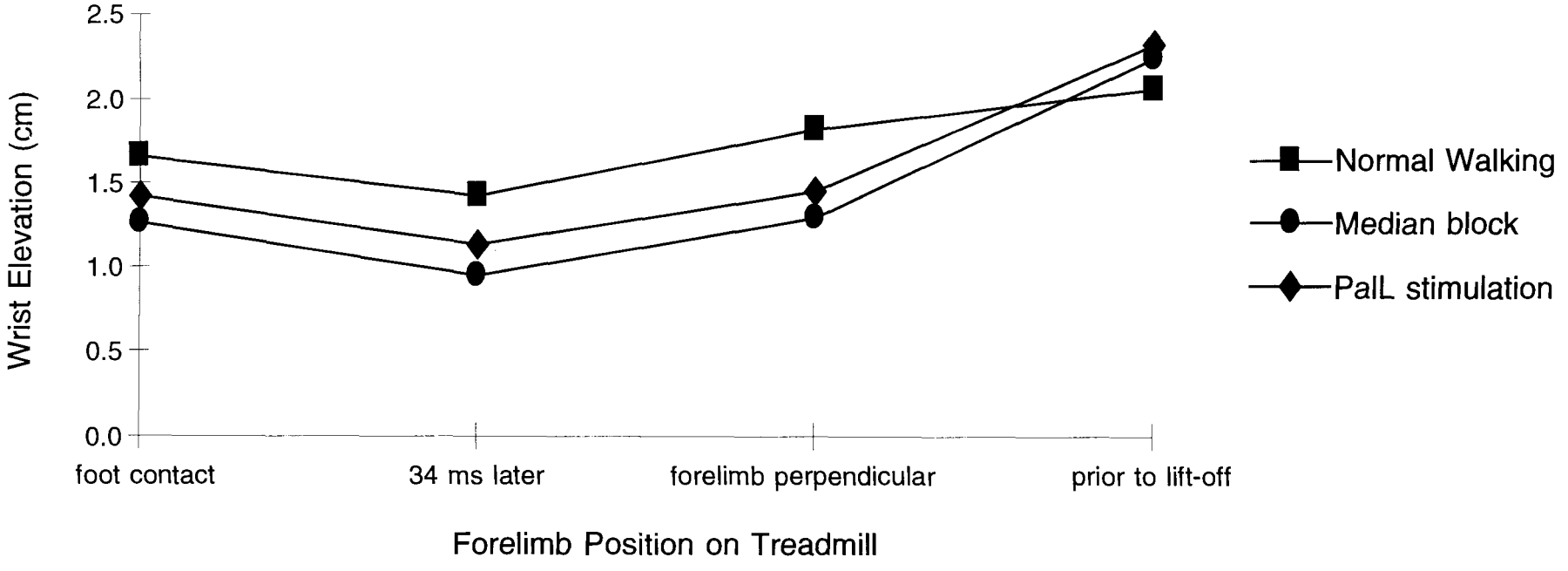

Figure 4.12: Results of closed-loop state controller experiments for level walking at 0.5 m/s (NIH-16, day 78) following Median nerve conduction block. The three traces represent wrist elevation averages for 10 consecutive steps in three situations: 1) normal walking (square), 2) walking following Median nerve conduction block (circle), and 3) FES-assisted walking following Median nerve conduction block. The experiments were conducted in this order to show that closed-loop stimulation of the PalL returned some function to the wrist following partial paralysis of all wrist flexors innervated by the Median nerve.

Figure 4.12 shows that partially blocking the Median nerve clearly resulted in a lower wrist position at foot contact and a lower wrist position for the duration of the stance phase. Stimulation resulted in an observable increase in plantar flexion throughout the stance phase, and a decrease in yield about the wrist following contact. The results were significant considering that only the PalL was stimulated and this was sufficient to return some function to the wrist during partial paralysis of most of the wrist flexors.

During prolonged recording sessions with anesthetic block, the cat would sometimes get fatigued and walk clumsily from side to side of the treadmill. In these cases, the step cycle and gait patterns were difficult to interpret and the state controller exhibited higher prediction errors. In some cases the cat also shook its paw and apparently noticed the lack of sensation from the paw.

4.4. DISCUSSION

The results of implementing the FES state controller described in this paper demonstrate that afferent sensory signals from nerve cuffs are a viable and useful source of feedback for control of FES. In the presence of closed-loop plantar-flexor muscle stimulation during the stance phase, the system performed reliably for a wide range of walking conditions.

The long-term stability of nerve cuff signals recorded from cutaneous nerves in the cat forelimb was shown in a companion paper (Strange et al., 1996), for implant periods up to and exceeding 180 days. This stability can be achieved with proper design of implantable devices, care for the nerves during implant surgeries by using appropriate materials and cuff closing techniques (Kallesøe et al., 1996), and special precautions in the routing of leadout wires exiting the body. In the future, fully implantable telemetry FES systems are expected to further reduce strain on implanted devices and tissues, and should reduce failures caused by internal wire breakages.

Although FES implementation presented here was developed for one cat, the simulations discussed in a companion paper (Strange and Hoffer, 1996) demonstrate the robustness of the state controller when tested with data from different cats on different days in a variety of walking conditions on the treadmill. Given the stability of implanted cuff impedances and evoked nerve CAPs over long implant periods, cutaneous ENG signals recorded during walking on the treadmill can be expected to be reliable feedback signals to the real-time FES state controller. An additional factor contributing to the stability of feedback signals was the low variation of the Median and Radial ENG activity patterns from step-to-step for each trial. Nerve signal amplitudes varied less than the corresponding EMG signals from forelimb muscles in the same steps. This consistency in the patterns of whole nerve cutaneous ENG signals provides confidence that the neural signals can be utilized as feedback with minimal need for calibration of thresholds for detecting gait events (Strange and Hoffer, 1996).

Clinical FES systems that implement ENG feedback will require methods to eliminate stimulus and evoked compound EMG artifacts. In this study, the bin-integrated neural signals were slightly reduced in overall amplitude during the stimulation phases, with the reduction dependent upon stimulation burst frequency and the length of the stimulus artifact blanking pulse. Although some stimulus artifact and switching noise was still present, the FES state controller continued to produce accurate predictions of the stance phase and timing of PalL activity. Alternate methods to eliminate stimulus artifact have been developed which include selective sampling of the neural signals at expected low-noise periods (Haugland and Hoffer, 1994b), and selectively pausing the recording channel with a sample and hold circuit (Nicolic et al., 1994).

Previous clinical FES systems that utilized cutaneous nerve signals from implanted cuffs used pre-programmed counters to specify the duration of states or phases. In an experimental system to correct for drop foot in humans, the Sural nerve provided an accurate signal of heel contact which was used to stop the stimulation of foot dorsiflexors at the end of the swing phase. Since in that application the Sural nerve signal could not provide an accurate foot lift-off signal, a counter was used to start stimulation of the dorsiflexors at a pre-specified time following heel contact (Haugland and Sinkjaer, 1995). In another state controller implemented in the cat hindlimb, the Tibial and Superficial Peroneal nerves were instrumented and provided independent information regarding the onset of Medial Gastrocnemius and Tibialis Anterior muscle activity respectively during walking. Counters were used to set the duration of activity for each muscle, based on average duration of muscle activity for an arbitrary gait pattern (Popovic et al., 1993). These types of systems are velocity-dependent, and will operate accurately within a narrow velocity range but may introduce errors outside this operating range.

The state controller presented here worked reliably because it utilized two independent neural inputs. This allowed for accurate detection of both foot contact and foot lift-off at a variety of treadmill velocities and slopes. Detection of both state transitions enabled the implementation of a

velocity-independent state controller that operated reliably for all conditions tested. This demonstrates the power of utilizing more than one independent feedback channel for improved closed-loop control of FES systems.

The simplicity of the state controller approach discussed here demonstrates the usefulness of including cutaneous neural feedback in FES control systems to detect the timing of events and phase changes in the step cycle. Closing the loop and stimulating the PalL following Median nerve block and partial paralysis of most wrist flexor muscles resulted in partial return of normal wrist function during walking. Stimulation of additional muscles with a multi-channel FES system would probably have produced even better results. It is expected that in clinical applications of this approach, the residual function in the affected limb and the functional effects of stimulation of remaining muscles must be evaluated to determine the most appropriate stimulation patterns for each individual case.

Although the present state controller accurately predicted the timing of the step cycle and of the activity of one muscle, it did not provide amplitude modulation of the stimulation control signal. In future FES systems it may be desirable to implement stimulation patterns (either current amplitude or pulse duration modulation) that more closely emulate natural EMG patterns recorded in normal individuals. Although the EMG patterns in normal subjects may not necessarily translate into efficient function in patients, the EMG signals could provide a useful starting point for developing efficient stimulation patterns.

The hand crafted rules with single thresholds developed here can be applied to relatively simple closed-loop FES systems with successful results, but more powerful nerve signal analysis tools may be required for more complex systems (Andrews et al., 1989; Veltink et al., 1990; Chizeck, 1992; Popovic, 1992). Machine learning techniques have been applied to automatic rule generation of control signals for closed-loop FES (Kostov et al., 1994; Kostov et al., 1995a,b,c). Recent preliminary results implementing adaptive logic networks have provided excellent

prediction of both timing and amplitude modulation of EMG signals (Kostov et al., 1996, in preparation).

4.5. CONCLUSIONS

In this study we have demonstrated that an FES state controller utilizing two sources of cutaneous neural feedback from the cat forelimb can accurately predict the start and end of the stance phase and the timing of PalL activity during walking on a treadmill. The controller used single threshold detection on each nerve cuff signal to accurately identify events in the step cycle such as foot contact and lift-off for a variety of treadmill speeds and slopes. The reliable nature of cutaneous nerve signals was demonstrated by the fact that the same neural thresholds were used from trial to trial and provided accurate results across all conditions tested with minimal need for threshold calibration.

The results of this study suggest that accurate, reliable feedback signals can be obtained from nerve cuffs implanted on cutaneous sensory nerves and utilized in closed-loop control of FES state controllers.

Chapter 5: General Discussion

The experiments discussed in this thesis were designed to address three central questions regarding the use of natural sensory signals as a source of feedback for FES: 1) are nerve signals recorded from nerve cuffs chronically implanted in the forelimbs of cats stable over long term implant periods? 2) can nerve cuff recordings from sensory nerves provide useful, reliable information regarding foot contact and other gait events? and 3) can sensory nerve signals be implemented in a closed-loop FES system to restore the use of paralyzed wrist plantar flexor muscles during walking?

Other key topics and results included the feasibility of state controller systems for FES, variability of neural signals over time and in different walking conditions, stimulus artifact rejection through blanking neural recording channels, and simulated paralysis through the use of local anesthetic to effect conduction block in the extremity.

5.1. LONG-TERM STABILITY OF NERVE CUFF SIGNALS

The average CAP results discussed in Chapter 2 suggest that recording nerve cuffs may be implanted for long term use without introducing extraordinary damage to the nerves. The averaged CAP amplitude and conduction latency data in the second series of implants showed that both the condition of the nerves and the implanted cuffs remained stable and functional for periods over six months. These are important results considering the longevity problems of other neural recording devices in the extremity, such as hatpin electrodes and silicon intrafascicular probes which have had problems due to their fragile nature, tendency to migrate within the nerve fascicle,

and tendency to suffer from encapsulation by connective tissue (Hoffer, 1990; Kallesøe and Hoffer, 1994; personal communications).

The recording nerve cuffs implanted in the second series of subjects included a number of improvements, namely a patented closing technique using interdigitated closing tubes and a baton to ensure the circumference of the cuff, and a method of shorting together the outer reference electrodes at the cuff rather than at the recording station. The cuffs with the new closing technique were much simpler and safer to implant as sutures were often difficult to tie tightly around the cuff. The removal of the sutures eliminated the possibility of local tissue reactions to the suture material and the sutures dissolving in long term implants, and reduced the possibility of the cuff opening over time. In addition, the use of a baton to close and fix the circumference of the nerve cuff also ensured that the cuff could not spiral in on itself, as observed in earlier experiments (Hoffer, 1975; unpublished observations).

The main drawback of using implanted nerve cuffs in the animal models was the use of wires to transmit information from the nerve cuff to a backpack connector. The wires showed a tendency to break in the presence of repeated movement where the wires crossed joints and especially where the wires exited the body and attached to the backpack. In a number of cases in the first series of implants, the wires were snagged and broken by the cats as they scratched at the backpack sutures. This problem was rectified in the second series of implants by the use of a fabric belly band which encircled the backpack and the belly of the cat and restricted access to the backpack sutures and wires. The use of improved backpack sutures made of No. 5 sutures enclosed by silicone tubing also reduced the chance of infection and irritation at the backpack sutures in the second series, resulting in a lower incidence of pulled or broken wires at the backpack.

The most obvious solution to broken wires due to repeated movement and snagging would be to remove the wires altogether and implement a telemetry system to transmit neural and other information out of the body. Of course this solution introduces a number of other technical

concerns, namely providing sufficient power to internal devices for recording purposes and designing a two-way telemetry system with minimal noise that both supplies power and transmits relatively small amplitude physiological signals through tissue. An interesting option once power is supplied into the body for telemetry, is to instrument and power some of the recording devices with instrumentation amplifiers and filters. Conditioning the neural signals at the source with active circuitry should lead to improved signal-to-noise ratios over traditional passive recording techniques. New approaches to totally implanted FES systems in humans would also benefit from the use of telemetry within the body to avoid the occurrence of broken wires in the body due to repetitive movements. In this case, though, power would be an issue as implanted batteries or a external telemetry power system would be required for all powered devices in the body, and FES stimulation and feedback signal transmission would be to other parts of the body rather than external to the body.

5.2. INFORMATION FROM NERVE CUFFS IMPLANTED ON SENSORY NERVES IN THE CAT FORELIMB

Recordings of neural activity from the Median, Ulnar, and Radial nerves during walking on the treadmill clearly showed modulations during the step cycle related to events such as paw contact and lift-off, modulations that were very consistent from step to step and over the length of the implant period for all implanted cats. The similarity of forelimb sensory ENG signals from different cats and different walking conditions demonstrated that the nerve cuff signals could provide a stable, reliable source of information about ground contact and gait phase transitions. The reliability of the nerve cuff signals as feedback sources is an important issue for closed-loop FES systems, as highly variable and relatively unstable feedback signals would lead to lower system accuracy and would necessitate frequent recalibration of the nerve cuff signals and FES system parameters.

The modelling experiments discussed in Chapter 3 showed that the nerve cuff signals from the Median and Superficial Radial nerves contained valuable information regarding the step cycle which could reliably be utilized as feedback in a closed-loop FES state controller. The Median nerve provided a very dependable foot contact sensor, which signalled the beginning of stance and also the onset of PalL activity. The Radial nerve provided a useful foot lift-off signal related to the changing wrist angle and deformation of the skin and hair receptors at the end of the stance phase. The simple state controller model produced very accurate PalL timing predictions when tested on different cats on different days in a range of walking conditions (treadmill speeds and slopes), and demonstrated the usefulness and reliability of including natural sensory feedback in clinical FES systems. A very useful result of the modelling experiments was the finding that a constant threshold (constant percentage of peak activity) analysis for both the Median and Radial nerves for all test data produced reasonably accurate results, thereby reducing the need for recalibration of the thresholds and increasing system reliability. Adaptive nerve cuff thresholds (running averages of fixed percentage of previous n neural peaks) should produce very accurate detection of neural events for FES controllers used in a wide range of conditions.

The whole-nerve recordings obtained from implanted nerve cuffs represent a summation of activity from all nerve fibres in the nerve, dominated by the largest diameter cutaneous afferents from the pads and hairy portions of skin in the paw. The signals were primarily sensory due to the distal location of the recording cuff below branch points to forelimb muscles, and stimulation of the recording cuffs resulted in little motor activity and showed that few motor fibres were present inside the cuff. The inclusion of all sensory modalities and large numbers of fibres in the nerve cuff provided a high level of signal stability over time, as evidenced by the CAP studies and the general repeatability of the forelimb nerve cuff signals during the implant periods.

The nerve cuffs were normally surrounded with connective tissue within a few days after the implant surgery, leading to stabilization of cuff impedances and nerve cuff signals amplitudes, and

minimal chance of migration of the electrode. Once the cuff electrode is fixed in position with connective tissue, whole-nerve recordings appear to be very stable and reliable method of obtaining neural signals.

An important issue concerning whole-nerve recordings with nerve cuffs is EMG pickup or contamination of the neural signal by electrical activity in nearby muscles (either voluntary of evoked by stimulation). EMG contamination decreases the ENG signal to noise ratio of the recording cuff and results in a loss of resolution of the signal of interest. EMG contamination of ENG signals can be addressed by proper design of the recording cuff and by using high pass filtering to remove the lower frequency EMG components.

EMG contamination can be minimized by constructing perfectly balanced tripolar nerve cuffs, where the outside reference electrodes "see" the same EMG signal originating outside the cuff which is used as the reference for the ENG signal inside the cuff seen at the middle electrode. In efficient nerve cuffs, the physical distance between middle and outer electrodes should be balanced and the impedances of the middle electrode should be matched to the impedances of the outer two connected in parallel, as in the normal tripolar recording configuration. Matched impedances will lead to a higher common mode rejection of EMG signals for a differential amplification of the difference between signals seen at the middle versus the outside electrodes. In addition, the differential amplifiers should be designed to have a high common mode rejection in the expected neural frequency range of 1 to 5 kHz to minimize EMG contamination of the ENG signals.

The recording nerve cuff's physical characteristics can be further optimized such that the cuff is snug (cuff inside diameter approximately 20% greater than nerve outside diameter to allow for post-surgery swelling) around the nerve to reduce the conductance of external EMG signals that enter the cuff at the ends and reach the centre electrode. The cuff length also plays an important role in minimizing EMG pickup, as a longer cuff length with increase the resistive pathway to the centre electrode from external sources of noise and will also increase the amplitude of ENG

signals recorded within the cuff (Hoffer, 1990). In addition, a tight seal along the longitudinal slit of the cuff is required to minimize paths for sources of noise to the interior of the cuff and the recording electrode. The new closing technique implemented in the second series of implants included an internal flap that overlapped both edges of the longitudinal slit and was pushed closed by connective tissue growth in the cuff (Kallesøe et al., 1996).

Secondary filtering of nerve cuff signals (Ithaco filter, 1 kHz highpass, 24 dB/octave or ~80dB/decade) sufficiently reduced EMG contamination and increased signal to noise ratios significantly. Highpass filtering was used to reduce the contamination of the ENG signals by both natural EMG and any evoked compound EMG resulting from stimulation of forelimb muscles during the FES experiments.

In the reported experiments, primarily cutaneous nerves have been targeted for instrumentation to obtain natural sensory feedback in animal and human experiment. Muscle nerves may offer alternative sources of sensory feedback, and could provide information regarding muscle length and force as transduced by muscle receptors such as muscle spindles and Golgi Tendon Organs. In a paralyzed limb, instrumenting a muscle nerve with a nerve cuff should result in a passive muscle length sensor, depending on the residual efferent (skeletomotor and fusimotor) control of the muscle. Muscle receptors, similar to cutaneous receptors, are not linear transducers of muscle length and force, but signals from nerve cuffs on the muscle nerves could still provide information useful as feedback for FES systems.

Appendix A includes a copy of NIH Progress Report #11, submitted to NIH on June 30, 1995, which discusses preliminary nerve cuff recordings from muscle nerves in the cat forelimb during experiments under anesthesia and during walking. NIH-15 was instrumented with small nerve cuffs, in the order of 0.5 mm ID and 5 mm in length, on the muscle nerves of the FDP and the EDL. The challenge in instrumenting these nerves was to scale down the size of the nerve cuffs and instrument the nerves without inflicting undue stress on the nerves. The miniature nerve cuffs

were mounted on a patch EMG electrode, which was sewn to the muscle belly just proximal to the nerve entry point to provide a stable platform which moved with the muscle. The nerve cuff was then opened and the muscle nerve was allowed to drop into the lumen of the cuff. A closing method consisting of a flap with interdigitated closing tubes and a baton was used to close the device.

Under anesthesia, manual perturbations of wrist angle and digit flexion/extension produced distinct modulations of the FDP and EDL muscle nerve signals, as shown in Fig. 1 of Appendix A. Figure 2 shows an time expanded version of the same data, and clearly shows the alternating pattern of modulation in FDP and EDL muscle nerve signals with alternating manual perturbations. These recordings from the passive limb of the anesthetized cat support the theory that muscle nerves in paralyzed limbs may provide useful muscle length and force information. Figure 3 shows recordings of muscle nerve cuffs during walking on the treadmill, and modulations in the ENG signals are evident. Motor activity is evident in Fig. 3 and can be correlated to EMG recordings from the instrumented muscle, but sensory signals from muscle afferents are also evident during periods of little EMG activity. These preliminary recordings suggest that muscle nerve signals may provide useful feedback for FES in clinical applications.

5.3. CLOSED-LOOP FES STATE CONTROLLER UTILIZING SENSORY NERVE FEEDBACK

A real-time FES state controller was developed from the model state controller, and was used in experiments to stimulate the PalL in the cat forelimb during walking. The state controller was designed completely in hardware to simplify the demonstration of the reliability and usefulness of including natural sensory signals as feedback in a closed-loop FES system. The state controller accurately predicted the timing of PalL activity based on feedback signals from the Median and Radial nerves for a variety of walking conditions. Although the closed-loop FES state controller

experiments were performed in only one cat as a proof-of-concept example, the earlier modelling experiments supported the general applicability of the approach to other experiments.

The FES state controller accurately detected the beginning and end of the stance phase for all normal steps in a variety of walking conditions (treadmill speeds up to 1.0 m/s and slopes of ±10%). The output of the state controller adapted to different rates of walking, as the controller detected both the beginning and end of the stance phase and did not need to implement timers to set the duration of either the stance or swing phase (Popovic et al., 1993; Haugland and Sinkjær, 1995). In a few isolated cases, the state controller predicted an error state for one step cycle because of an abnormal step pattern such as a hesitation step. In these cases, the state machine corrected itself by the next step once the cat began to walk normally.

In the open-loop experiments where the state controller predicted the timing of PalL but did not provide stimulation to the muscle, the cat walked normally and the Median and Radial ENG signals were very stereotyped and provided reliable feedback to the system. The resulting PalL timing prediction was very good for all walking conditions tested, and supported the earlier simulation results. In these experiments, the cat walked for periods of up to 30 minutes and the state controller performed consistently.

In the closed-loop state controller experiments that consisted of stimulating the PalL over naturally-occurring EMG and then stimulating the PalL following Median nerve conduction block to remove voluntary control of the muscle, the added element of stimulus artifact contamination of the neural signals was addressed by inserting switching circuitry on the neural channels. By switching the neural channel to ground for 2 to 3 ms just prior to the stimulation pulse being delivered to the PalL, the stimulus artifact normally observed in the nerve cuff signals was omitted. By using this stimulus artifact switching approach, a small percentage of the overall neural signal was lost, equal to 2-3 ms multiplied by the stimulation frequency. For example, in the case of a stimulation rate of 25 Hz and a blanking pulse of 3 ms, 75 ms out of 1 s of

stimulation was lost, or 7.5%. In multi-channel FES systems, the percentage of neural signals lost to blanking will increase as more stimulation channels are added with similar frequency rates.

Even with the switching circuitry, evidence of stimulus artifact was observed in some Median nerve recordings during stimulation of the PalL. In these cases, the stimulus parameters (pulse amplitude and duration) required to generate muscle contraction were also large enough to produce a stimulus artifact that outlasted the blanking pulse width of 3 ms. Some stimulus artifact noise was observable on the Median ENG envelope, although bin-integration of the neural signals reduced the effect of the short-duration stimulus artifacts. This noise did not appear to affect the performance of the FES state controller.

In the experiments with stimulation over the natural PalL EMG, stimulation did not visibly alter the function of the wrist during the step cycle. The wrist did not appear to be at a higher elevation when stimulated which showed that stimulation of the active PalL during walking did not enhance PalL output or produce a net affect on the wrist joint. A possible reason for this lack of functional result could be that the muscle is normally very active during the stance phase and that stimulation at these stimulus pulse amplitudes and durations through a patch electrode on the muscle belly could not supplement the natural muscle activity. The PalL is just one of many wrist and digit flexors that are active during the stance phase, and perhaps coordinated stimulation of a number of these muscles would produce a visible result at the wrist during normal walking.

In the experiments with the Median nerve conduction block, stimulation of the PalL during the Lidocaine block of muscle output for all wrist and digit flexors innervated by the Median nerve resulted in a partial return of function to the wrist during walking. Once again, the state controller accurately predicted the timing of PalL activity, although the output of the state machine could no longer be compared to the PalL EMG. The output of the state machine was judged to be correct based on visual inspection of the output versus the Median and Radial ENG patterns, and by visual inspection of the stimulus LED in the video versus the timing of the step cycle.

Although a complete Median nerve conduction block was achieved under anesthesia, a complete block was not achieved in the awake, freely moving cat (approximately 37% of the PalL EMG still occurred during normal walking). A possible reason for this incomplete block is the increased circulation and movement surrounding the blocking cuff during walking, which would act to flush out the local anesthetic more quickly. A more concentrated Lidocaine solution may have resulted in a complete conduction block. However, even though a complete block was not achieved, weakness in the wrist and a decrease in the wrist elevation during walking were observed during the Median nerve block. In these trials, stimulation of the PalL returned partial function to the wrist and increased the wrist elevation during the stance phase.

5.4. FUTURE WORK WITH FES AND NATURAL SENSORY FEEDBACK

The state controller approach to closed-loop FES demonstrated in this thesis was a simplified example of a FES system with only one stimulation channel, but it served to demonstrate that natural sensory signals from nerve cuffs in the periphery are a useful and reliable source of feedback. Recently, a variety of state controllers for FES have been investigated (Popovic et al., 1993; Haugland and Hoffer, 1994b, Haugland and Sinkjaer, 1995), and are attractive for clinical use because of their simplicity. More complex FES controllers are currently being designed that include adaptive control to increase the range that the systems can operate in, and pattern recognition to better analyze feedback signals (both natural and artificial) to recognize system variables and increase accuracy and reliability (Veltink, 1990; Chizeck, 1992; Stein, 1992; Popovic et al., 1993; Kostov et al., 1995a). Future clinical FES approaches that include natural sensory feedback may result in systems that benefit from the accuracy and reliability demonstrated in this thesis.

In order for natural sensory sources of feedback to be implemented in clinical FES systems in humans, future research should address such issues as: 1) continued development of implantable nerve cuff electrodes suitable for chronic implantation in humans that better suit the surrounding tissue environment, 2) development of telemetry systems to remove problems associated with implanted wires and connectors, 3) development of improved signal extraction techniques to increase the dimensionality and quality of data obtained from peripheral sensory nerves through the use of, e.g. multi-contact nerve cuffs or intrafascicular electrodes, 4) further investigation of the modalities of information available in sensory nerves such as contact, slip, pressure, muscle length, and muscle force, 5) development of miniaturized nerve cuffs that are safe for use on muscle nerves, and 6) employment of machine learning techniques and neural networks to improve nerve signal pattern recognition and feature extraction.

The work presented in this thesis represents a significant portion of the work contracted to Dr. Andy Hoffer as P.I. of a three year National Institutes of Health contract entitled "Sensory Feedback Signal Derivation from Afferent Neurons", No. NIH-NINDS-NO1-NS-3-2380. In addition, the work presented in this thesis has led to a collaborative project with Dr. Aleks Kostov of the University of Alberta to investigate the use of adaptive logic networks in neural pattern recognition and closed-loop control of FES (Kostov et al., 1996). Based partially on the results discussed in this thesis, a further three year contract has been awarded by NIH, entitled "Sensory Information from Afferent Neurons", No. NIH-NINDS-NO1-NS-6-2339, beginning on March 31, 1996, which addresses a number of the issues discussed above.

References

Andrews B.J., Barnett R.W., Phillips G.F., Kirkwood C.A., Donaldson N., Rushton D.N., and Perkins T.A., (1989), Rule-based control of a hybrid FES orthosis for assisting paraplegic locomotion. *Automedica*, Vol. 11, pp. 175-200.

Crago, P.E., Nakai, R.J., and Chizeck, H.J., (1991), Feedback regulation of hand grasp opening and contact force during stimulation of paralyzed muscle, *IEEE Trans. Biomed. Eng.*, vol. 38, pp. 17-28.

Chizeck, H.J., (1992), Adaptive and nonlinear control methods for neural prostheses, In: *NEURAL PROSTHESES: Replacing Motor Function after Disease or Disability*, R.B. Stein, P.H. Peckham and D. Popovic, editors. Oxford Univ. Press, pp. 298-328.

Crouch, J.E., (1969), *Text-Atlas of Cat Anatomy*, Lea and Febiger, Philadelphia, PA.

Creasy, G.H., (1993), Electrical stimulation of sacral roots for micturition after spinal cord injury, *Spinal Cord Injury*, Vol. 20, No. 3, pp. 505-515.

Davis, L.A., Gordon, T., Hoffer J.A., Jhamandas, J. and Stein, R.B, (1978), Compound action potentials recorded from mammalian peripheral nerves following ligation or resuturing. *J. Physiol.* 285: 543-559.

English, A., (1976), An electromyographic analysis of forelimb muscles during overground stepping in the cat, *J Exp. Biol.*, Vol. 76, pp. 105-122.

Hambrecht, F.T., (1992), A brief history of neural prostheses for motor control of paralyzed extremities, In: *NEURAL PROSTHESES: Replacing Motor Function after Disease or Disability*, R.B. Stein, P.H. Peckham and D. Popovic, editors. Oxford Univ. Press, pp. 3-14.

Haugland M.K., Hoffer A., and Sinkjær T., (1994), Skin contact force information in sensory nerve signals recorded by implanted cuff electrodes, *IEEE Trans.Rehab.Eng.*, Vol. 2, No. 1, pp. 18-28.

Haugland, M.K. and Hoffer, J.A., (1994a), Slip information provided by nerve cuff signals: application in closed-loop control of functional electrical stimulation, *IEEE Trans. Rehab. Eng.*, Vol. 2, pp. 29-36.

Haugland, M.K. and Hoffer, J.A., (1994b), Artifact-free sensory nerve signals obtained from cuff electrodes during functinal electrical stimulation, *IEEE Trans. Rehab. Eng.*, Vol. 2, pp. 37-40.

Haugland, M. and Sinkjær, T., (1995), Cutaneous whole nerve recordings used for correction of footdrop in hemiplegic man, *IEEE Trans. Rehab. Eng.*, Vol. 3, pp. 307-317.

Haugland, M., Lickel, A., Riso, R., Adaniczyk, M.M., Keith, M., Jensen, I.J., Haase, J., , and Sinkjaer, T., (1995), Restoration of lateral hand grasp using natural sensors, in *Proc. of 5th Vienna Int. Worksjop of FES*, Vienna, AS.

Hoffer, J.A., (1975), Long-term peripheral nerve activity during behaviour in the rabbit: The control of locomotion. Ph.D. Thesis, Johns Hopkins Univ., Nov. 1975. Publ. No. 76-8530, University Microfilms, Ann Arbor, Michigan; 124 pp.

Hoffer, J.A., (1988), Closed-Loop, Implanted-Sensor, Functional electrical stimulation system for partial restoration of motor functions. U.S. Patent No. 4,750,499.

Hoffer, J.A., (1990), Techniques to record spinal cord, peripheral nerve and muscle activity in freely moving animals. In: Neurophysiological Techniques: Applications to Neural Systems. NEUROMETHODS, Vol. 15, A.A. Boulton, G.B. Baker and C.H. Vanderwolf, Editors. Humana Press, Clifton, N.J., pp. 65-145.

Hoffer, J.A., and Haugland, M. (1992), Signals from tactile sensors in glabrous skin suitable for restoring motor functions in paralyzed humans. In *Neural Prostheses: Replacing Motor Function after Disease or Disability*, R.B. Stein, P.H. Peckham, and D. Popovic, editors. Oxford Univ. Press, pp. 99-125.

Hoffer, J.A., Loeb, G.E. and Pratt, C.A., (1981), Single unit conduction velocities from averaged nerve cuff electrode records in freely moving cats, *J. Neurosci. Methods* 4: 211-225.

Hoffer, J.A., Stein, R.B., Haugland, M., Sinkjær, T., Durfee, W.K., Schwartz, A.B., Loeb, G.E. and Kantor, C., (1996), Neural signals for command control and feedback in functional neuromuscular stimulation, *J. Rehab. Res. & Dev.* (in press).

Hoffman, P., Illert, M., and Wiedemann, E., (1985), EMG recordings from the cat forelimb during unrestrained locomotion, *Neuro Lett.*, S22:S126.

Kallesøe, K., Hoffer, J.A., Strange, K., Valenzuela, I., (1996), Implantable cuff having improved closure. U.S. Patent 5,487,756, awarded Jan. 30, 1996.

Kallesøe, K., Valenzuela, I., Viberg, D., and Hoffer, J.A., (1994), Interfacing to single peripheral axons using flexible silicon multicontact probes, in Absrt. of Neural Prostheses: Motor Systems IV, Deer Creek, Ohio, July 23-28, p. 17.

Kallesøe, K., Haugland, M., and Hoffer, J.A., (1992), Gait assistance with FES controlled by the cutaneous ENG, *Abstr Soc.Neuroscience 22nd Meeting*, Anaheim, CA, Vol. 18, Part 2, p. 1553.

Kirkwood C.A., and Andrews B.J., (1989), Finite-state control of FES systems: Application of AI inductive learning techniques, in *Proc. 11th Annual International IEEE - EMBS Conference*, Seattle, USA, pp. 1020-1021.

Kobetic R., and Marsolais E.B., (1994), Synthesis of paraplegic gait with multichannel functional neuromuscular stimulation, *IEEE Trans.Rehab.Eng.*, Vol. 2, No. 2, pp. 66-79.

Kostov A., Popovic D., Stein R.B., and Armstrong W.W., (1993), Learning of EMG-patterns by Adaptive Logic Networks, in *Proc 15th Annual International IEEE - EMBS Conference*, San Diego, California, U.S.A., Vol. 3, pp. 1135-1136.

Kostov, A., Stein, R.B., Popovic, D., and Armstrong, W.W., (1994), Improved methods for control of FES for locomotion, in *Proc. of Modeling and Control in Biomedical Systems*, Galveston, pp. 422-427.

Kostov, A., Andrews, B.J., Popovic, D.B., Stein, R.B., and Armstrong, W.W. (1995a), Machine learning in control of functional electrical stimulation systems for locomotion, *IEEE Trans.Biomed.Eng.*, Vol. 42, No. 6, pp. 541-551.

Kostov, A., Stein, R.B., Armstrong, W.W., Thomas M., and Popovic, D.B., (1995b), Integrated control system for FES-assisted locomotion after spinal cord injury, in *Proc. 17th Annual IEEE - EMBS Conference*, Montreal, Canada, Sep. 20-23.

Kostov, A., Andrews, B., and Stein, R.B., (1995c), Inductive machine learning in control of FES-assisted gait after spinal cord injury, in *Proc. 5th Vienna International Workshop on Functional Electrostimulation*, August 17-19, 1995, Vienna, Austria.

Kostov, A., Strange, K., Stein, R.B., and Hoffer, J.A. (1996), Artificial neural networks application in EMG-prediciton using sensory nerve signals recorded in the cat's forelimb during walking, in preparation.

Kralj, A., Bajd, T., Turk, R., et al., (1994), Eleven years of experience in FES assisted gait of psinal cord injured patients, J. of Biomechanics, Vol. 27, pp. 805.

Marsolais, E.B., Scheiner, A., Miller, P.C., Kobetic, R., and Daly, J.J., (1994), Augmentation of transfers for a quadriplegic patient using an implanted FNS system: case report, *Paraplegia*, Vol. 32, No. 8, pp. 573-579.

Mortimer, J.T., (1990), Electrical excitation of nerve. In *Neural Prostheses: Fundamental Studies*, W.F. Agnew and D.B. McCreery, editors, Prentic Hall, pp. 67-83.

Mortimer, J.T., (1981), Motor Prostheses. In *Handbook of Physiology, The Nervous System II*, pp. 155-187.

Nathan, R.H., (1993), Control strategies in FNS systems for the upper extremities, *Critical Reviews in Biomedical Engineering*, Vol. 21, No. 6, pp. 485-568

Peckham, P.H., and Keith, M.W., (1992), Motor prostheses for restoration of upper extremity function, In: *NEURAL PROSTHESES: Replacing Motor Function after Disease or Disability*, R.B. Stein, P.H. Peckham and D. Popovic, editors. Oxford Univ. Press, pp. 162-189.

Popovic, D.B., (1992), Functional electrical stimulation for lower extremities, In: *NEURAL PROSTHESES: Replacing Motor Function after Disease or Disability*, R.B. Stein, P.H. Peckham and D. Popovic, editors. Oxford Univ. Press, pp. 233-251.

Popovic D., Stein R.B., Jovanovic K., Dai R.C., Kostov A., and Armstrong W.W., (1993), Sensory nerve recording for closed-loop control to restore motor functions, *IEEE Trans.Biomed.Eng.*, Vol. 40, No. 10, pp. 1024-1031.

Nicolic, Z., Popovic, D.B., Stein, R.B., and Kenwell, Z., (1994), Instrumentation for ENG and EMG recordings in FES systems, *IEEE Trans. Bio. Eng.*, Vol. 41, pp. 703-706.

Riso, R , Slot, P.J., Haugland, M., and Sinkjaer, T., (1995), Characterization of cutaneous nerve responses for control of neuromotor prostheses, in *Proc. of 5th Vienna Int. Workshop of FES*, Vienna, AS.

Sinkjær, T., Haugland, M., and Haase, J., (1992), The use of natural sensory nerve signals as an advanced heel-switch in drop-foot patients. in *Proc. of the 4th Vienna Workshop on FES*, pp. 134-137.

Stein, R.B., Belanger, M., and Wheeler, G., (1993), Electrical systems for improving locomotion after incomplete spinal cord injury: an assessment, Arch. of Phys Med and Rehab, Vol 74, pp. 954-959.

Stein, R.B., (1992), Feedback control of normal and electrically induced movements, In: *NEURAL PROSTHESES: Replacing Motor Function after Disease or Disability*, R.B. Stein, P.H. Peckham and D. Popovic, editors. Oxford Univ. Press, pp. 281-297.

Stein, R.B., Charles, D., Gordon, T., Hoffer, J.A. and Jhamandas, J., (1978), Impedance properties of metal electrodes for chronic recording from mammalian nerves. *IEEE Trans. BME* 25: 532-537.

Stein, R.B., Gordon, T., Hoffer, J.A., Davis, L.A. and Charles, D., (1980), Long-term recordings from cat peripheral nerves during degeneration and regeneration: Implications for human nerve repair and prosthetics. In *Nerve Repair: its Clinical and Experimental Basis*, D.L. Jewett and H.R. McCarroll, Eds. C.V. Mosby: St. Louis; Ch. 17, pp. 166-176.

Strange K.D., Hoffer J.A., Kallesøe K., Schindler S.M., and Crouch D.A., (1995), Long-term stability of nerve cuffs implanted in the cat forelimb, in *Proc. of RESNA '95*, Vancouver, Canada, June 1995, pp. 372-374.

Strange, K. and Hoffer, J.A., (1995a), Using cutaneous neural signals to predict cat forelimb muscle activity during walking, in *Proc. of IEEE SMC*, Vancouver, Canada, Oct. 1995, vol.2, pp. 1199-1204.

Strange, K. and Hoffer, J.A., (1995b), Cutaneous neural feedback can be used to predict timing of muscle activation in the cat forelimb during locomotion, *Abstr Soc. Neuroscience 25th Meeting*, San Diego, CA , Vol. 21, Part 1, page 419.

Strange, K.D. and Hoffer, J.A., (1996), Sensory signals from cat paw cutaneous receptors during walking: applicability for closed-loop control of FES, submitted concurrently.

Strange K.D, Kallesoe, K., and Hoffer, J.A., (1996), Long-term stability of signals recorded from cat forelimb nerves with cuff electrodes, submitted concurrently.

Sunderland, S., (1968), *Nerves and Nerve Injuries.* London: Livingstone.

Upshaw, B.J., Sinkjaer, T., and Haase, J., (1995), Natural vs. artificial sensors applied in peroneal nerve stimulation, in *Proc. of 5th Vienna International Workshop on FES*, August, 1995, Vienna, Austria.

Veltink P.H., Rijkhoff N.J.M., and Rutten W.L.C., (1990), Neural networks for reconstructing muscle activation from external sensor signals during human walking, in *Proc. of IEEE Intelligent Motion Control*, Istanbul, pp. 469-473.

Webster, J.G., (1992), Artificial sensors suitable for closed-loop control of FNS, In: *NEURAL PROSTHESES: Replacing Motor Function after Disease or Disability*, R.B. Stein, P.H. Peckham and D. Popovic, editors. Oxford Univ. Press, pp. 88-98.

Yoshida, K., and Horch, K., (1994), FNS control of ankle position using neural feedback, in Absrt. of Neural Prostheses: Motor Systems IV, Deer Creek, Ohio, July 23-28, p. 40.

Appendix A:

Quarterly Progress Report #11 submitted to National Institutes of Health

Sept. 30, 1995

Contract No.: NIH-NINDS-NO1-NS-3-2380

"Sensory feedback signal derivation from afferent neurons"

Sensory feedback signal derivation from afferent neurons

Contract No.: **NIH-NINDS-NO1-NS-3-2380**

QUARTERLY PROGRESS REPORT #11

for the period

1 June 1995 - 31 Aug. 1995

Principal Investigator: J.A. Hoffer, PhD

Co-investigators: K. Strange, BASc
Y. Chen, PhD
P. Christensen, BASc
D. Crouch, BSc (Hon)
K. Kallesøe, MScEE
C. Kendall, RVT

Origin: School of Kinesiology
Faculty of Applied Sciences
Simon Fraser University
Burnaby, British Columbia V5A 1S6, Canada

Subcontractor: D. Popovic, PhD
University of Miami, Miami, Florida, USA

Date of submission of this report: 30 Sept. 1995

Table of Contents

I. Summary of the Overall Project

In this study we are exploring the feasibility of extracting 1) cutaneous sensory information about fingertip contact and slip, and 2) proprioceptive sensory information about wrist or finger position. We use implanted nerve cuff electrodes to record peripheral nerve activity in animal models.

Our overall **objectives** for the 3-year duration of this contract are as follows:

1. Investigate, in cadaver material, implantation sites for nerve cuff electrodes from which cutaneous and proprioceptive information relevant to the human fingers, hand and forearm could be recorded.
2. Select a suitable animal preparation in which human nerve dimensions and electrode placement sites can be modeled and tested, with eventual human prosthetic applications in mind.
3. Fabricate nerve cuff electrodes suitable for these purposes, and subcontract the fabrication of nerve cuff electrodes of an alternate design.
4. Investigate the extraction of information about contact and slip from chronically recorded nerve activity using these animal models and electrodes. Specifically,
   a. Devise recording, processing and detection methods to detect contact and slip from recorded neural activity in a restrained animal;
   b. Modify these methods as needed to function in an unrestrained animal and in the presence of functional electrical stimulation (FES);
   c. Record activity for at least 6 months and track changes in neural responses over this time.
5. Supply material for histopathological examination from cuffed nerves and contralateral controls, from chronically implanted animals.
6. Investigate the possibility of extracting information about muscle force and limb position from chronically recorded neural activity.
7. Cooperate with other investigators of the Neural Prosthesis Program by collaboration and sharing of experimental findings.

II. Summary of Progress in the Eleventh Quarter

During the eleventh quarter, we made significant progress obtaining usable neural signals from nerves to individual muscles using small scale tripolar nerve cuffs. We also made significant progress in our histological analysis and initial results are presented in this report. In addition, our collaborative project of applying machine learning techniques to analyzing neural signals and predicting muscle activity has produced outstanding results. Three full manuscripts on the subjects of nerve signal stability, cutaneous nerve signals recorded during locomotion, and machine learning techniques applied to closed-loop control of functional electrical stimulation have been developed.

III. Details of Progress in the Eleventh Quarter

A. Chronic Recordings from Individual Nerves to Forelimb Muscles

Small nerves supplying individual cat forelimb muscles were targeted for instrumentation with cuff electrodes to obtain electroneurographic (ENG) recordings of motor and proprioceptive sensory information during voluntary tasks.

1. Implant Protocol

Nerves to individual muscles in the forelimb were assessed in terms of functional role, accessiblity and ease of instrumentation. Superficial forelimb muscles such as Palmaris Longus (PalL), Flexor Carpi Ulnaris (FCU), Extensor Carpi Ulnaris (ECU), Extensor Digitorum Communis (EDC), and Extensor Digitorum Lateralis (EDL), are usually innervated by small nerves (approximately 0.3 to 1.0 mm in diameter) which branch from the parent nerves (Median, Ulnar, and Deep Radial) below the elbow. These muscle nerves are difficult to instrument due to their fragile nature and the fact that they are usually surrounded by muscles, making it difficult to stabilize the device with respect to the other structures. Furthermore, accessing superficial muscle nerves is often difficult because the nerve entry point is on the underside of the muscle when looking at the surgical site.

Nerves to deep forelimb muscles such as Abductor Pollicis Longus (APL) and Flexor Digitorum Profundus (FDP, 5th head) are similar in diameter to the superficial muscle nerves, but the deep muscle nerves are generally shorter. A significant advantage to targeting deep muscles is that their nerves are more easily accessible from a top view of the surgical site when the superficial muscles are reflected.

We developed a miniature nerve cuff based on the tripolar design reported in Strange et al. (1995), consisting of a small cuff (ID of 0.5 - 1.0 mm, length of 0.5 to 1.0) mounted on a bipolar electromyogram (EMG) patch electrode (Hoffer, 1990). The nerve cuff was closed by an external flap and a locking mechanism involving closing tubes and a baton that has recently been allowed a U.S. Patent (Kallesøe et al, 1994). The patch was sewn to the muscle belly with 8-0 sutures just proximal to the nerve entry point, and the nerve was allowed to drop into the inside of the cuff when it was held open. The outside electrodes of the cuff were shorted together at the cuff and the four lead wires (two cuff - 631 Cooner wire - and two EMG - 634 Cooner wire) exited the device and were routed distal to the device. A strain relief loop was introduced distal to the cuff and the wires were passed subcutaneously to the backpack (Hoffer, 1990; Strange et al., 1995).

In subject NIH 15 we instrumented the nerves to EDL and FDP (5th head) with nerve cuffs of this design, and we instrumented the Median and Radial nerves with proximal and distal nerve cuffs and electroneurogram (ENG) patch electrodes as described in Strange et al. (1995b) and Strange and Hoffer (1995b). The EDL nerve was instrumented with a 5 mm long, 0.6 mm ID cuff mounted on a 5x5 mm patch, and the FDP was instrumented with a 5 mm long, 0.8 mm ID cuff mounted on a 5x5 mm patch. We also implanted EMG patch electrodes on PalL and EDC to record muscle activity during voluntary tasks from a total of four muscles (PalL, FDP, EDC, and EDL).

2. Recordings Under Anesthesia

We periodically monitored the status of the implanted devices by following the compound action potentials (CAPs) as outlined in Strange et al. (1995a,b). The CAP amplitudes recorded from nerves to FDP and EDL declined to 7% and 31% of the day 0 amplitude respectively (on day 14), but showed substantial recovery to 23% and 78% respectively (on day 40). Neural and EMG

recordings from the instrumented muscles during walking on the treadmill showed increasing amplitudes and confirmed the recovery in the instrumented nerves, which was similar to earlier observations from cutaneous nerves (Strange et al., 1995a,b).

While the subject was under anesthesia, we investigated the ENG signals in nerves to FDP and EDL during manual oscillations of the paw and digits. All physiological signals were processed according to the methods of Strange and Hoffer (1995). In one experiment the paw was held at zero degrees flexion, and the digits were rigorously flexed and extended at a rate of 2 to 3 cycles per second. Data from this experiment are presented in Figs. 1 and 2 which show neural signals in the top four traces (FDP, EDL, Rad, and Med) and EMG signals in the bottom four traces (PalL, FDP, EDC, and EDL). All signal traces are displayed in microvolts.

We observed that all four nerve signals were modulated with the manual oscillations of the digits, while none of the EMG signals showed significant activity or modulation. These observations demonstrated that reflexes were almost totally suppressed by anesthesia and that recorded neural signals were predominately sensory in nature. The cutaneous Radial and Median signals showed bursts of activity with each perturbation regardless of direction (flexion or extension), while the FDP nerve showed a burst only during (or after) digit extension and the EDL showed a burst only during (or after) digit flexion. The direction of the perturbation suggested that the recorded signals were produced by spindle afferents that fired as the passive muscle was stretched. Figure 2 shows the same data as Fig. 1 on an expanded time scale. The opposite directional dependence of the FDP and EDL ENG signals is clearly demonstrated.

Further experiments under anesthesia showed that the FDP and EDL nerve signals were sensitive to both position and velocity of the perturbation. The manual oscillation of the paw and digits was difficult to calibrate and repeat reliably, and an improved perturbation task will be required to fully characterize the responses in the nerves to individual muscles when the subject is under anesthesia.

3. Recordings During Walking on the Treadmill

We examined the FDP and EDL signals recorded during walking on the treadmill to assess the information available from nerves to individual forelimb muscles. The recording protocol, a discussion of signals recorded from Median and radial cutaneous nerves during walking, and a discussion of recorded EMG signals and the role of selected forelimb muscles are found in Strange and Hoffer (1995).

Figure 3 presents data recorded from NIH 15 on day 28 post implant. The treadmill was level and the speed was 0.5 m/s. Once again, the top four traces represent neural signals (FDP, EDL, Rad, and Med) and the bottom four represent EMG signals (PalL, FDP, EDC, and EDL). All signals are displayed in microvolts. The first observation to note is that all four muscle signals are modulated with the step cycle as shown by the lines signifying contact and lift-off. The PalL showed the highest amplitude signals and was activated just prior to contact and during most of the stance phase. The FDP had relatively low levels of EMG activity throughout the step cycle, possibly as a result of partial nerve injury due to instrumentation, but it was well modulated with activity occurring prior to lift-off and into the swing phase. The EDC and EDL were both modulated with the step cycle, with peaks in activity occurring just prior to contact to stabilize the wrist joint. The timing and relative amplitudes of muscle activity generally agreed with earlier recordings as reported in Strange and Hoffer (1995).

The nerve signals shown in Fig. 3 are all modulated with the step cycle, with the Radial and Median nerve signals similar to recordings in earlier experiments (Strange and Hoffer, 1995). The FDP is strongly modulated with the step cycle with higher levels of activity during stance and peaks occurring prior to lift-off. The signal was surprisingly strongly modulated with the step cycle, considering the partial injury to the nerve as assessed by the CAP. The nerve to each instrumented muscle contained both motor and sensory fibres, and their relative contribution in whole nerve

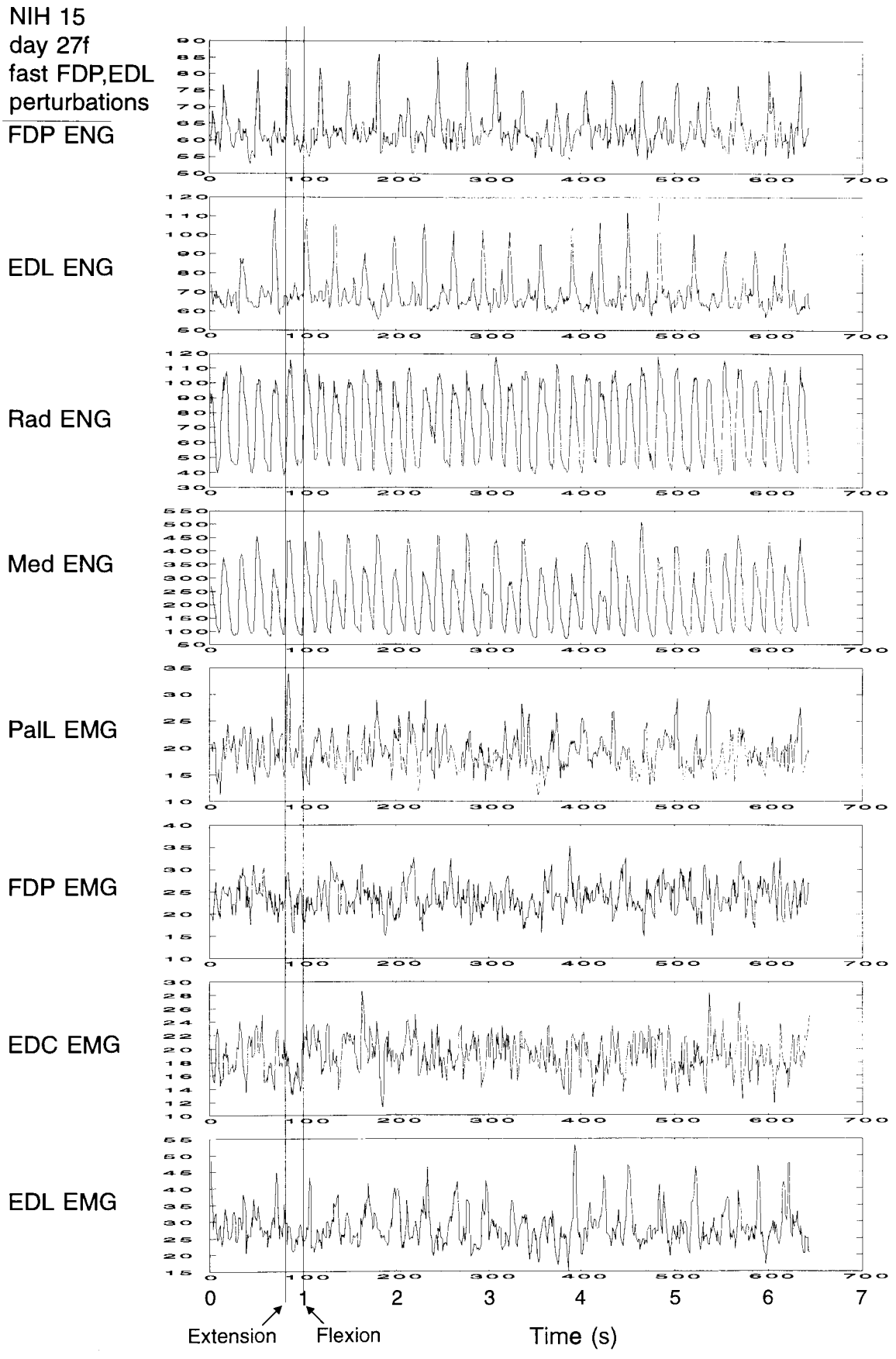

Figure 1: ENG and EMG data recorded under anesthesia from cat forelimb, with mechanical perturbations of the wrist and digits (data from NIH 15)

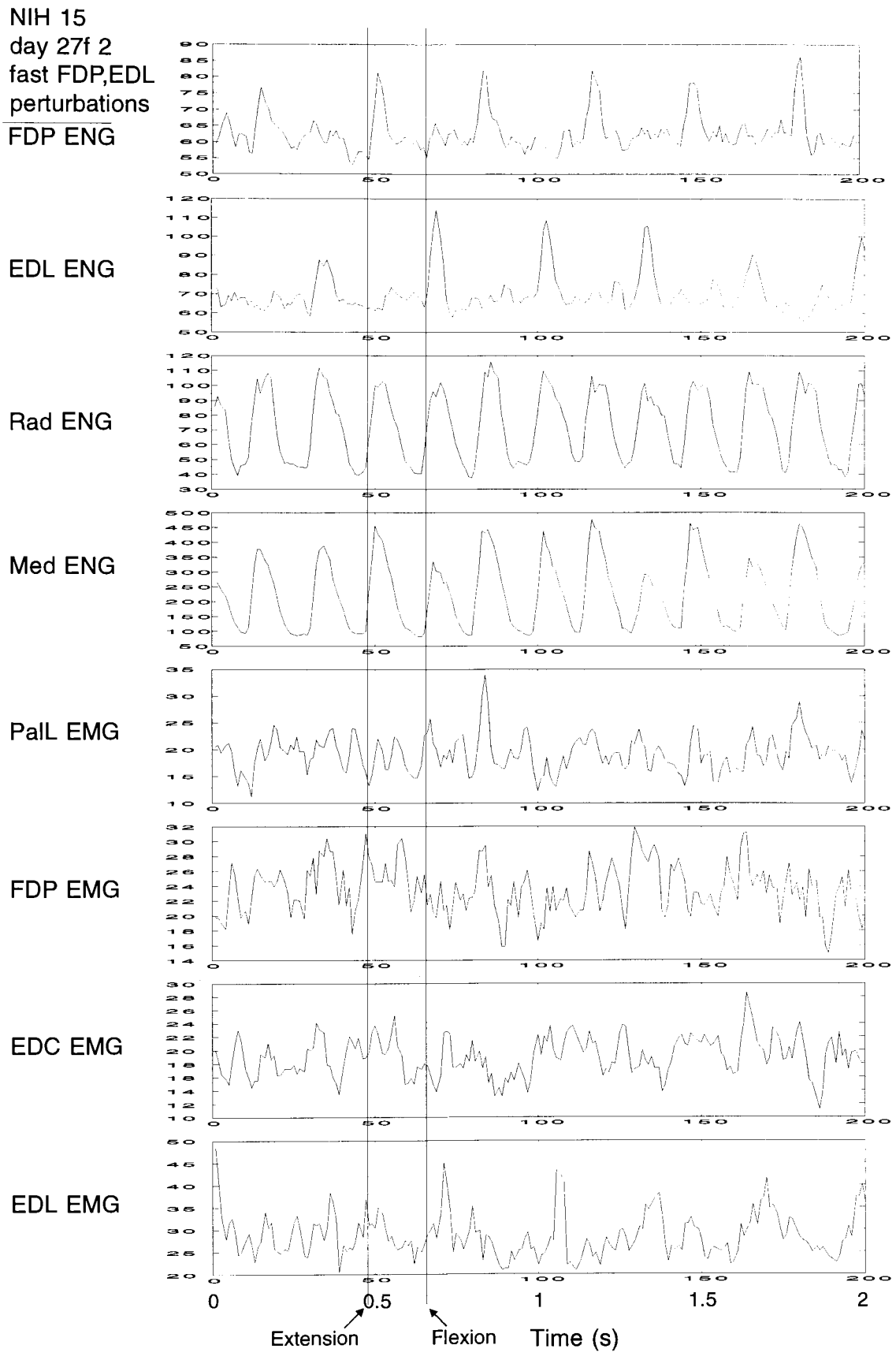

Figure 2: ENG and EMG data recorded under anesthesia from cat forelimb, with mechanical perturbations of the wrist and digits (data from NIH 15)

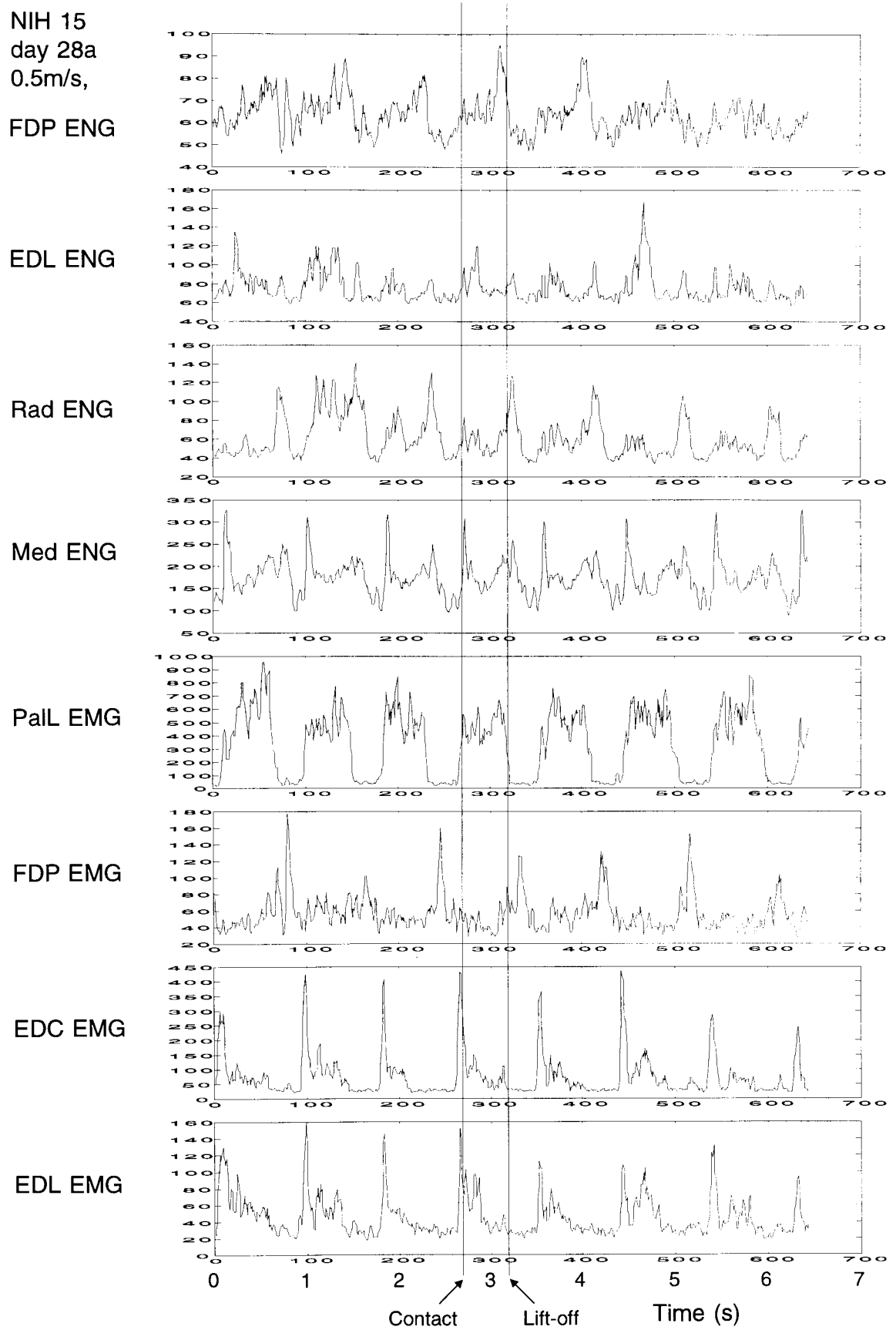

Figure 3: ENG and EMG data recorded from cat forelimb during walking on a treadmill (data from NIH 15, level treadmill, 0.5 m/s)

signals shown in Fig. 3 is unknown. The FDP ENG showed increasing activity throughout stance, possibly a sensory signal resulting from loading the muscle as the body moved forward and the muscle lengthened. The large burst in ENG prior to lift-off is thought to be a volley of motor signals activating the muscle to provide force during lift-off and swing, and the sharp decrease in activity following lift-off indicated absent motor signals and absent sensory signals as the muscle is inactive and unloaded.

The EDL showed modulations with the step cycle, although the signal is quite variable and the relationship between EDL ENG and EMG is not as clear as in the FDP recordings. The limited, variable activity of the extensor muscles during walking may play a role in the variability in the EDL ENG recordings shown in Fig. 3 and represents an interesting aspect of control that warrants further investigation.

4. EMG Contamination of Nerve Cuff Signals

We investigated the amount of EMG contamination of nerve cuff signals recorded in NIH 15 during walking, and determined the EMG rejection properties of the implanted nerve cuffs and the ENG patch electrode. ENG signals were sampled at 20 kHz and processed by the method described in Strange and Hoffer (1995). FFTs of the signals produced the power spectra of the four ENG signals both before and after secondary Ithaco filtering.

Figures 4 and 5 present the power spectra of the four ENG signals recorded in NIH 15 walking on a level treadmill on day 28, which is the same recording session as shown in Fig. 3. Figure 4 shows the spectra for FDP, EDL, Radial, and Median ENG signals (top to bottom), along with device dimensions, filtering characteristics, and calculated ENG-to-EMG signal-to-noise ratio (SNR) for each signal. The SNR was calculated by integrating the spectra up to 1 kHz (the frequency range for EMG), and integrating the spectra from 1 kHz to 10 kHz (the frequency range for ENG). The spectra are derived from signals in volts and the units for the spectra are volts squared.

All four panels in Fig. 4 show that considerable EMG pickup is present in the recorded signal following bandpass filtering with the Bak amplifiers. The peaks of EMG occur at 300 to 600 Hz and are approximately two orders of magnitude larger than the ENG component above 1 kHz, seen in Fig. 4 as the bumps on the falling edges of the EMG peaks.

Figure 5 presents the signals from Fig. 4 following secondary highpass filtering at 1 kHz with Ithaco filters (Strange and Hoffer, 1995). The EMG component has been reduced and the peaks in the signals now occur at or above 1 kHz. The SNR for each device is shown in the figure (average = 4.65 $\pm$2.9, n = 4), along with the increase in SNR due to Ithaco filtering. These values are comparable to SNR values reported for Ulnar, Median, and Radial recordings in Strange and Hoffer (1995). The EDL and Radial ENG signals appear to still contain some EMG components as shown by the sharp peak at 1 kHz, although the majority of EMG contamination has been filtered out.

The data in Figs. 4 and 5 suggest that highpass filtering of signals from nerve cuff and patch electrodes can remove the majority of EMG contamination and produce clean ENG signals as shown in Fig. 3. Nerve cuff signals essentially free of EMG contamination may be used as feedback signals for closed-loop control of functional electrical stimulation systems. In particular, feedback signals from individual nerves to forelimb muscles would be useful for controlling limb position during reaching or other voluntary activities.

NIH 15, day 28a
0.5 m/s, level, fsamp = 20 kS/s
file: psd28a2.idw

FM7, FDP nerve cuff
0.8 mm ID, 5 mm long
BP filtered @ 50Hz-1kHz, Bak
ENG:EMG ratio = 0.37
(threshold at 1 kHz)

FM8, EDL nerve cuff
0.6 mm ID, 5 mm long
BP filtered @ 50Hz-1kHz, Bak
ENG:EMG ratio = 0.41
(threshold at 1 kHz)

FM9, Radial nerve patch
10 * 30 mm
BP filtered @ 50Hz-1kHz, Bak
ENG:EMG ratio = 0.068
(threshold at 1 kHz)

FM10, Median nerve cuff
2.0 mm ID, 20 mm long
BP filtered @ 50Hz-1kHz, Bak
ENG:EMG ratio = 0.61
(threshold at 1 kHz)

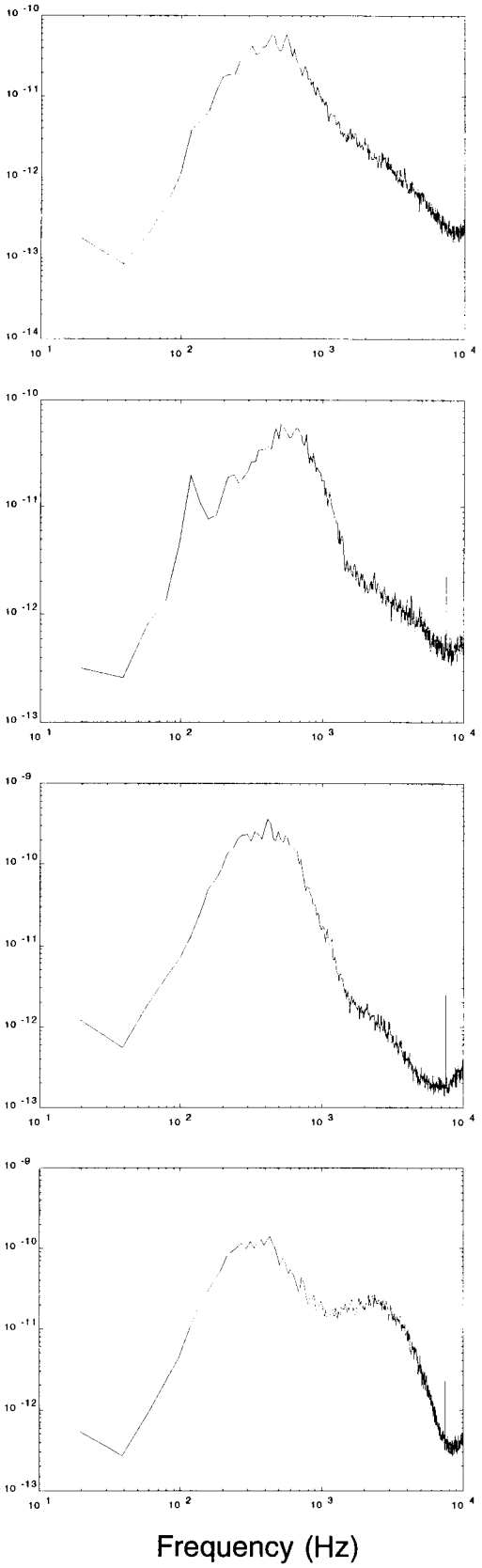

Figure 4: Power spectral densities of nerve cuff recordings from the cat forelimb during walking, prior to high pass filtering with Ithaco filters (data from NIH 15, level treadmill, 0.5 m/s)

NIH 15, day 28a
0.5 m/s, level, fsamp = 20 kS/s
file: psd28a.idw

FM1, FDP nerve cuff
0.8 mm ID, 5 mm long
HP filtered @ 1kHz, Ithaco
ENG:EMG ratio = 8.39 (x22.7)
(threshold at 1 kHz)

FM2, EDL nerve cuff
0.6 mm ID, 5 mm long
HP filtered @ 1kHz, Ithaco
ENG:EMG ratio = 5.47 (x13.4)
(threshold at 1 kHz)

FM3, Radial nerve patch
10 * 30 mm
HP filtered @ 1kHz, Ithaco
ENG:EMG ratio = 2.29 (x33.8)
(threshold at 1 kHz)

FM4, Median nerve cuff
2.0 mm ID, 20 mm long
HP filtered @ 1kHz, Ithaco
ENG:EMG ratio = 2.43 (x4.0)
(threshold at 1 kHz)

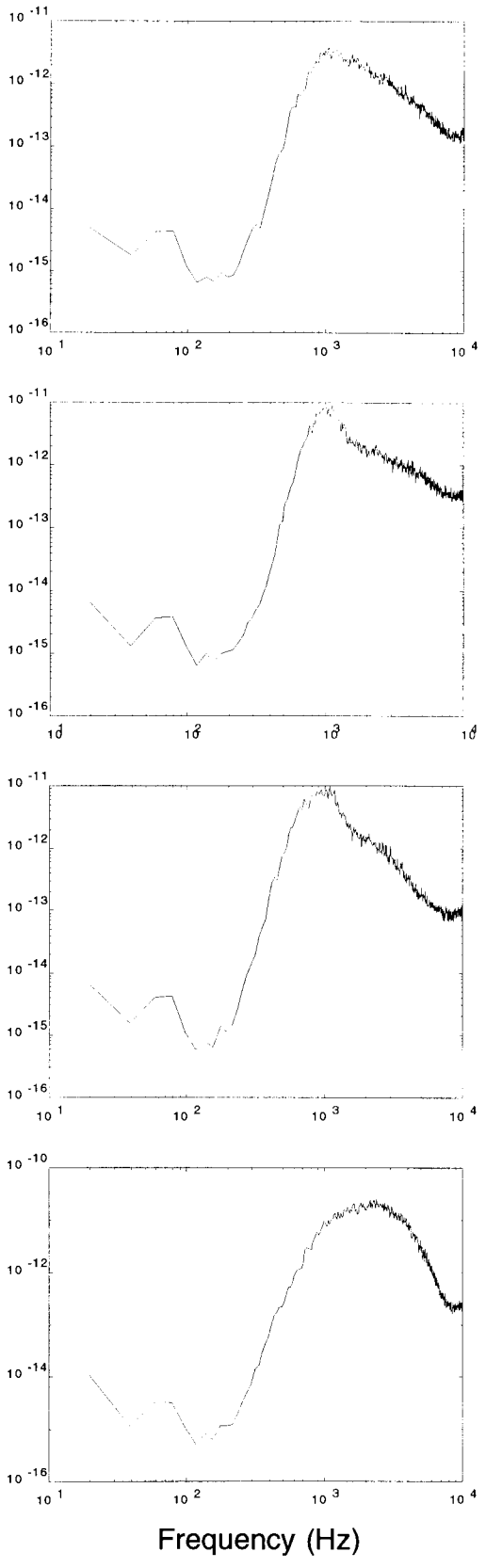

Figure 5: Power spectral densities of nerve cuff recordings from the cat forelimb during walking, after high pass filtering with Ithaco filters (data from NIH 15, level treadmill, 0.5 m/s)

B. Preliminary Histological Findings

Male cats were chronically implanted with recording cuffs for a period ranging from 180 to 300 days as described by Strange et al (1995a,b). Preliminary results show that this chronic implant schedule does not seem to cause damage that is quantifiable from histological samples. We interpret this to indicate that this long term implant protocol is safe for most animals. Further analysis is ongoing.

1. Methods

One centimeter long nerve samples were immersed in Karnovsky's fixative (Karnovsky, 1965), dehydrated and then osmicated for four hours. The osmicated samples were embedded in Jembed 812 (J.B.EM services, Quebec) and then 0.5 μm sections were cut using a glass knife. The 0.5 μm sections were counterstained with a 2:1 mixture of Richardson's stain and Toluidine blue. Sections were examined under a light microscope and photographs were taken at X800 magnifications using a dry objective. The photographs were developed into 4" by 6" prints and then these prints were scanned by a Hewlett Packard Scan Jet Plus. The scanned images were saved as PICT files and then these files were imported into NIH Image 1.52, an image analysis software package. Following image enhancement, the outside and inside perimeters of the axons were separately traced with a mouse. The area and perimeters of the axons and fibers were computed with NIH Image and this information was used to compute the true circular axon and fiber diameters as well as the myelin sheath thickness (Auer, 1994). The data were not corrected to account for shrinkage due to histological processing.

2. Preliminary Results

A preliminary examination of the data indicates several interesting features. The nerve samples from beneath the nerve cuffs tend to show both a characteristic increase in the amount of epineurial connective tissue and an increase in the amount of extraneural connective tissue that encapsulates each cuffed sample. These two connective tissue zones are distinctly demonstrated under low magnification (Fig. 6b). The corresponding control samples do not demonstrate this phenomenon (Fig. 6a). Qualitatively, the axons of a cuffed and a non-cuffed nerve are virtually indistinguishable . Axonal shapes and size distributions appear to be similar between the control (Fig. 7a) and the cuffed (Fig. 7b) samples.

The histograms showing the distribution of the fiber diameters show the bimodal population distribution typically seen in many other nerves samples. Other researchers (Friede and Beuche, 1985; Usson et al., 1987) have suggested that the occurrence of these peaks represent two separate normally distributed populations which are centered around two different modal averages. In this case, the data shows a large group of fibers centered around 11 μm and a smaller population centered around 5 μm. The plots of myelin thickness versus the axon diameter further (Figs. 8b and 9b) support the separation of the distribution into a large diameter and a small diameter population. Although a nearly linear relationship is demonstrated between axon size and myelin sheath thickness, a clear break appears in the distribution of the larger and the smaller fibers. The larger axons (>8 μm) from one subpopulation as do the axons that are smaller than 8 μm

A close examination of the histograms of NIH 13 and NIH 11 (Figs. 8a and 9a) reveals that the distributions of both populations are similar. This result is somewhat surprising given that NIH 11 experienced a decrease in the ulnar nerve compound action potential (CAP) to 40% of its initial value (at day 0 of the experiment) while NIH 13 maintained its signal at 92% of its original value (Strange et al., 1995a,b) . We expected that there would be difference in the fiber distribution between the two populations that might help to account for the difference in ENG amplitude but this result does not appear to have occured. Further work is required to assess whether a differential loss of fibers located near the edge of the nerve could be contributing to these results. Research conducted by Rydevik and Lundborg (1977) suggests that there may be reason to expect that the more outwardly located neurons are more susceptible to damage.

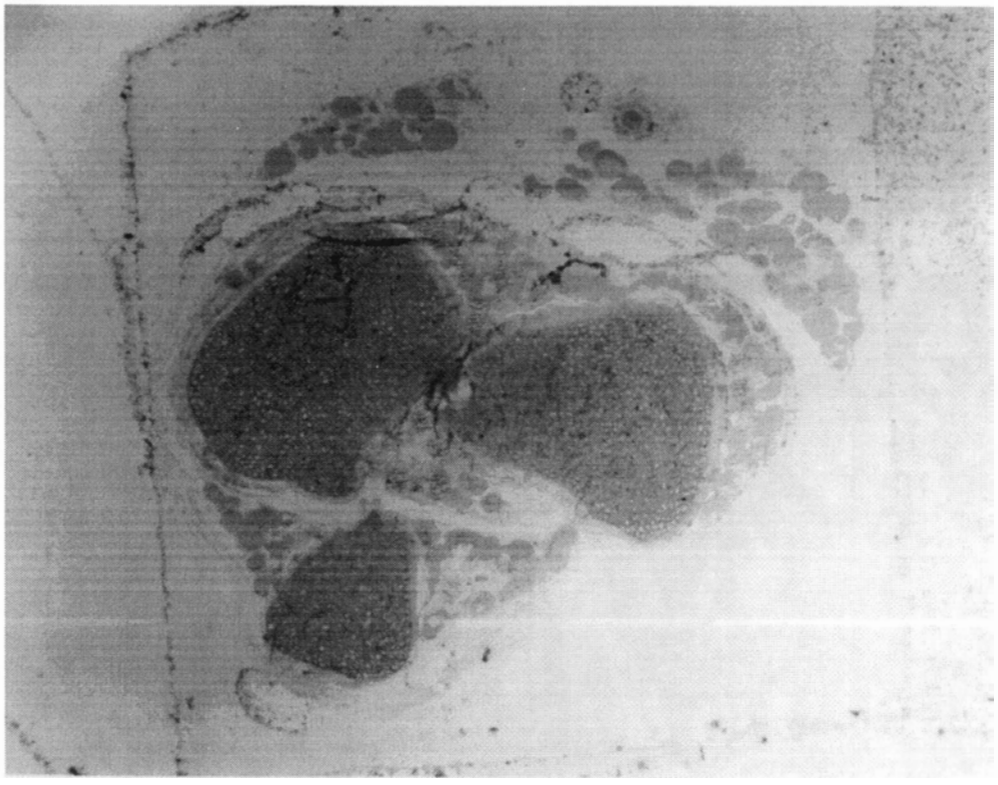

Figure 6a: Histology of NIH 13 distal Ulnar nerve control, low magnification (45X)

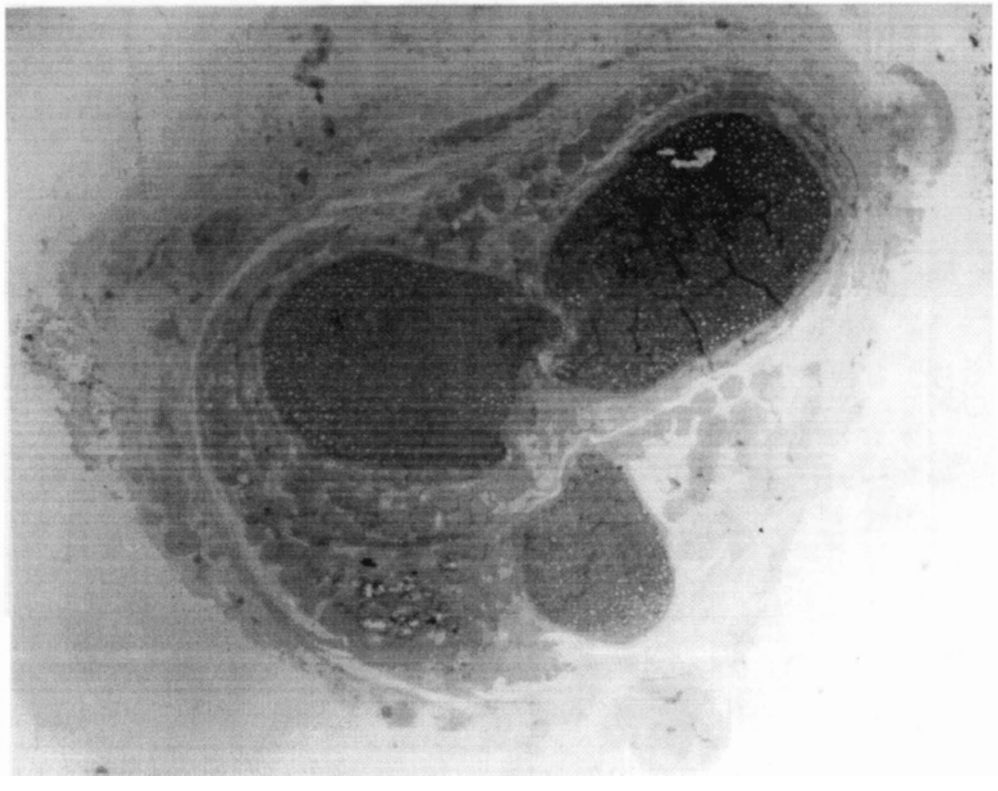

Figure 6b: Histology of NIH 13 distal Ulnar nerve experimental, low magnification (45X)

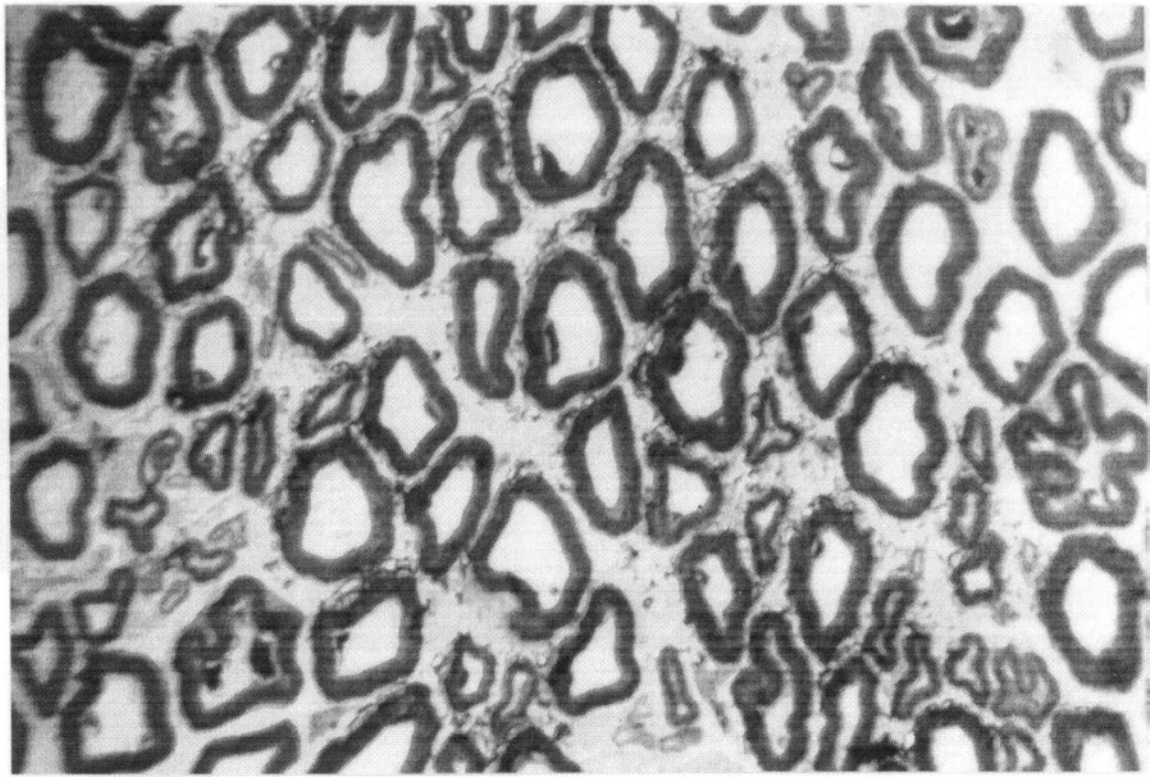

Figure 7a: Histology of NIH 14 distal radial nerve control. High magnification (800X)

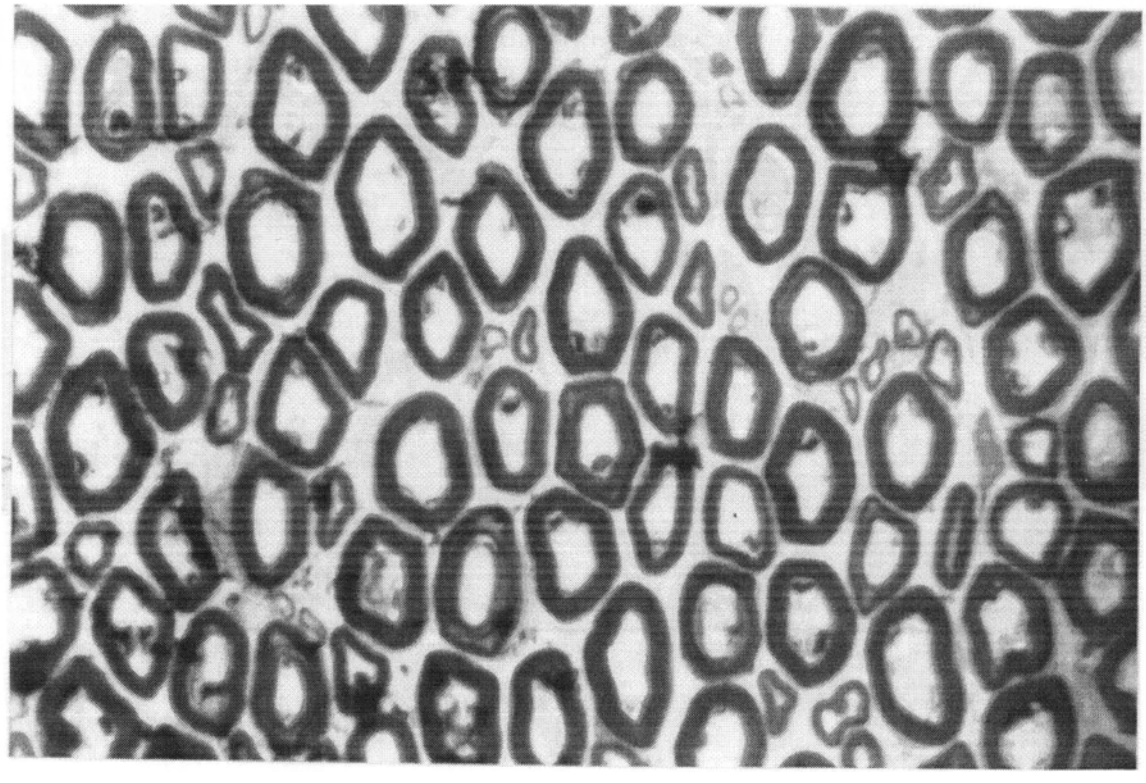

Figure 7b: Histology of NIH 14 distal radial nerve experimental. High magnification (800X)

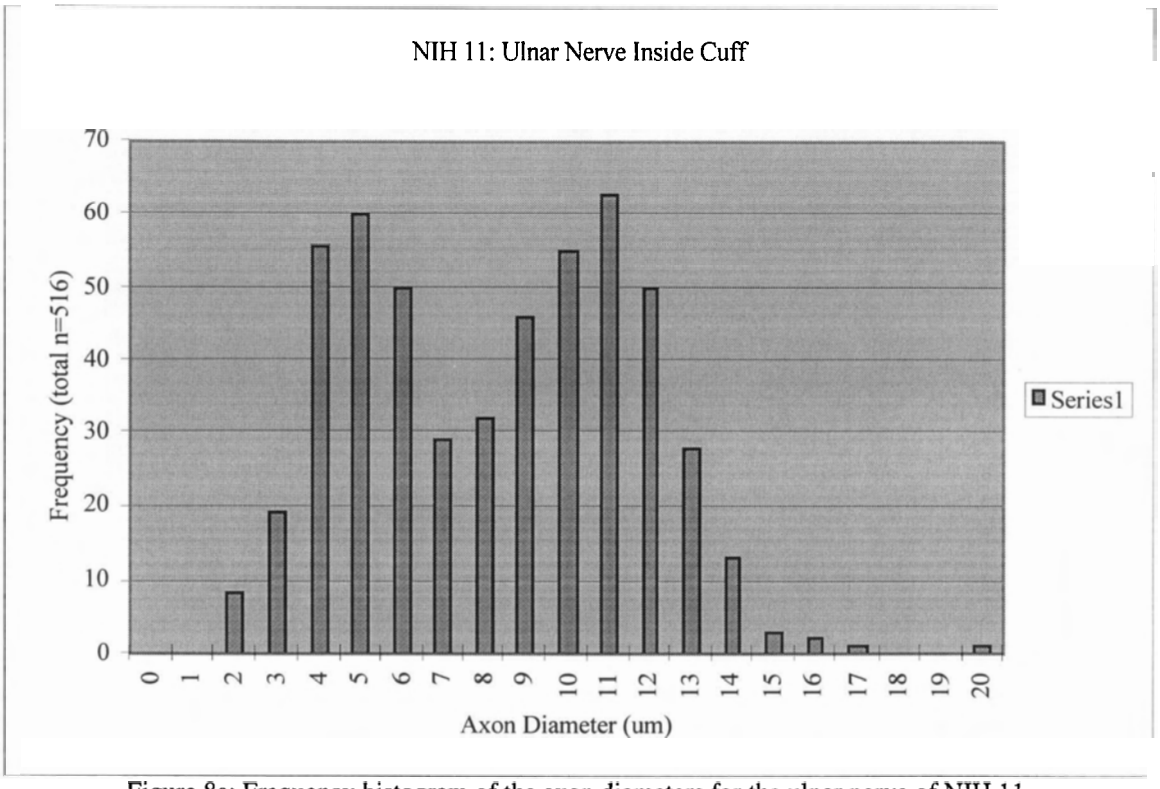

Figure 8a: Frequency histogram of the axon diameters for the ulnar nerve of NIH 11.

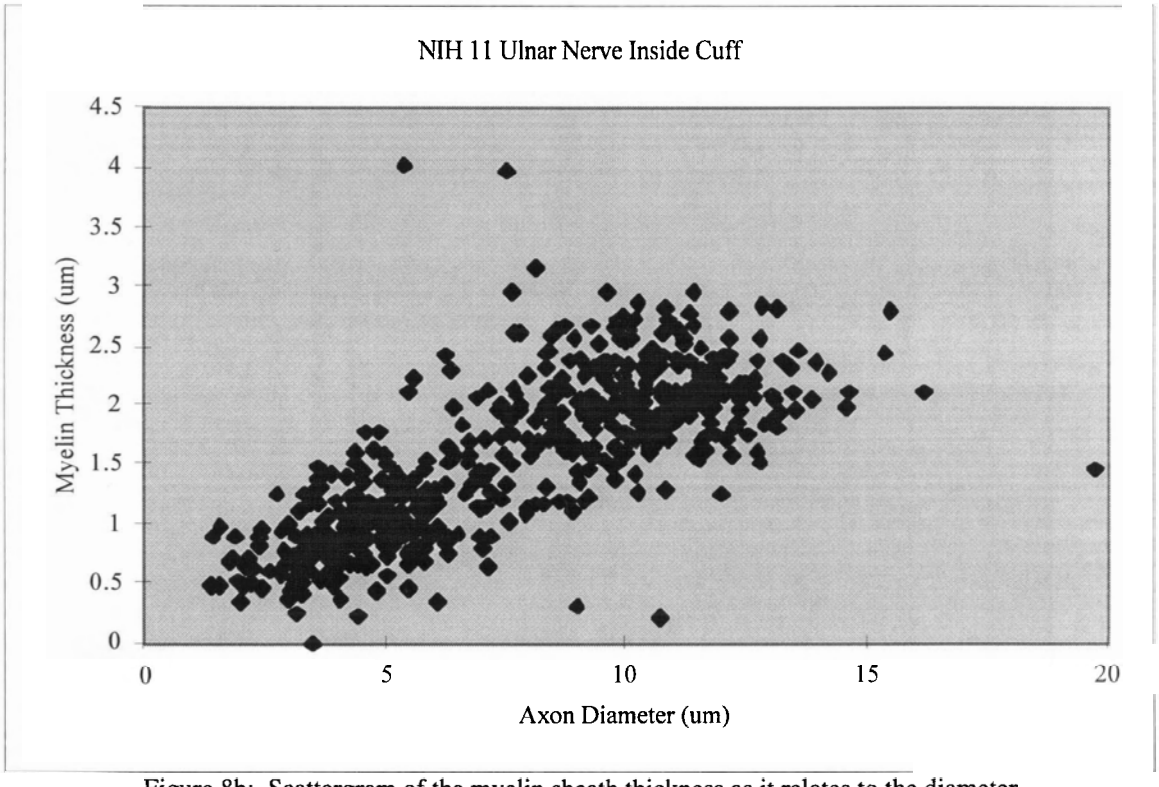

Figure 8b: Scattergram of the myelin sheath thickness as it relates to the diameter of the axon for the ulnar nerve of NIH 11..

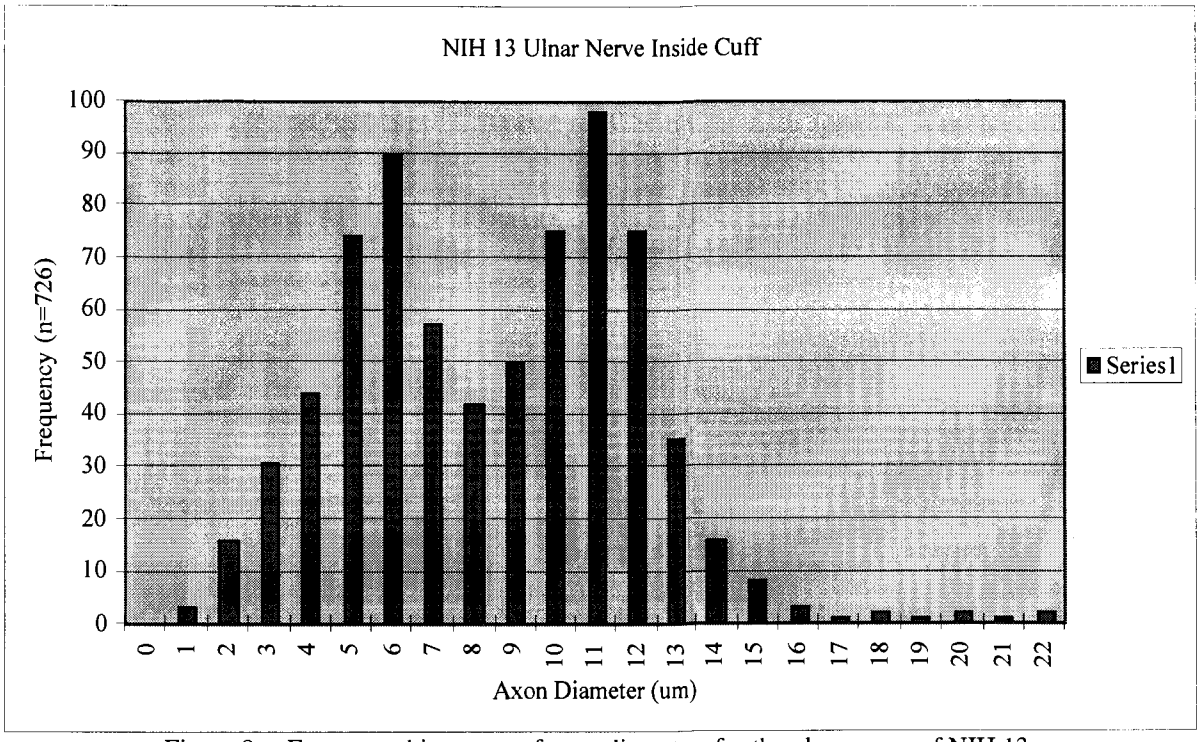

Figure 9a: Frequency histogram of axon diameters for the ulnar nerve of NIH 13.

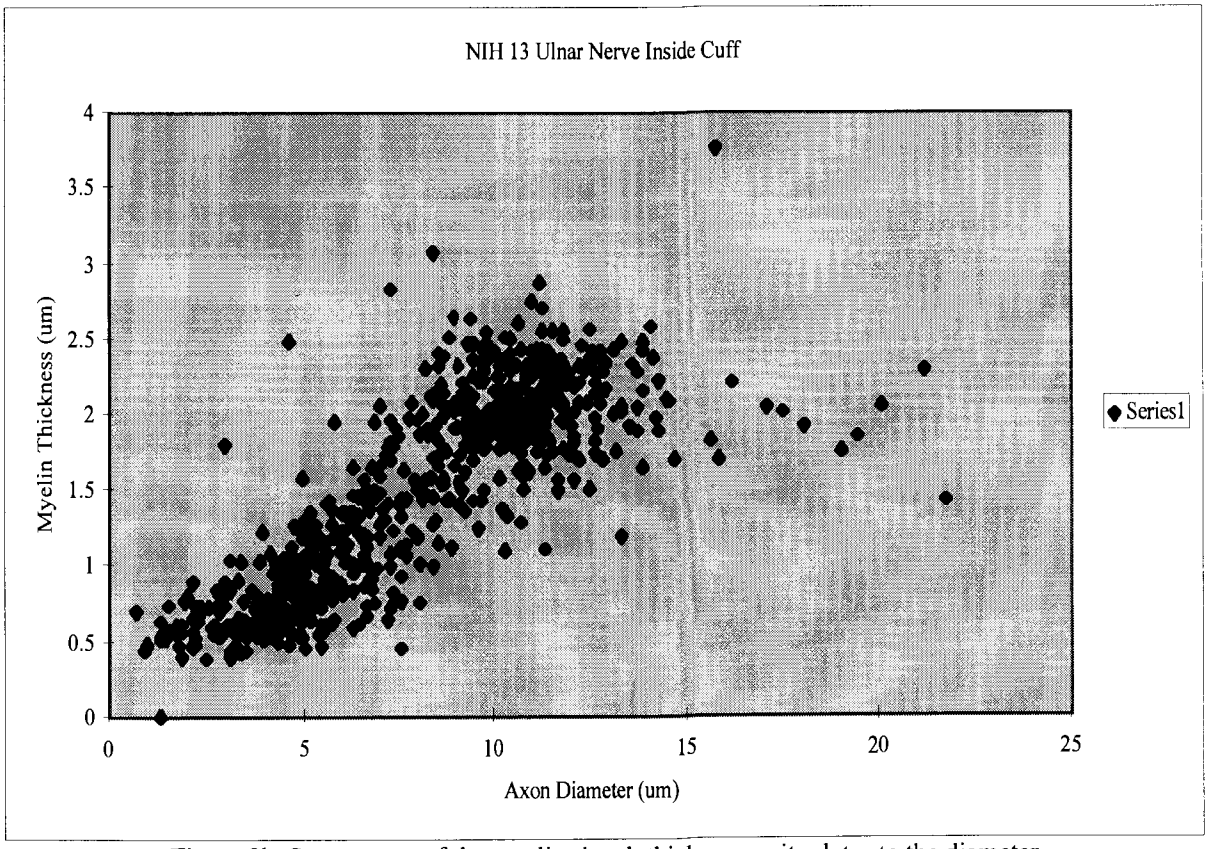

Figure 9b: Scattergram of the myelin sheath thickness as it relates to the diameter of the axon for the ulnar nerve of NIH 13.

C. Progress with Collaborators

During the eleventh quarter, we continued our collaboration with Drs. A. Kostov and R.B. Stein of the University of Alberta, concentrating on developing manuscripts based on our investigations of implementing machine learning techniques to analyze neural signals and predict muscle activity. We have developed a plan for further experiments to analyze data developed in the Year Two series of NIH implants as outlined in Progress Report #10 and future implementations of machine learning techniques in closed-loop control of functional electrical stimulation.

D. Publications and Meetings

1. Publications

During the eleventh quarter, the investigators developed three manuscripts for peer-reviewed journals based on results obtained from the current NIH contract. The three manuscripts are nearly ready for submission, and are outlined as follows:

Manuscript 1:

Title: Long term stability of nerve cuff signals recorded from the cat forelimb.

Authors: K. Strange, K. Kallesøe, and J.A. Hoffer

Manuscript 2:

Title: Sensory signals from the cat paw cutaneous receptors during walking: Applicability for closed-loop control of FES.

Authors: K. Strange and J.A. Hoffer

Manuscript 3:

Title: Artificial neural networks application in EMG-prediction using sensory nerve signals recorded in the cat's forelimb during walking.

Authors: A. Kostov, K. Strange, R.B. Stein, and J.A. Hoffer

2. Meetings

During the eleventh quarter, Kevin Strange and Andy Hoffer had an abstract published in the Proceedings of Neuroscience 25th Annual Meeting, Nov. 1995, San Diego, CA. The abstract is included in Appendix A.

IV. Plans for Twelfth Quarter

In the twelfth quarter we intend to:

1. examine histopathologically the nerves from Year One and Year Two cats (objective 5)

2. continue Year Three series of implants, implanting cuffs appropriate for smaller proprioceptive nerves (objective 3)

3. complete the construction of an 8-channel stimulator to be used for FES of forelimb muscles (objective 4b)

4. complete the construction of hardware and begin the software design for controlling the reaching task (objective 4a,b)

5. develop a model of closed loop control of FES during walking utilizing neural feedback (objective 4)

6. analyze walking data with our collaborators (objective 7)

V. References

Auer, R., (1994), Automated nerve fibre size and myelin sheath measurements using microcomputer-based digital image analysis: theory methods and results, *Journal of Neuroscience Methods*, 51: 229-238.

Friede, R, and Beuche, W., (1985), Combined scatter diagrams of sheath thickness and fibre caliber in human sural nerves: changes with age and neuropathy, *Journal of Neurology, Neurosurgery and Psychiatry*, 48: 749-756.

Hoffer, J.A., (1990), Techniques to record spinal cord, peripheral nerve and muscle activity in freely moving animals. In: Neurophysiological Techniques: Applications to Neural Systems. *NEUROMETHODS*, Vol. 15, A.A. Boulton, G.B. Baker and C.H. Vanderwolf, Editors. Humana Press, Clifton, N.J., pp. 65-145.

Kallesøe, K., Hoffer, J.A., Strange, K., and Valenzuela, I., (1994), Implantable Cuff Having Improved Closure. Pat. Pend. in US and Canada, Dec. 24. 1994.

Karnovsky, M.J., (1965), A formaldehyde fixative of high osmolarity for use in the electron microscope, *Journal of Cell Biology*, 27: 137A.

Rydevik, B, and Lundborg, G., (1977), Permeability of intraneural microvessels and perineurium following acute, graded experimental nerve compression, *Scandanavian Journal of Plastic and Reconstrive Surgery*, 11: 179-187.

Strange, K.D., and Hoffer, J.A., (1995), Sensory Signals From Cat Paw Cutaneous Receptors During Walking: Applicability for Closed-Loop Control Of FES, in preparation

Strange K.D., Hoffer J.A., Kallesøe K., Schindler S.M., and Crouch D.A., (1995a), Long term stability of nerve cuffs implanted in the cat forelimb, in *Proc. of RESNA '95*, Vancouver, Canada, June, 1995

Strange K.D, Kallesoe, K., and Hoffer, J.A., (1995b), Long Term Stability of Nerve Signals Recorded in the Cat Forelimb, in preparation.

Usson, Y, Torch, S, and Drouet d'Aubigny, G., (1987), A method for automatic classification of large and small myelinated fibre populations in peripheral nerves, *Journal of Neuroscience Methods*, 20: 237-248.

VI. Appendix A

Abstract published in Soc. Neuroscience, Abstr. 21: 419, Nov. 1995, San Diego, CA.